学位論文

Development of chemical post-translational modification reactions on azoline-containing peptides expressed in a reconstituted cyclodehydratase-coupled translation system

(試験管内生合成されたアゾリン含有ペプチドの化学的翻訳後修飾反応の開発)

平成 28 年 12 月　博士（理学）申請

東京大学大学院理学系研究科
化学専攻
加藤　保治

Abstract

Backbone modifications such as azoles, azolines and azolidines are often seen in bioactive peptidic natural products. Since these heterocyclic structures would provide peptides with several characteristics such as rigid global conformation, hydrogen bonding sites with fixed orientations, improved proteolytic resistance, and cell membrane permeability, they are important motifs of the bioactive peptides and the backbone modifications would be a general strategy for organisms to develop a wide variety of bioactive peptides.

Our laboratory has previously developed an *in vitro* biosynthesis system for azoline-containing peptides by integrating the Flexible *In vitro* Translation (FIT) system and a post-translational cyclodehydratase, PatD, which is involved in the biosynthesis of patellamides. In the *in vitro* biosynthesis system, referred to as FIT–PatD system, Cys/Ser/Thr residues involved in translated peptides are modified by PatD to the corresponding azoline moieties, allowing one-pot synthesis of azoline-containing peptides. We have revealed an unprecedented substrate tolerance of PatD and demonstrated that this system can be applied for diverse azoline-containing peptides.

In order to expand structural diversity, which is accessible by *in vitro* translation and subsequent post-translational modifications, in my doctoral studies, chemical methodologies were developed, which generate peptides containing a wide range of backbone modifications by the integration of enzymatic cyclodehydration by PatD and chemical modifications such as oxidation and reduction.

In chapter 2, based on a serendipitous observation that one of the two consecutive thiazolines in peptidic backbone is prone to be oxidized, chemical oxidation method was developed for *in vitro* synthesis of various thiazole-containing peptides. In addition, site-specific deuterium labeling method was developed, which identified the oxidation site and provided insights on reaction mechanism. Investigation of substrate scope of the oxidation method demonstrated *in vitro* synthesis of various thiazole-containing peptids.

In chapter 3, reduction of thiazoline moiety in peptidic backbone was attempted for *in vitro* synthesis of thiazolidine-containing peptides. Based on a serendipitous finding that thiazoline can be reduced into $\Psi[CH_2NH]$ structure via thiazolidine moiety, *in vitro* synthetic method of

Ψ[CH_2NH]-containing peptides was developed. The formation of thiazolidine and Ψ[CH_2NH] structure was confirmed by model reactions. The reduction method enabled facile synthesis of a wide variety of Ψ[CH_2NH]-containing peptides.

In conclusion, in this research I have developed novel methods involving the post-translational enzymatic cyclodehydration by PatD and chemical modifications on ribosomally synthesized peptides to yield peptides with various backbone modifications such as thiazole moiety (Chapter 2) and Ψ[CH_2NH] structure as well as thiazolidine moiety (Chapter 3). The installation of thiazoles and thiazolidines, which are prevailing in bioactive peptidic natural products as well as Ψ[CH_2NH] structures, which is one of the well known peptidomimetic structures, would provide unique structural scaffolds into peptides, which possibly leads to the development of novel bioactive peptides.

Table of contents

Chapter 1 General introduction

1.1 Non-standard peptides as drug candidates for protein–protein interactions (PPIs) and peptidic natural products as a source of non-standard peptides

Protein–protein interactions (PPIs) have emerged as challenging targets of great importance in chemical biology and medicinal chemistry.[1-7] It has been argued that PPIs are difficult to be targeted by small molecules, which are mainly employed in drug discovery today[8] because of larger interaction surface area involved in PPIs (1500–3000Å) compared to protein-small molecule interaction surface area (300–1000Å).[9] In addition, though antibodies can actually modulate PPIs, they cannot target intracellular proteins of therapeutic interest because they cannot penetrate cell membrane. Although intensive studies have recently provided successful examples of targeting PPIs by small molecules,[7] it is still challenging to develop small molecule PPI modulators and non-standard peptides have been getting much attention as candidates of drugs and bioactive molecules for modulation of intracellular PPIs.[10, 11]

Since detailed mechanism of PPIs can be attributed to the interactions between peptides embedded in proteins of interest, peptides would be the most natural approach to modulate PPIs by mimicking proteins.[12,13] Moreover, the fact that peptidic natural products exemplified by cyclosporin A (**Figure 1.1**), which is far from the rule of thumb on bioavailability of small molecules (or Lipinski's rule of five[14]) can penetrate cell membrane[15], encouraged the utilities of non-standard peptides as molecular scaffold for the development of novel bioactive peptides. (Note that "non-standard peptides" here denote the peptides containing "non-standard structures", which is not found in linear peptides composed of 20 kinds of proteinogenic amino acids.) Although peptides generally can not permeate cell membrane, a number of non-standard structures in cyclosporin A such as non-proteinogenic side chains, D-amino acids, *N*-methylation, and macrocyclic structure would cooperatively contribute to the membrane permeability of cyclosporin A.

In addition to above-mentioned non-standard structures found in cyclosporin A, peptidic natural products in general exhibit huge structural diversity, which is reviewed in the following part. This structural diversity must be advantageous for the development of novel bioactive peptides,

however, alternative approaches than "natural product-based drug development" would be desired for the development of peptides against some targets of therapeutic interest. Except for antimicrobial agents, the activities of peptidic natural products would have nothing to do with human diseases and the production of such molecules would not be the selective pressure in the process of evolution. The immunosuppressant activity of cyclosporin A would be just a product of chance. Thus, for the development of novel bioactive peptides with non-standard structures, peptides, which possess natural product-like structures, but as a whole, structurally different from original natural products would be required.

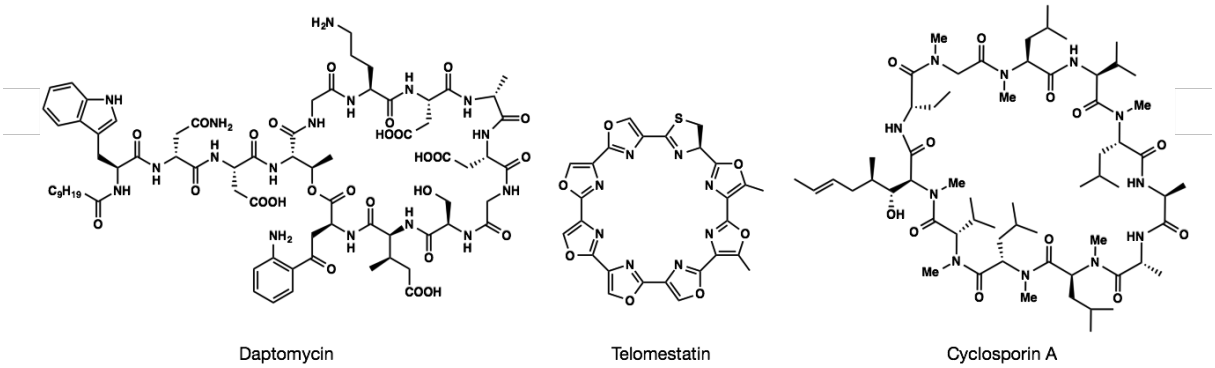

Figrue 1.1 Examples of peptidic natural products biosynthesized by non-ribosomal peptide synthetases (NRPS).

1.2 The development of bioactive peptides by rational design and high-throughput screening

In general, mainly two approaches can be employed for *de novo* development of bioactive peptides. First, PPI modulator can be rationally designed based on proteins of interests.[12] For example, based on co-crystallization structures, mimicry of peptide strands in either of proteins involved in targeted PPIs can be synthesized.[7] The designed peptides can interact with the targeted proteins and thus competitively inhibit the targeted PPIs. By the aid of computational analysis, which predict regions of proteins, which are critical for PPIs, constrained peptides can be also designed.[16] However, the potential problems of these approaches are; (i) crystal structures are required for the structure-based design, (ii) it would be generally difficult to obtain stronger affinity against a target protein than that of the native counterpart protein, (iii) it is difficult to design peptides, which bind to unexpected sites or exhibit PPI modulation in allosteric mechanism and (iv) it is difficult to design peptides based on a non-structured binding region, which is also prevalent in PPIs.[17]

The other approach is construction of peptide library and subsequent screening of active peptides from the library (**Figure 1.2**). This method has actually isolated (i) binding peptides against target proteins, which crystal structure was not solved,[18] (ii) binding peptides with pM affinities,[19] (iii) active peptides, which bind target proteins at unexpected sites and regulate PPIs in an allosteric manner.[20] (iv) Additionally, since this screening approach does not mimic naturally occurring binding peptide strands, no structured binding region is required.

In *de novo* development of bioactive peptides by high-throughput screening approach, the diversity of peptide libraries is highly important. Antibodies would be a good reference of such relationship between diversity and activity. Since antibodies can strongly bind to a specific target molecules, they have been widely used in biological research and clinically.[21] These characteristics are the basis of fundamental molecular detection techniques such as ELISA[22, 23] and western blotting[24-26] in biological research, and therapeutic antibodies is growing modality for drug development.[8]

In general, therapeutic antibodies have low nM order of dissociation constants (K_D). For example, K_D values are 2.6–3.1 nM for nivolumab[27, 28], 30–550 pM for adalimmub[29-31], 21 pM–9.1 nM for infliximab[29, 30], 160 nM for rituximab[32] and 2.2–16.6 nM for bevacizumab[33, 34].

On the other hand, the diversity of antibodies has been estimated[35, 36] as $>10^{10}$, suggesting that highly diverse peptide library may provide active peptides which bind to target molecules of interest with strong affinity comparable to antibodies. Actually, screening approach using genetically encoded peptide library has been yielded a number of active peptides showing antibody-like activities.[37]

In short conclusion, construction of non-standard peptide library and a subsequent screening have great advantages for the development of bioactive peptides. In order to accomplish this approach, facile synthetic methods are required for the construction of highly diverse (10^{10}–10^{11}) non-standard peptide libraries.

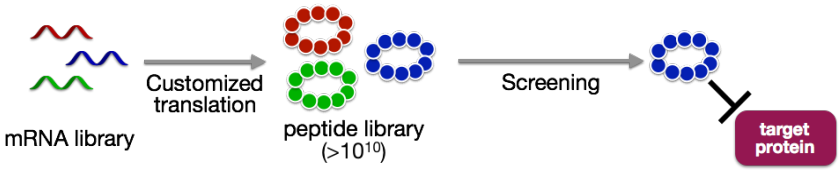

Figure 1.2 Schematic illustration of the screening for bioactive peptides. In this figure, mRNA display-mediated screening of bioactive peptides is illustrated.

1.3 Chemical synthesis and NRPS-mediated biosynthesis of non-standard peptides

Both chemical synthesis and enzymatic synthesis can be employed for the synthesis of non-standard peptides. By organic synthesis, various non-standard structures can be introduced, and structures can be controlled at atomic level. However, the diversity of peptide library is at most 10^8 even with combinatorial methods.[38] On the other hand, biosynthetic machinery can also be employed for the synthesis of non-standard peptides. A number of peptidic natural products including cyclosporin A are biosynthesized by non-ribosomal peptide synthetases (NRPS) (**Figure 1.1**). In general, peptidic natural products biosynthesized by NRPS exhibit huge structural diversity and several peptides are clinically used.[39] For example, cyclosporin A contains a number of non-standard structures, and being an orally available immunosuppressant. Although *in vitro* reconstitution and engineering of NRPS have been investigated and made success in the synthesis of natural product analogs[40, 41], the property of NRPS that several huge proteins are responsible for the polymerization of amino acids as well as modification reactions[42] has limited the diversity of natural product analogs synthesized by engineered NRPS and thus application of NRPS in the *de novo* development of bioactive peptides.

1.4 Post-ribosomal peptide synthesis (PRPS) for non-standard peptide biosynthesis

In addition to NRPS-mediated biosynthesis, many peptidic natural products are biosynthesized via ribosomal pathway. Such peptidic natural products with ribosomal origin are called "ribosomally synthesized and post-translationally modified peptides (RiPPs)" and examples are shown in **Figure 1.3**. The biosynthetic pathways of RiPPs are called "post-ribosomal peptide synthesis (PRPS)",[43] and PRPS are found in all the three domains of life, comprising universal biosynthetic pathway of peptidic natural products.[43]

Biosynthesis of RiPPs by PRPS literally initiates with ribosomal expression, or translation of a longer precursor peptide (**Figure 1.4**). Precursor peptides typically composed of 20–110 amino acid residues, and a region, which is processed to yield final natural product is named "core peptide" In some cases, multiple core peptide regions are encoded in a single precursor peptide (e.g. patellamides). In most precursor peptides of RiPPs, the core peptide is flanked by a N-terminal "leader peptide", which is usually important for the post-translational modifications and export.[44] In the case of biosynthetic pathway of bottromycins, the leader peptide is not at N-terminus but at C-terminus and thus called "follower peptide". In addition, the core peptide is followed by a C-terminal "recognition sequence" in some cases, which is recognized by a protease of macrocyclase (e.g. patellamides). In the presence of the leader peptide and several other regions, core peptides are extensively modified by a series of post-translational modifications, which is the basis of the structural diversity of RiPPs.

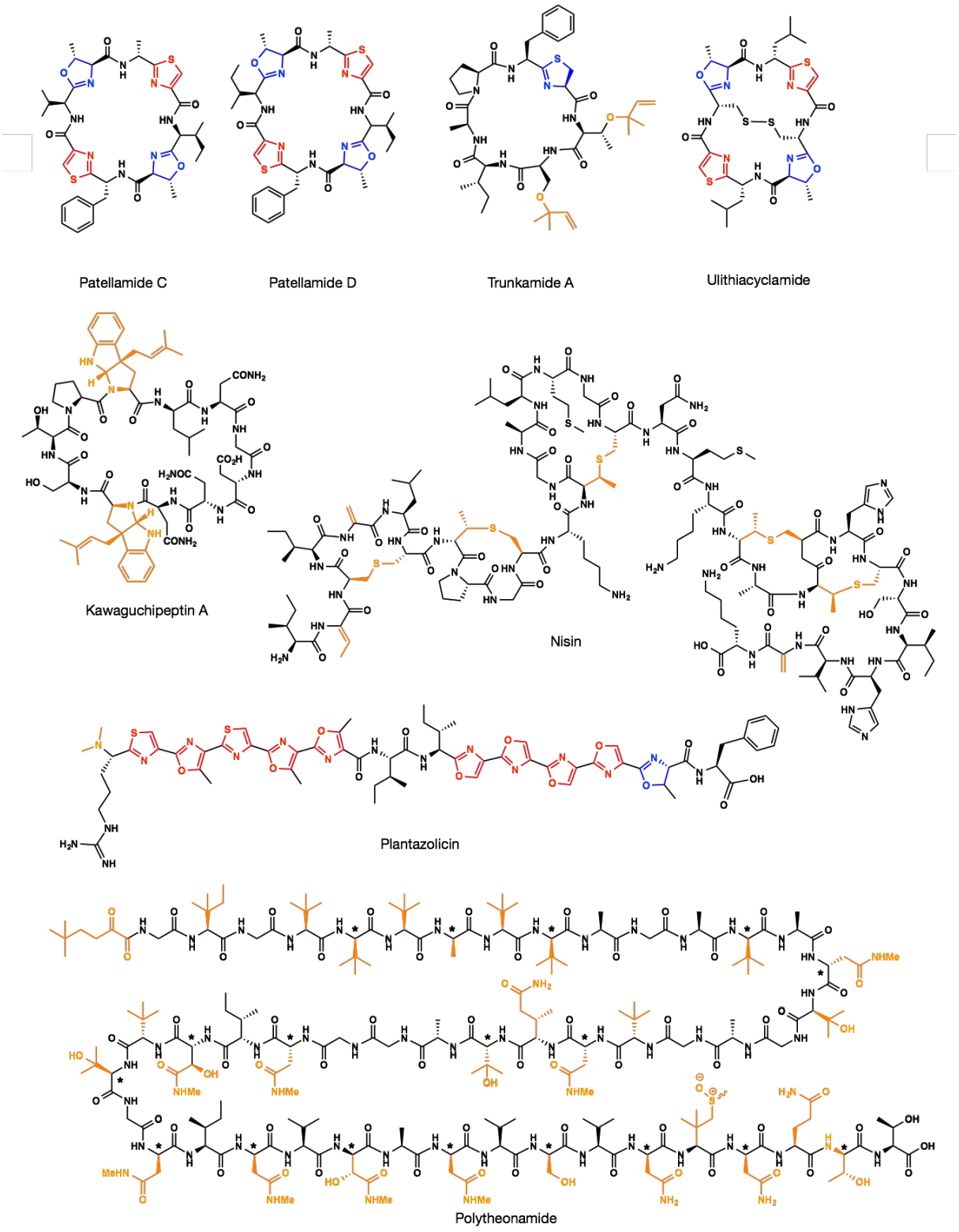

Figure 1.3 Examples of ribosomally synthesized and post-translationally modified peptides (RiPPs). Azolines, azoles and other non-standard structures are shown in blue, red and orange, respectively. In the structure of polytheonamide, amino acid residues with D-configuration are labeled with asterisk (*).

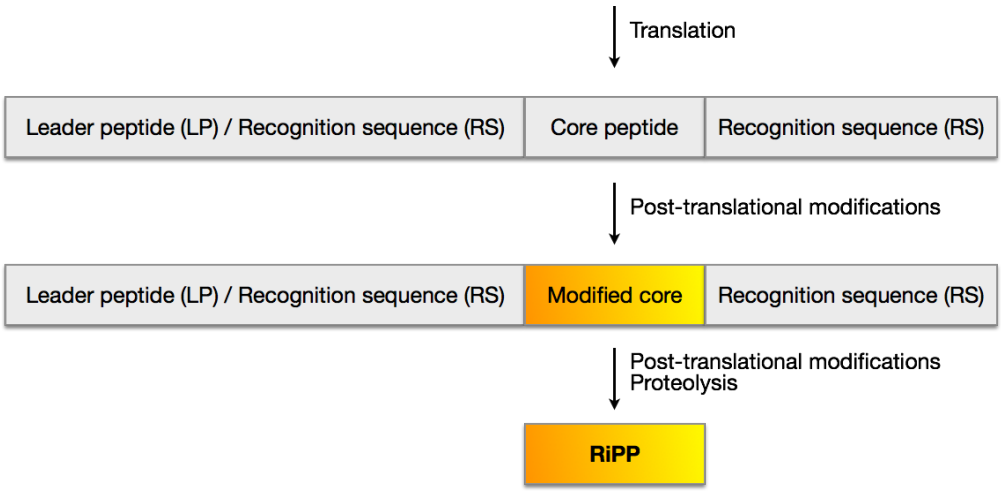

Figure 1.4 Schematic irustration of post-ribosomal peptide synthesis (PRPS): Biosynthetic pathway of ribosomally synthesized and post-translationally modified peptides (RiPPs).

1.5 Structural diversity in ribosomally synthesized and post-translationally modified peptides (RiPPs)

1.5.1 Modifications at side chain of precursor peptides

Structures found in ribosomally synthesized and post-translationally modified peptides (RiPPs) are diverse,[45] and they can be divided into modification of (i) side chains, (ii) main chains, and (iii) side chains and main chains. In the following text, structural diversity of post-translational modifications is reviewed.

Dehydration

One prevalent modification found in RiPPs is dehydration of Ser and Thr residues resulting in dehydroalanine (Dha) and dehydrobutyrine (Dhb), respectively. Incorporation of Dha and Dhb can contribute to structural rigidity and protease resistance of peptides.[46] In addition, Dha and Dhb endow peptides with reactivity against sulfhydryl and amine groups. For example, natural product nisin[47] (**Figure 1.3**), which exhibit antibacterial activity has Dha and Dhb residues, suggested to be michael acceptor reactive to membrane sulfhydryl groups of bacteria.[48]

Dha residues can also react with intramolecular sulfhydryl groups. Michael addition between Dha residues and cysteine residues form lanthionine, which is defined as two alanine residues bridged by thioether bond. (In the case of Dhb, intramolecular micahel addition provide methyl lanthionine. Both of the thioether bridge can be seen in the structure of nisin shown in **Figure 1.3**) Another derivatization of dehydro amino acids is formal [4 + 2] cycloaddition, which is involved in biosynthesis of pyridine ring formation of thiopeptides. For example, that type of cycloaddition was biochemically demonstrated with TclM[49]. Additionally, michael addition of dehydro amino acid residues and oxidatively decarboxylated C-terminal cysteine residues forms similar thioether bridge with aminovinyl cysteine. Examples can be seen in epidermin[50] and cypemycin[51, 52]. Another variation is lysinoalanine, which is derived from dehydro amino acid residues and lysine residues exemplified by duramycin[53].

Epimerization

Another example of side chain modification is epimerization. For example, epimerization takes place in the biosynthesis of polytheonamides (**Figure 1.3**).[54, 55] Although epimerization itself does not provide peptides with new functional group, stereochemical conversion can contribute to protease resistance of peptides.[56] (Polytheonamides contain D-amino acids with non-proteinogenic side chains as well as D-Ala.)

O-Prenylation

Trunkamide (**Figure 1.3**) is a macrocyclic peptidic natural product isolated from *Lissoclinum patella*[57, 58] and later, production by symbiotic *Prochloron* spp. was revealed[59]. Along with macrocyclic structure and a backbone thiazoline, *O*-prenylation of Ser and Thr residues can be found as non-standard structures. Also, *O*-prenylation on Tyr residue can be seen in prenylagaramides[60] and a number of prenylation are reported in small cyclic peptides produced by cyanobacteria, or cyanobactins.[61] These *O*-prenylation is catalyzed by prenylases, exemplified by LynF enzyme.[62] LynF prenylate Ser/Thr/Tyr residues in macrocyclic peptides, unlike typical post-translational modification enzymes requiring N-terminal leader peptides.

Although *C*-prenylation on Tyr residue was also reported as seen in aestuaramides,[63] *C*-prenylation was attributed to spontaneous Claisen rearrangement.[62] Another example of C-prenylation is found on Trp residue, which is discussed in the main-chain modification part.

Disulfide formation

In general, disulfide formation between intramolecular cysteine residues can spontaneously proceed. Actually, for biosynthetic gene cluster of ulithiacyclamide[59, 64] (**Figure 1.3**), which is a macrocyclic peptidic natural product with disulfide bond linkage as well as backbone heterocycles, no oxidase has been reported to be involved in the disulfide formation. However, in some cases, enzymatic oxidation would be involved in biosynthesis of disulfide linkage. For example, some conotoxins are very difficult to synthesize chemically,[65] which suggests assistance by some mechanisms exist to correctly and efficiently fold the precursor peptide into the mature product

in vivo. This assumption is consistent with the report that in the case of thermophilin 9, the disruption of disulfide oxidase altered inhibitory spectrum of the producing strain[66] and that protein disulfide isomerases (PDIs) was major soluble proteins in *Conus* venom duct extracts[67]. This enzymatic assistance would be, at least in some cases, necessary for the biosynthesis of conotoxins. It would be worth noting, however, that for bioactivities of conotoxins, constrained structures rather than disulfide bonds themselves would be important based on the report that the replacement of disulfide forming cysteines by allyl glycines retained the bioactivity of leucocin, which is attributable to hydrophobic intermolecular interactions of the diallyl side chains.[68]

1.5.2 Modifications at main chain of precursor peptides

Probably, most prevalent main-chain modification is cleavage of leader peptide since almost all precursor peptides of RiPPs have leader peptides. It would be necessary for RiPPs producers to append leader peptides to precursor peptides in order to protect peptides/proteins from unnecessary modifications. And also in some cases, leader peptides would provide the producers with immunity since some RiPPs are inactive before the cleavage of the N-terminal leader peptides.[44] N to C macrocyclization is also common main-chain modification in RiPPs biosynthesis. A number of bioactive peptides have macrocyclic structures.[43]

C-prenylation

C-prenylation of tryptophan residue is also example of main chain modification. (*O*-prenylation is mentioned above.) Kawaguchipeptins are macrocyclic peptidic natural products, which are isolated from *Microcystis aeruginos*a NIES-88.[69, 70] Kawaguchipeptin A contains two prenylated tryptophan residues as well as a D-leucine residue[69] unlike kawaguchipeptin B, which is composed of proteinogenic amino acid residues (**Figure 1.3**).[70] A post-translational modification enzyme, KgpF catalyzes the prenylation at γ-position resulting in a tricyclic structure containing newly introduced pyrrolidine ring and KgpF can modify linear peptides and macrocyclic peptides[71] as well as Fmoc-Trp-OH[72]. *C*-prenylation of tryptophan residue can also be seen in ComX phormone.[73-75] C-prenylation in ComX phormone catalyzed by ComQ and in Kawaguchipeptin A

catalyzed by KgpF share the same scaffold with opposite stereochemistry.[72]

Backbone heterocycles such as azolines and azoles

Peptidic backbone heterocycles would rigidify global structure of the peptides and would endow peptides with protease resistance. Moreover, there are diverse interactions known between heterocycle-containing peptidic natural products and proteins/nucleic acids/metal ions.[76] Moreover, patellamide C (**Figure 1.3**), one of the macrocyclic peptidic natural products containing backbone heterocycles exhibited membrane permeability even higher than cyclosporin A, which is a clinically used and orally available peptidic natural product, by the parallel artificial membrane permeability assay (PAMPA).[77] PAMPA is a cell-free membrane permeability assay, which has been widely used for small molecules[78] and peptides[15] in order to evaluate passive membrane diffusion behavior of the compounds. The high membrane permeability should be attributed to backbone heterocycles as well as macrocyclic structure of patellamide C, demonstrating potential advantage of backbone heterocycles in the development of bioactive peptides.

The heterocyclic structures such as azolines and azoles are post-translationally introduced into peptidic backbone by cyclodehydratases and dehydrogenases, respectively. The cyclodehydratases introduce thiazoline, oxazoline, and methyloxazoline from Cys, Ser and Thr, respectively. The cyclodehydratases are YcaO domain-containing proteins and the cyclodehydration is dependent on ATP and magnesium ion[79] with two proposed intermediates for the mechanism of backbone amide activation, phosphorylated hemiorthoamide[80, 81].

The resulting azolines sometimes further derivatized by flavin mononucleotide (FMN)-dependent dehydrogenase to form thiazole, oxazole, and methyloxazole from thaizoline, oxazoline and methyloxazoline, respectively.[79] In some cases these heterocycle-related post-tranlsational modification enzymes cooperatively catalyze the reaction exemplified by the case of microcin B17 biosynthesis, where three proteins, the cyclodehydratase McbB, oxidase McbC, and putative docking protein McbD were required for the oxidation as well as cyclodehydration.[82]

1.6 Biosynthetic pathway of patellamdies, as an example of PRPS-mediated biosynthesis

From the technical point of view, the major advantage of the synthesis of non-standard peptides in a post-translational manner would be its compatibility with high-throughput screening system such as mRNA display system as long as post-translational modification enzymes have enough wide substrate scope, or promiscuity. In this context, we focused on post-translational introduction of backbone heterocycles because of (i) the abovementioned properties of heterocycles, which would be advantageous for the development of bioactive peptides and (ii) difficulties in direct incorporation of backbone heterocycles into translated peptides.

Based on such assumption, we have previously focused on the biosynthetic pathway of patellamides. Patellamides were isolated from *Lissoclinum patella.*[83] and later structures were revised[84-87]. They were revealed to be RiPPs, produced by *Prochloron spp*., which is cyanobacterial symbionts.[88] As for patellamide D, anti-multi drug resistance activity was reported.[89] In addition, patellamide C showed high membrane permeability.[15]

Biosynthetic genes of patellamides are composed of patA–patG[88], of which patA, patD, patE, and patG were denoted as essential[90] (with a citation[88]). patE encodes precursor peptide, which is composed of N-terminal leader peptide (LP), core peptides (CP) flanked by upstream and downstream recognition sequences (uRS and dRS), aligned as LP-uRS-CP-dRS-uRS-CP-dRS, where the sequences of two CPs are not exactly the same, corresponding to the two different patellamides as final products (**Figure 1.5**).

PatA is a protease, which cleaves amide bonds at the N-terminal side of the core peptides (CPs) with recognition sequences G(L/V)E(A/P)S. Protease domain of PatA was fully active similar to the full-length PatA and more stable than the full-length PatA.[91]

PatD is a YcaO domain-containing cyclodehydratase,[79] which modify Cys, Thr and Ser residues into thiazoline, oxazoline and methyloxazoline respectively. The X-ray crystal structure of PatD itself has not been reported, but structure of TruD, a homolog of PatD was reported.[81] TruD activates amide bond to be modified by adenylation using ATP.[81] In addition, ATP binding residues conserved among YcaO domains were revealed on the basis of X-ray crystal structure and biochemical studies,[92] but catalytic mechanism of the cyclodehydration is still elusive.

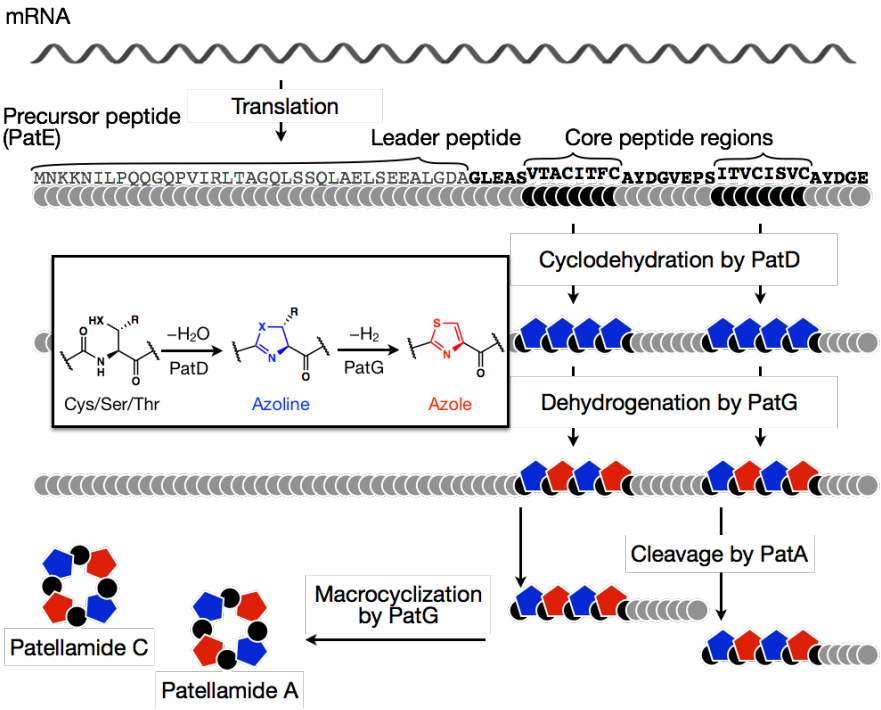

Figure 1.5 Biosynthetic pathway of patellamides.

PatG is composed of three domains, an N-terminal dehydrogenase domain, a central domain with unknown function, and a C-terminal protease (macrocyclization) domain. The macrocyclization reaction between N-terminal amine and C-terminal residues, which have downstream sequences, AYDG(E/V) was reconstituted *in vitro* and the synthesis of a wide variety of macrocyclic peptides was demonstrated.[93, 94] X-ray crystal structure of the macrocyclase domain of PatG was solved and structural basis for the macrocyclization was proposed.[95]

PatF was predicted as a prenylase and required for the production of patellamides,[90] But there is no prenyl group in known patellamides, and thus mysterious protein. The lack of prenyl group in patellamides was rationalized by mutations in catalytic residues in PatF.[96] Involvement of PatF as well as PatB and C in patellamide biosynthesis is unclear at this point, because to the best of my knowledge, reconstitution or heterologous expression of total biosynthetic pathway of patellamides has not been clearly demonstrated.

Collectively, proposed biosynthetic pathway is depicted in **Figure 1.5**. First, the precursor peptide PatE is ribosomally expressed. In the presence of N-terminal leader peptide, the cyclodehydratase PatD and the dehydrogenase domain of PatG install thiazole and (methyl)oxazoline. PatA liberate α-amino group at the N-terminal end of the core peptides, which is subsequently macrocyclized by the macrocyclase domain of PatG. Note that the cognate substrate of PatG oxidase is still elusive and oxidation of thiazolines into thiazoles after macrocyclization, for example, is also possible.

1.7 FIT–PatD system; integration of a customized cell-free translation system and a post-translational cyclodehydratase PatD

*This section is based on the publication from our laboratory; "One-pot synthesis of azoline-containing peptides in a cell-free translation system integrated with a posttranslational cyclodehydratase", Yuki Goto, Yumi Ito, Yasuharu Kato, Shotaro Tsunoda, Hiroaki Suga, *Chem. Biol.*, **2014**, 21, 766-774.

We have previously devised an *in vitro* biosynthetic system for azoline-containing peptides[97] by integrating the post-translational cyclodehydratase PatD, which is involved in patellamide biosynthesis[88] and a reconstituted cell-free translation system[98]. The *in vitro* biosynthetic system enabled one-pot synthesis of a wide variety of azoline-containing peptides in a template DNA dependent manner. In addition, the *in vitro* biosynthetic system enabled extensive mutagenesis studies, unveiling recognition determinants by which modification reaction is governed and unexpectedly high substrate tolerance of the cyclodehydratase PatD (**Figure 1.6**). In brief, (i) dRS can be truncated. (ii) uRS tolerates mutations and the length from leader peptide dictates core peptide region. (iii) The C-terminal region of the leader peptide (26L–37A) is necessary for the efficient cyclodehydration and peptides bearing that region at N-terminus can be efficiently modified by PatD. (iv) Precursor peptides without leader peptides were modified to some extent in the presence of a separate leader peptide. This "*in trans* modification" suggested "PatD-activation" mechanism by the leader peptide. In addition, (a) PatD can heterocyclize all of the Cys/Thr/Ser residues, with higher modification efficiency in this order. (b) PatD can accept various artificial core peptide sequences with (b-1) various amino acid length, (b-2) various amino acid compositions including hydrophilic residues and (b-3) consecutive cysteine residues to be modified, which are all rare in naturally-occurring core peptide sequences. Collectively, unprecedented substrate tolerance of post-translational cyclodehydratase PatD was demonstrated and these observations were the basis of the present studies, which are described in the following chapters.

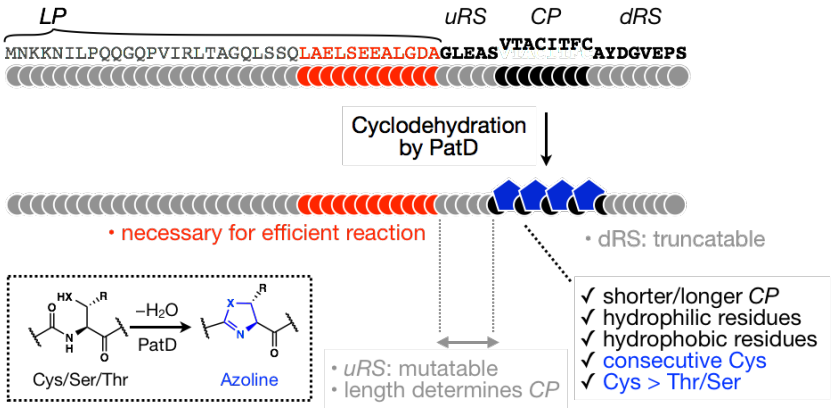

Figure 1.6 Summary of the mutagenesis experiments in our previous study, which is related to the experimental design in the present thesis.

1.8 Technological backgrounds

1.8.1 Translation reaction as peptide synthetic method and its molecular mechanism

Translation is a biosynthetic reaction of proteins, in which ribosome[99] polymerize amino acids in a mRNA template dependent manner. Since peptide synthesis by translation reaction proceeds rapidly (12–22 amino acids/sec)[100, 101] and precisely (error rate ~1/1000)[102], translation is a powerful tool as peptide synthetic method. Relationship between the sequence of peptides and the sequence of template mRNAs (nucleotides) is governed by codons, sequences of three nucleotides.[103] For example, the codon UUU is corresponding to phenylalanine, and thus poly U sequence direct the synthesis of poly phenylalanine sequence.[104] In principle there are 64 kinds of codons (= 4^3), and the relationship between codons and amino acids are summarized as the genetic code.[105]

As above mentioned, relationship between codons and amino acids are strictly controlled. In molecular level, this control can be attributed to the adopter molecule, tRNA, and the relationship can be rationalized from two points (**Figure 1.7**), (i) paring between codons and tRNAs and (ii) paring between tRNAs and amino acids. (i) First, every tRNA has the sequence called anticodon, which is a complementary sequence to the corresponding codon, and thus base paring between codons and anticodons can link codons and tRNAs properly. (ii) Aminoacylation reactions of amino acids on tRNAs are catalyzed by aminoacyl tRNA synthetases (ARSs), which selectively catalyze the reaction using corresponding tRNAs and amino acids. For example, Trptophanyl aminoacyl tRNA synthetase (TrpRS) catalyze aminoacylation of $tRNA^{Trp}_{CCA}$ by tryptophan selectively, and the substrate specificities of ARSs can link tRNAs and amino acids properly. Note that $tRNA^{Trp}_{CCA}$ denotes that the tRNA is corresponding to tryptophan and its anticodon sequence is 5'-CCA-3', which is complementary to tryptophan codon 5'-UGG-3'.

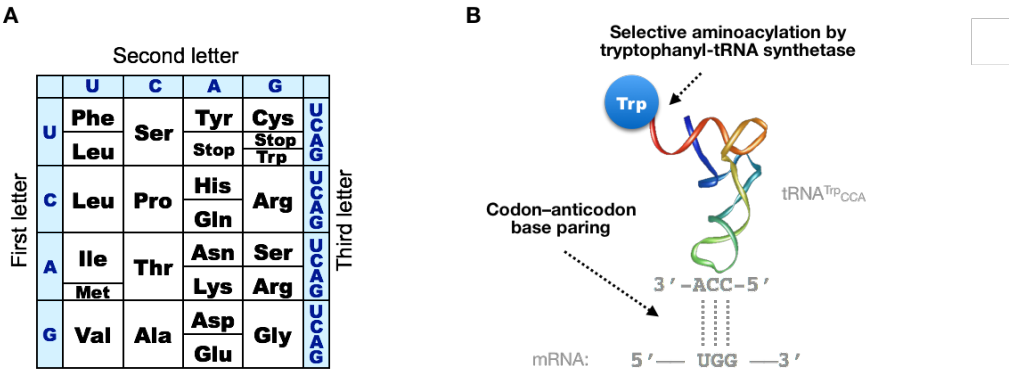

Figure 1.7 The genetic code and molecular mechanism of sequence dependency of translation.

1.8.2 Ribosomal synthesis of non-standard peptides by mis-acylated tRNAs

The mechanism for fidelity control in translation reaction is consistent with the fact that ribosome must tolerate 20 kinds of proteinogenic amino acids as the building blocks for peptide synthesis. Although translation system, as a whole, can only synthesize canonical peptides, the property that ribosome does not recognize side chains of amino acids charged onto tRNAs is the basis of the engineering of translation system discussed in the following text.

Based on the background, synthetic methods of misacylated tRNA with non-proteinogenic amino acids have been investigated. Early examples are, albeit not non-proteinogenic, the replacement of cysteine by alanine upon the Raney-nickel mediated desulfurization on Cys-tRNA^{Cys},[106] being an early indication of the successful incorporation of a wide variety of non-proteinogenic amino acids by the "misacylation strategy". For the synthetic methods of misacylated tRNAs, semi-enzymatic synthesis, in which a chemically synthesized aminoacyl-dinucleotide and tRNA body are ligated by T4 RNA ligase [107, 108] and artificially evolved aminoacyl tRNA synthetase[109] have been mainly used, but these methods limit the variety of non-proteinogenic amino acids, which may be tested for the ribosomal incorporation and subsequent biological or chemical events.

Promiscuity of the aminoacyl tRNA syntheases, though they were basically specific enzymes, can also be utilized for the introduction on non-proteinogenic amino acids.[110] ARS can

aminoacylate tRNA with non-proteinogenic amino acids structurally-relevant to the original proteinogenic amino acid. Although this method require only a cell-free translation system depleted with a specific amino acid and addition of the corresponding non-proteinogenic amino acid, the major limitation is the structural variety of non-proteinogenic amino acids are limited to the original proteinogenic amino acid-like structures. In addition, since ARS recognize tRNA species, it is hard to "reasign" a proteinogenic amino acid into codons different from the original codon. For example, assignment of cysteine at tryptophan codon (UGG), which is the key technological manipulation in the chapter 2, would be difficult with such approaches.

1.8.3 Potential of flexizymes for preparations of mis-acylated tRNAs.

Flexizymes, an artificially evolved ribozyme, which have previously developed in our laboratory[111, 112], enabled facile aminoacylation of tRNAs with non-proteinogenic amino acids (**Figure 1.8**). Several flexizymes have been developed, which catalyze aminoacylation of tRNA bearing 3' CCA end by aminoacyl substrates activated with leaving groups with different substrate selectivity for each flexizyme. The flexizyme, eFx recognize aromatic moieties in side chain of amino acid derivatives activated with cyanomethyl ester, whereas the flexizyme dFx recognize aromatic dinitrobenzyl group in the leaving group itself. Combined with other variants, virtually any amino acids can be acylated onto tRNAs.

The versatility of the flexizyme-mediated aminoacylation reaction enabled the utilization of a wide variety of non-proteinogenic amino acids, including ones with reactive moieties for post-translational chemical modification reactions. Such non-proteinogenic amino acids include D-amino acids[113-115], β-aminoacids[116], *N*-methyl/*N*-substituted amino acids[117, 118] and α-hydroxy acids[119, 120], and amino acids containing chloroacetyl group[121, 122], which is reactive with intramolecular thiol, azido-/alkyne- containing amino acids[123], and 5-hydroxy tryptophan/benzyl amine-containing amino acids[124].

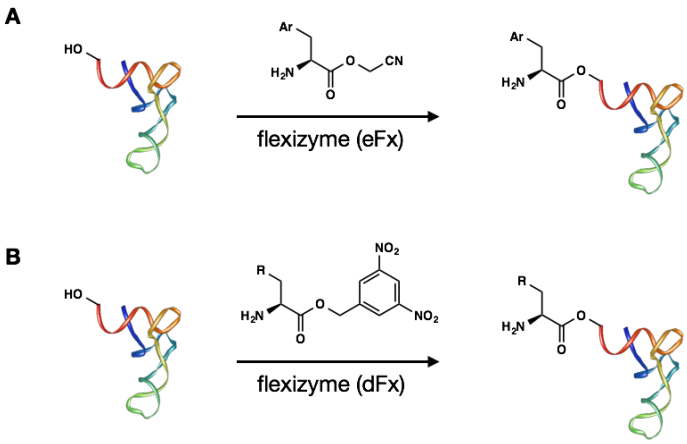

Figure 1.8 Aminoacylation of tRNAs by activated amino acids catalyzed by flexizymes.

1.8.4 Orthogonal tRNA for customized cell-free translation of non-standard peptides

Another important aspect in the customized translation system is orthogonality of tRNAs against aminoacyl tRNA synthetases since undesired aminoacylation by one of the 20 aminoacyl tRNA synthetases of liberated tRNAs originally charged with non-proteinogenic amino acids would cause contamination at the specific codon to be reprogrammed. To circumvent such undesired aminoacylation, *in vitro* transcribed $tRNA^{AsnE2}$, which was previously developed in our laboratory[119] was utilized for the flexizyme-mediated aminoacylation reactions in the present study.

Chapter 2 Development of *in vitro* synthetic method of azole-containing peptides

Parts of this chapter were published in: "Attempts at in Vitro Reconstitution of a Post-translational Dehydrogenase toward Synthesis of Azole-containing Peptides", Yasuharu Kato, Yuki Goto, Hiroaki Suga, *Peptide Science 2014*, **2015**, 137-138. and "Laser-induced oxidation of a peptide-embedded thiazoline by an assistance of adjacent thiazoline", Yasuharu Kato, Yuki Goto, Hiroaki Suga, *Peptide Science 2015,* **2016**, 27-28

Introduction

In nature, there are often found bioactive peptidic natural products with backbone azole structures and they are important structural motif of bioactive peptides[125]. Especially, consecutive azole/azoline structures are often seen in peptidic natural products as discussed in chapter 1. Since azoles in peptidic backbone would provide peptides with fascinating characteristics for peptide drug development such as peptidase resistance, structural rigidity, conjugated π electron system and cell membrane permeability, facile synthetic method of diverse azole-containing peptides would be of great use for the development of bioactive peptides including peptide drug development.

Our laboratory has previously developed an *in vitro* biosynthesis system for azoline-containing peptides by integrating the Flexible *In vitro* Translation (FIT) system[111] and a post-translational cyclodehydratase, PatD, which is involved in the biosynthesis of patellamides[88] . In the *in vitro* biosynthesis system, referred to as FIT–PatD system, Cys/Ser/Thr residues involved in translated peptides are modified by PatD to the corresponding azoline moieties, allowing one-pot synthesis of azoline-containing peptides. We have revealed an unprecedented substrate tolerance of PatD and demonstrated that this system can be applied for diverse azoline-containing peptides.

In order to devise *in vitro* synthetic method of thiazole-containing peptides, *in vitro* reconstitution of a post-translational dehydrogenase PatG, which is involved in the biosynthesis of patellamides together with the cyclodehydratase PatD was first attempted. However, all the reaction

conditions including constructs of post-translational modification enzymes, precursor peptides to be modified, and the addition of cofactors did not provide detectable oxidation activity by the dehydrogenase PatG. As a consequence, structural diversity of peptides, which can be synthesized by ribosomal peptide synthesis and subsequent modification reactions was limited to azoline moieties.

In the present study, in order to expand structural diversity, which is accessible by *in vitro* translation and subsequent post-translational modification reactions, oxidation of thiazoline moieties in peptidic backbone was attempted. Based on a serendipitous observation that one of the two consecutive thiazolines is prone to be oxidized during MALDI-TOF-MS analysis, chemical oxidation method was developed for *in vitro* synthetic method of various thiazole-containing peptides by integrating FIT–PatD system and chemical post-translational oxidation reaction. The synthetic method of thiazole-containing peptides developed here, combined with molecular evolution methods, would enable the development of novel bioactive peptides with natural product-like backbone thiazoles.

Results

Attempts at in vitro reconstitution of a post-translational dehydrogenase PatG toward synthesis of azole-containing peptides (Summary of my master's studies)

First, a model DNA template encoding a peptide containing N-terminal leader sequence and a downstream core peptide to be modified bearing the wild-type sequence was designed (**Figure 2.1A**). The model DNA template was incubated with translation mixture in 37°C for 30 min, and the resulting translation product was desalted with C18 column and directly analyzed by Matrix-assisted laser desorption/ionization time-of-flight mass spectrometry (MALDI-TOF-MS). MALDI-TOF-MS showed a sole peak corresponding to the expected precursor peptide (**Figure 2.1B**). Then, the translation product was treated with PatD at 25°C for 16 h. MALDI-TOF-MS detected a decrease in molecular mass by 72 Da, indicating the formation of two methyloxazolines (meOxH) and two thiazolines (Thz) (**Figure 2.1C**). The translation product was also incubated in the presence of both PatD and PatG, where the decrease in molecular mass by 76 Da due to cyclodehydration forming two methyloxazolines (meOxH) and two thiazolines (ThH) by PatD followed by dehydrogenation from two thiazolines (ThH) into thiazoles (Thz) by PatG. However, MALDI-TOF-MS of the modification product only gave the peak corresponding to the azoline-containing peptide (**Figure 2.1D**), indicating that the dehydrogenation by PatG did not proceed. Although we tested several reaction conditions including constructs of recombinant enzymes (*e.g.* His10-tagged, MBP-tagged, or tag-free proteins), variants of precursor peptides and addition of possible cofactors (FMN, FAD^+, NAD^+, and $NADP^+$) the formation of thiazoles (Thz) was not observed in all tested reaction conditions (data not shown). From these results it was concluded that the dehydrogenase PatG was not actively reconstituted *in vitro* in tested conditions.

In summary, post-translational azole formation has not been achieved by the dehydrogenase PatG *in vitro*. Based on these results, further studies are required for *in vitro* synthesis of various azole-containing peptides such as oxidation of peptidic azoline moieties by using PatG homologs or by chemical modification methods.

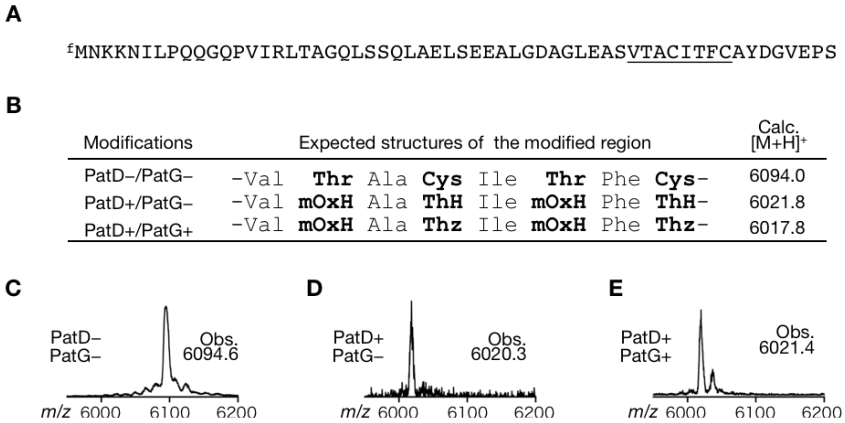

Figure 2.1 (A) Sequence of a model peptide. The region to be modified is underlined. N-terminal ^{f}M stands for *N*-formyl methionine. (B) List of expected molecular mass for each reaction condition. ThH, mOxH, and Thz indicate thiazoline, methyloxazoline and thiazole, respectively. (C-E) MALDI-TOF-MS spectra of each reaction product, (C) translation, (D) cyclodehydration by PatD and (E) modification by PatD and PatG.

Laser induced oxidation of one of two consecutive thiazolines in peptidic backbone

The chemical oxidation reaction developed here is based on the following observations. When a model template DNA coding a model peptide containing two consecutive cysteines and N-terminal truncated leader peptide (**Figure 2.2A**) was incubated in a cell free translation mixture at 37°C for 30 min, Matrix-assisted laser desorption/ionization time-of-flight mass spectrometry (MALDI-TOF-MS) detected a major peak corresponding to the designed model precursor peptide containing two consecutive cysteines (mixture of peptides with free thiols and intramolecular disulfide. **Figure 2.2B**) Then to the resulting translation product was added the cyclodehydratase PatD and further incubated at 25°C for 16 h. MALDI-TOF-MS detected a loss of 36 Da in molecular mass, suggesting that the two consecutive cysteines in the model precursor peptide were modified to consecutive thiazolines by the cyclodehydratase PatD (**Figure 2.2C**). Intriguingly, the major peak corresponding to the dehydrated peptide (*) was accompanied by a minor peak smaller in molecular mass by 2 Da (†). Such a "byproduct" was not observed in the case of other model peptides containing separate cysteines or single cysteine. Based on these results, it was hypothesized that the byproduct would be generated by oxidation of one of the thiazolines to thiazole by assistance of the other thiazoline (**Figure2.2D**).

To test this hypothesis, hydrolysis assay under acidic conditions was attempted. The experimental design is shown in **Figure 2.3A**. Thiazolines will be hydrolyzed under acidic conditions to provide original cysteine residues whereas aromatic thiazoles will not be hydrolyzed. After incubation of dehydration product by PatD with f.c. 2% of TFA at 42°C for 30 min, MALDI-TOF-MS detected a major peak corresponding to the complete hydrolysis and little acid resistant peak was observed. One possible scenario, which can rationalize these results, is that the byproduct was the peptide containing thiazole-thiazoline structure generated by oxidation during MALDI-TOF-MS measurement and thus undetectable in MALDI-TOF-MS analysis after hydrolysis in acidic conditions.

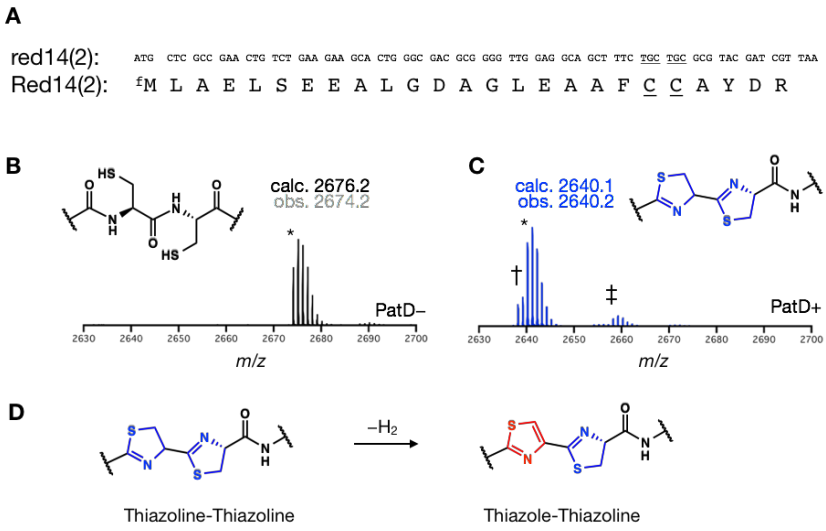

Figure 2.2 An experimental indication for laser-induced oxidation of consecutive thiazolines in peptidic backbone. (A) DNA sequence and the corresponding model peptide used in this experiment. The consecutive cysteine residues to be modified by the cyclodehydratase PatD are underlined. N-terminal ^{f}M stands for *N*-formyl methionine. (B and C) MALDI-TOF-MS spectra of reaction products, (B) translation product and (C) cyclodehydration product by PatD (D) Proposed oxidation reaction for the side peak labeled with dagger (†) in Figure 1C. Oxidation of the N-terminal thiazoline was confirmed in the following experiments.

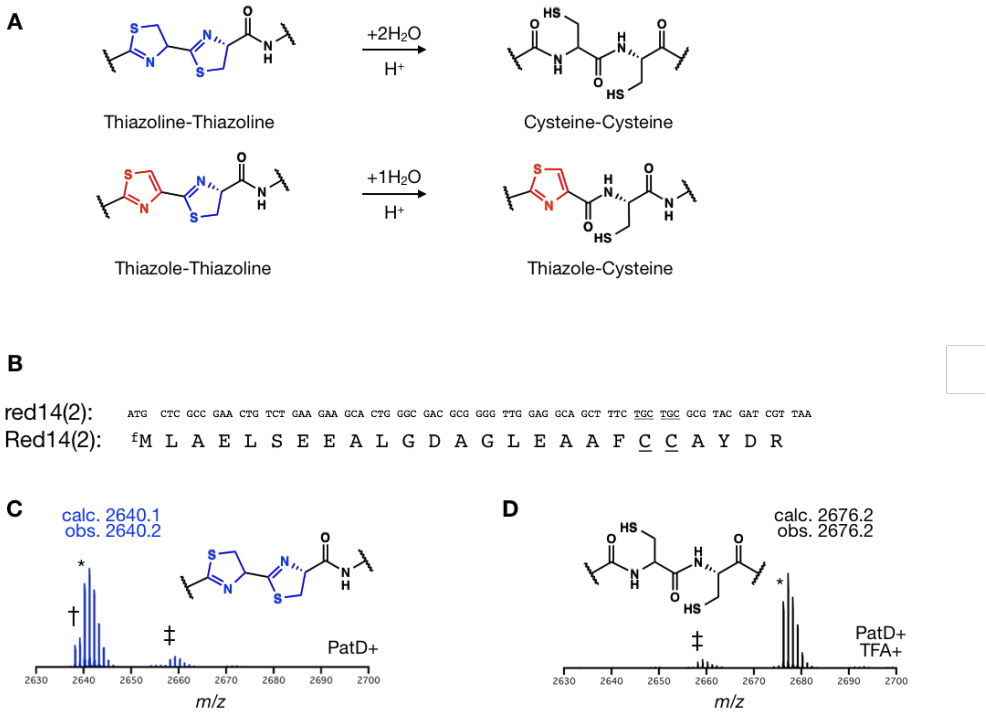

Figure 2.3 Hydrolysis assay in acidic conditions for the detection of thiazole structure. (A) Experimental design of the hydrolysis assay for the detection of thiazoles. The difference in stability in acidic conditions would provide different peak shift for oxidized and unoxidized structures, enabling detection of thiazoles. (B) DNA sequence and the corresponding model peptide used in this experiment. The consecutive cysteine residues to be modified by the cyclodehydratase PatD are underlined. N-terminal ^{f}M stands for *N*-formyl methionine. (C and D) MALDI-TOF-MS spectra of reaction products, (C) cyclodehydration product by PatD and (D) hydrolysis product in acidic conditions. In the spectra, monoisotopic peaks are labeled with asterisk (*) and peptides containing a single thiazoline are labeled with double dagger (‡). The peak corresponding to the supposed oxidation product is labeled with dagger (†)

Deuterium labeling assay by ribosomal incorporation of deuterated cysteine (d_3Cys) for the detection of thiazole formation

To investigate whether oxidation of thiazoline into thiazole was involved in the formation of the byproduct, next deuterium labeling assay was attempted by introducing deuterium labeled cysteine (cysteine-2,3,3-d_3 or d_3Cys) instead of canonical cysteine by a cell-free translation system. The introduction of deuterium labeled cysteine would enable detection of the formation of thiazole

by the loss of deuterium just by MALDI-TOF-MS analysis. After the incubation of the model template DNA with a customized cell-free translation mixture, in which canonical cysteine was substituted with d_3Cys, MALDI-TOF-MS detected a major peak corresponding to the designed model peptide containing two consecutive d_3Cys (**Figure 2.4 A and B**). And the translation mixture was further incubated in the presence of the cyclodehydratase PatD at 25°C for 16 h. MALDI-TOF-MS detected a major peak corresponding to the two consecutive thiazolines accompanied by a peak corresponding to a byproduct which was smaller in molecular mass by 4 Da, which was consistent to the loss of two deuteriums, suggesting the formation of thiazole structure at either of two consecutive cysteines during MALDI-TOF-MS analysis (**Figure 4C**).

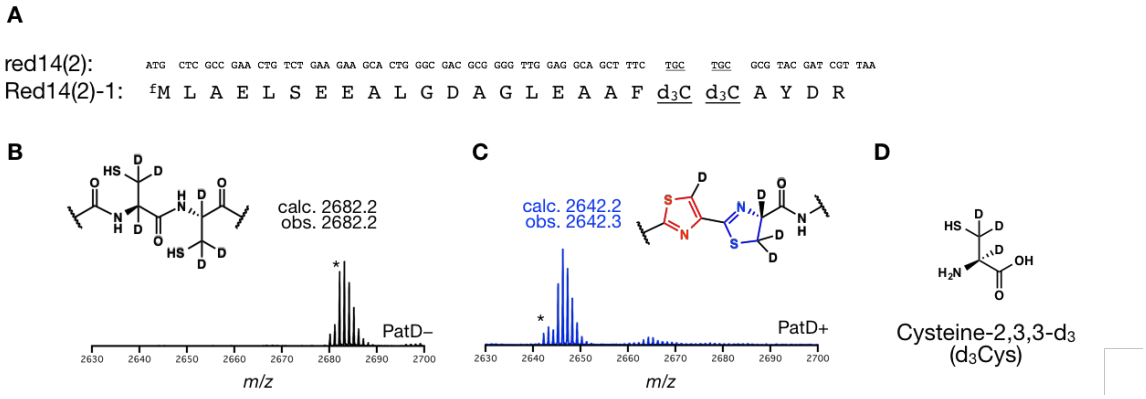

Figure 2.4 Deuterium labeling assay for the detection of thiazoles. (A) DNA sequence and the corresponding model peptide expressed in a customized cell-free translation system containing cysteine-2,3,3-d_3 (d_3Cys) instead of canonical cysteine. (B, C) MALDI-TOF-MS spectra of reaction products, (B) translation product and (C) cyclodehydration product. The monoisotopic peaks are labeled with asterisk (*). In the case of dehydration product (C), The peak labeled with asterisk is corresponding to the oxidation product, in which two deuterium were lost upon the PatD modification. The spectrum showed a major peak corresponding to the loss of one deuterium upon the cyclodehydration due to isomerization, which is discussed in the following part of the main text.

Chemical oxidation on enzymatically introduced thiazoline moieties in peptidic backbones

The proposed side oxidation at one of the two consecutive thiazolines discussed above then suggested the two consecutive thiazolines would prone to be oxidized since such a loss of hydrogen at thiazoline structure was not observed in the case of the experiment using a peptide containing single thiazoline moiety. And the application of this "oxidation-prone property" of two consecutive thiazolines would enable *in vitro* synthesis of thiazole-containing peptides. Based on this assumption, next acceleration of the oxidation reaction was attempted. After investigation of reaction conditions, hydrogen peroxide was found to efficiently convert the consecutive thiazolines to the thiazole-thiazoline structure.

For the chemical oxidation experiments, first the same template DNA to the previous experiment was incubated with a customized translation mixture. (**Figure 2.5A**) In this customized translation mixture, initiator AUG codon was suppressed with ^{Ac}Phe instead of *N*-formyl methionine to prevent possible side oxidation at thioether in the side chain of methionine. After translation reaction at 37°C for 30 min, the resulting peptide was incubated with the cyclodehydratase PatD and the MALDI-TOF-MS detected the peak shift corresponding to the formation of two consecutive thiazolines, confirming the N-terminal mutation from methionine to ^{Ac}Phe had little effect on the modification efficiency by the cyclodehydratase PatD (**Figure 2.5C and D**). Then the dehydration product by PatD was further incubated with hydrogen peroxide at 42°C for 1 h at pH 5, in the presence of f.c.100 mM of hydrogen peroxide. The peak shift corresponding to the decrease in molecular mass by 2 Da was detected and the peak corresponding to the peptide containing thiazole-thiazoline structure was observed as major peak (**Figure 2.5E**). The oxidation product was then treated with f.c. 2% of TFA for the hydrolysis of unoxidized thiazoline. MALDI-TOF-MS analysis detected an acid resistant peak as a major peak corresponding to the peptide containing a single thiazole suggesting efficient oxidation of the two consecutive thiazolines into the thiazole-thiazoline structure (**Figure 2.5F**).

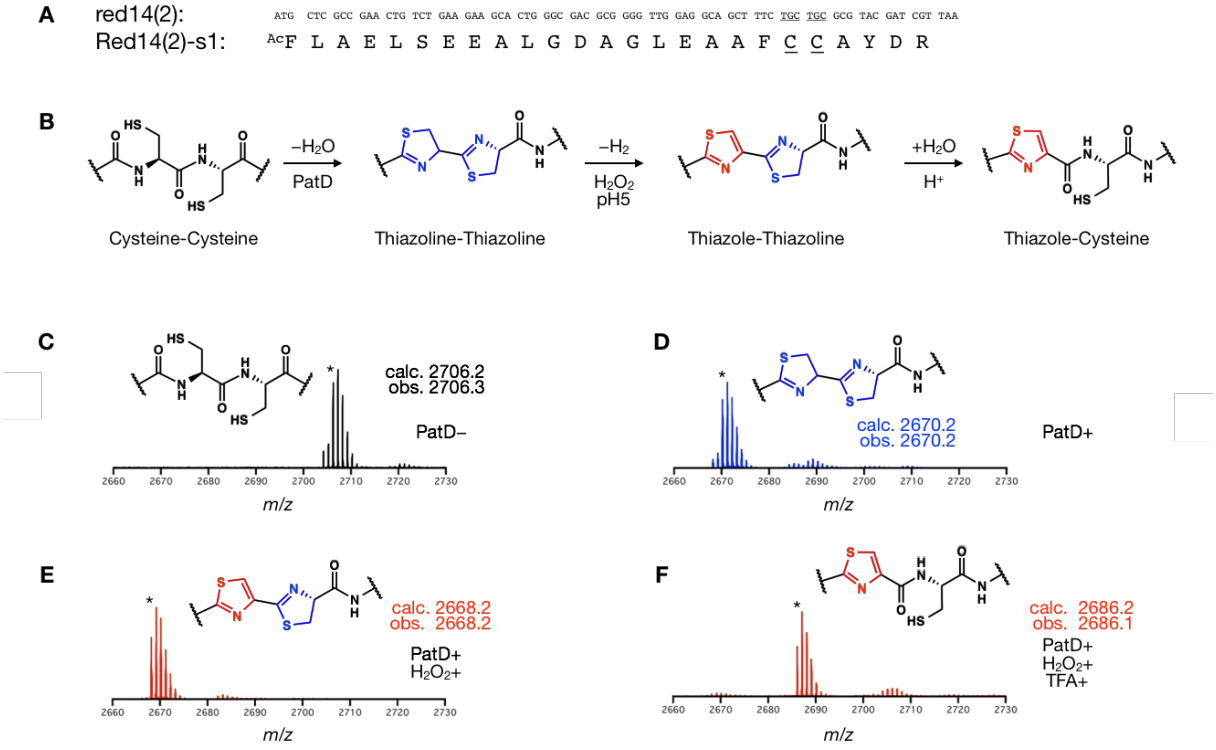

Figure 2.5 Chemical oxidation of one of two consecutive thiazolines in peptidic backbone (A) DNA sequence and the corresponding model peptide used in this experiment. The consecutive cysteine residues to be modified by the cyclodehydratase PatD are underlined. N-terminal ^{Ac}F stands for *N*-acetyl phenylalanine, which is incorporated into the model peptide instead of methionine in order to prevent side oxidation at thioether of methionine. (B) Reaction scheme of the *in vitro* synthesis of thiazole-containing peptides. After translation, cyclodehydration, and the oxidation reaction by hydrogen peroxide, the resulting peptide was treated in acidic conditions to clearly distinguish oxidized and unoxidized products as described previously. After the incubation in each condition, the resulting peptides were analyzed by MALDI-TOF-MS. (C-F) MALDI-TOF-MS spectra of reaction products, (C) translation product, (D) cyclodehydration product by PatD, (E) oxidation product by hydrogen peroxide and (F) acid-mediated-hyrolysis product. In all the spectra, monoisotopic peaks are labeled with asterisk (*).

As a control experiment, the same modification procedure was applied on the peptide containing two separated cysteines as well as N-terminal ^{Ac}Phe. A model template DNA was incubated with the customized translation mixture and further incubated with the cyclodehydratase PatD, hydrogen peroxide, and TFA. The resulting peptides of each step were analyzed by MALDI-TOF-MS analysis (**Figure 2.6**). The incubation with hydrogen peroxide did not provide a

peak shift corresponding to the formation of thiazole and hydrolysis reaction in acidic conditions gave almost complete hydrolysis yielding the peptide containing two consecutive cysteines, suggesting the importance of the two consecutive thiazoline structures for the oxidation reaction.

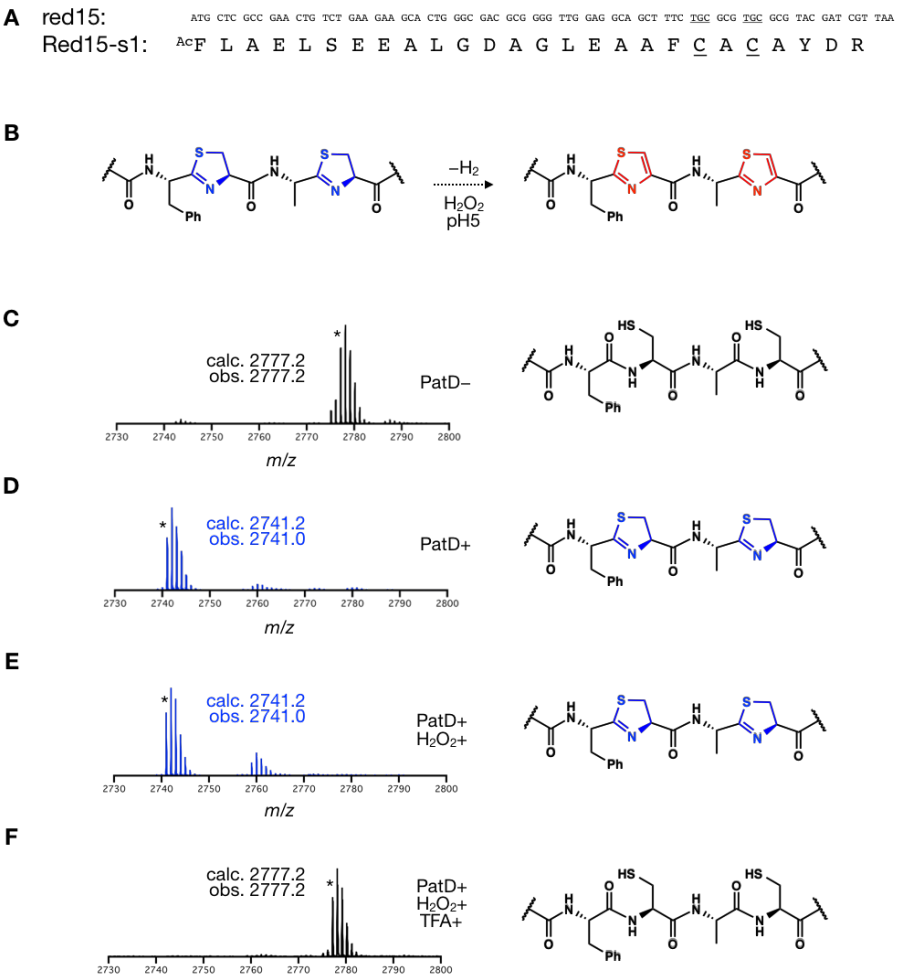

Figure 2.6 (A) DNA sequence and the corresponding model peptide used in this experiment. The consecutive cysteine residues to be modified by the cyclodehydratase PatD are underlined. N-terminal ^{Ac}F stands for *N*-acetyl phenylalanine, which is incorporated into the model peptide instead of methionine in order to prevent side oxidation at thioether of methionine. (B) Reaction scheme, which was tested in this control experiment. (C-F) MALDI-TOF-MS spectra of reaction products, (C) translation product, (D) cyclodehydration product by PatD, (D) oxidation product by hydrogen peroxide and (E) acid mediated-hydrolysis product. In all the spectra, monoisotopic peaks are labeled with asterisk (*).

Investigation of the oxidation site by site-selective labeling by deuterium

Although the oxidation of one of two consecutive thiazolines was demonstrated and oxidation at N-terminal thiazoline was hypothesized, the oxidation site remained to be confirmed. In order to identify the oxidation site, MS/MS analysis was first attempted. Although the series of fragment peaks supported the oxidation at either of thiazolines, it was hard to distinguish the oxidation site by the MS/MS analysis (See supporting results)

In order to further investigate the oxidation site, site-selective deuterium labeling assay was next attempted by means of genetic code reprograming method. If the oxidation reaction proceeded in a site selective manner, deuterium substitution at the specific hydrogen, which is involved in the oxidation reaction can offer direct evidence of the oxidation site.

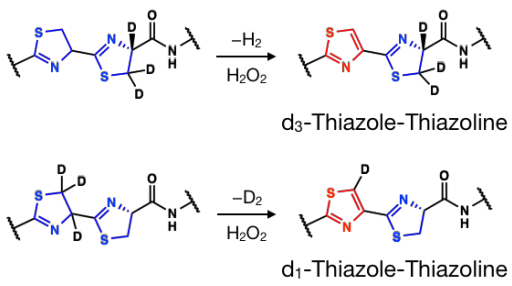

Figure 2.7 Experimental design for the detection of oxidation site by site-selective deuterium labeled substrate peptides. When hydrogens involved in the oxidation reaction are substituted by deuteriums, the loss of deuteriums would be detected by mass spectrometry.

Experimentally, site-selective deuterium labeling was introduced by means of genetic code reprogramming method (See supporting results for the detail of the incorporation of d_3Cys as well as canonical cysteine in a site selective manner). In short, in this experiment, genetic code was reprogrammed in that canonical cysteine was incorporated into peptide at TGG codon instead of Trp, whereas d_3Cys was incorporated at TGT and TGC codons instead of canonical cysteine. This reassignment of d_3Cys and Cys was achieved by the addition of d_3Cys and externally aminoacylated tRNA by means of Flexizyme, and the elimination of Cys and Trp from the cell-free translation mixture. Under the reprogrammed genetic code, d_3Cys as well as canonical Cys were site-selectively

incorporated in a template dependent manner and the peptides site-selectively labeled with deuteriums can be expressed. In addition, ^{Ac}Phe was also incorporated at N-terminus, instead of *N*-formyl methionine (^{f}Met) as in the previous experiments in order to prevent side oxidation at side chain thioether.

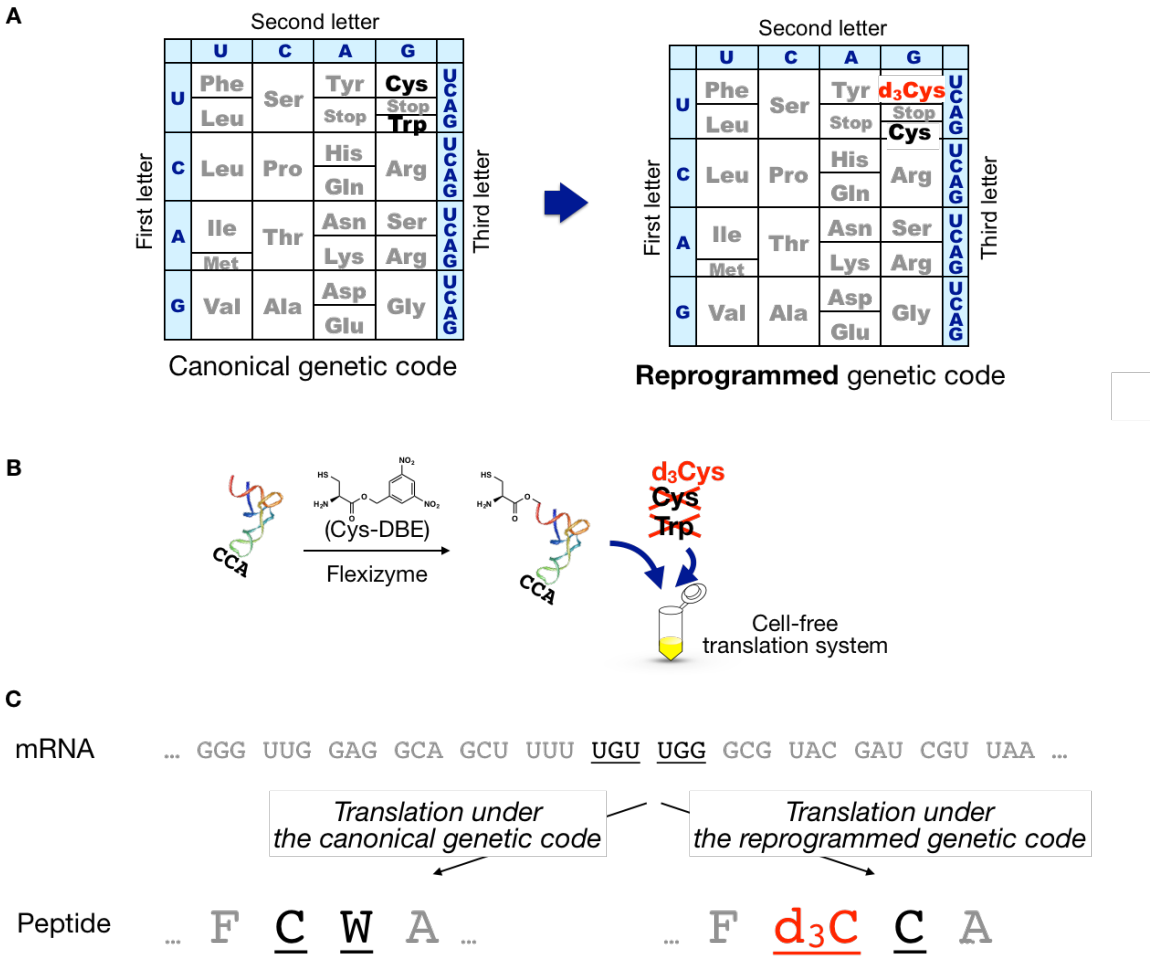

Figure 2.8 Genetic code reprogramming for site-selective incorporation of d_3Cys and canonical cysteine. (A) Schematic illustration of reprogrammed genetic code. Genetic code was reprogrammed by substitutions of Cys and Trp to d_3Cys and Cys, respectively. (B) Schematic illustration of genetic code reprogramming. tRNA was aminoacylated externally by means of flexizyme with canonical cysteine and added into translation mixture together with d_3Cys. And instead, Trp and canonical Cys were removed from the translation mixture. (C) Schematic illustration of translation of a model mRNA by canonical genetic code and the reprogrammed genetic code. In the reprogrammed genetic code, d_3Cys and Cys are site-selectively incorporated in a template dependent manner.

When a model DNA template containing 5'-TGGTGT- 3' sequence, which originally encode -TrpCys- was incubated in the customized translation mixture, MALDI-TOF-MS detected the major peak corresponding to the designed peptide containing Cys-d_3Cys sequence as well as N-terminal ^{Ac}Phe (**Figure 2.9A and B**). The site selective incorporation was confirmed by MS/MS analysis. (See supporting results). After the cyclodehydrtion by PatD, the resulting dehydration product was incubated with hydrogen peroxide. MALDI-TOF-MS of the products before and after the oxidation reaction detected a peak shift corresponding to the decrease in molecular mass by 2 Da (**Figure 2.9C and D**), suggesting the deuterium at C-terminal thiazoline did not participate in the oxidation event. In addition, the resulting oxidation product was hydrolyzed in acidic conditions. MALDI-TOF-MS detected a major peak corresponding to the peptide containing a single thiazole and three deuteriums (**Figure 2.9E**), which was consistent with the "N-terminal oxidation" (**Figure 2.9F**)

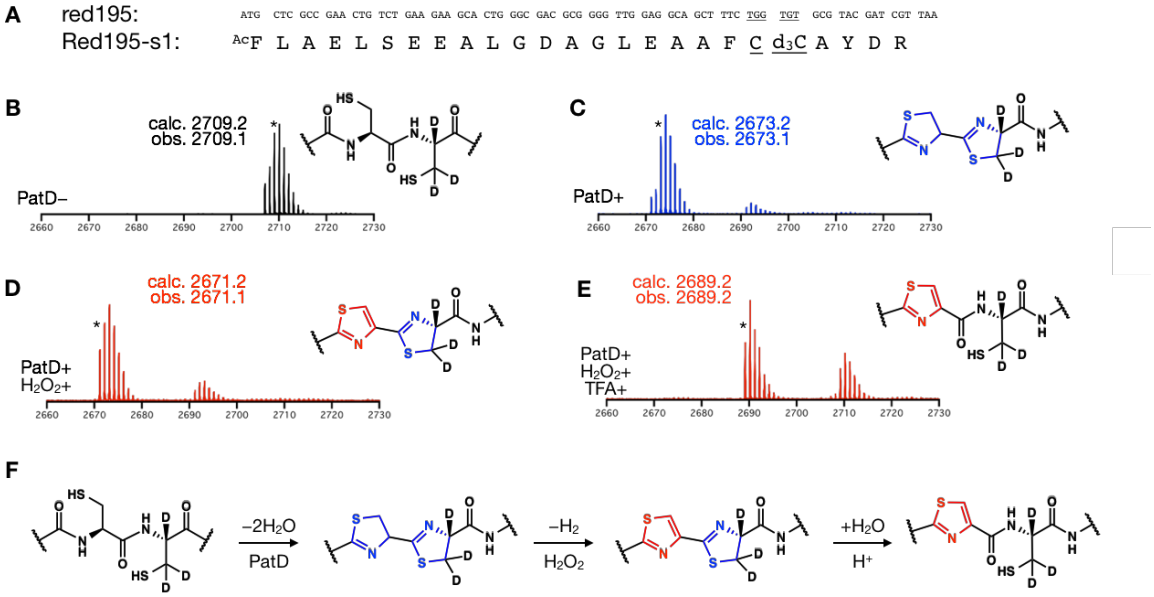

Figure 2.9 Deuterium labeling assay with a model peptide containing C-terminal deuterium labeling (Cys-d_3Cys). (A) DNA sequence and the corresponding model peptide used in this experiment. The consecutive cysteine residues to be modified by the cyclodehydratase PatD are underlined. N-terminal ^{Ac}F stands for *N*-acetyl phenylalanine, which is incorporated into the model peptide instead of methionine in order to prevent side oxidation at thioether of methionine. (B-E) MALDI-TOF-MS spectra of reaction products, (B) translation product, (C) cyclodehydration product by PatD, (D) oxidation product by hydrogen peroxide and (E) acid-mediated hydrolysis product. (F) Summary of the oxidation reaction with the C-terminally deuterium labeled substrate peptide based on the MALDI-TOF-MS spectra.

On the other hand, a model DNA template with swapped sequence, 5'-TGTTGG- 3', expressed the peptide containing d_3Cys-Cys sequence (**Figure 2.10A and B**) Oxidation by hydrogen peroxide after the cyclodehydration by PatD, provided a peak shift corresponding to the loss of two deuteriums (**Figure 2.10 C-E**), confirming the site-selective oxidation at N-terminal thiazoline (**Figure 2.10F)**. In addition, the loss of one deuterium after the cyclodehydration by PatD was also observed by MALDI-TOF-MS suggesting the isomer, which is discussed in the following part.

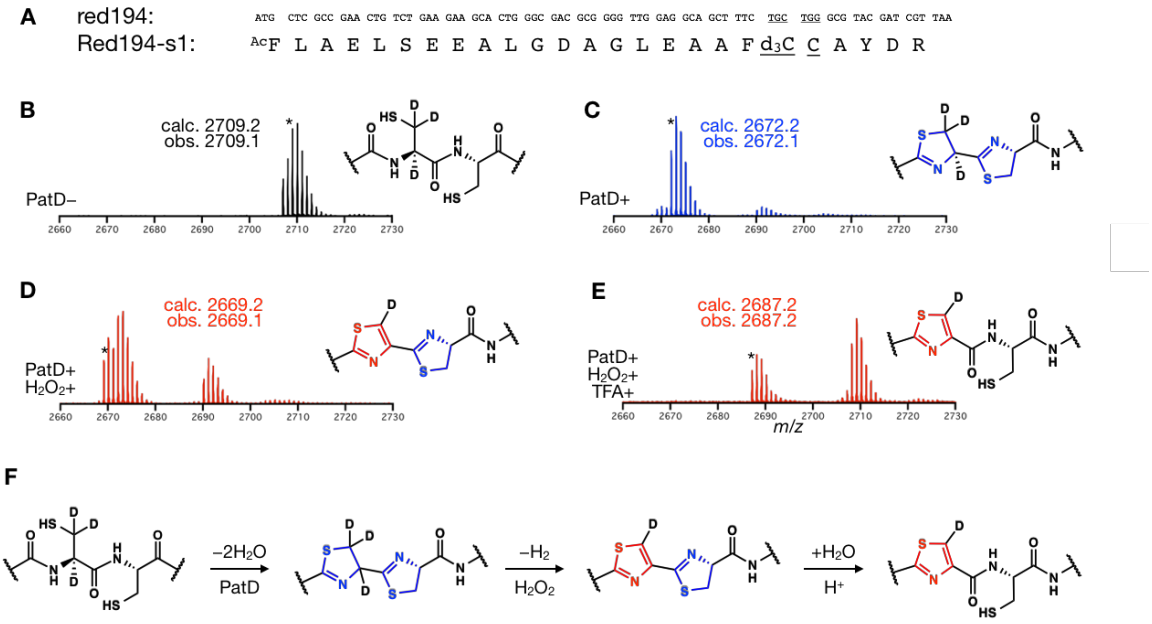

Figure 2.10 Deuterium labeling assay with a model peptide containing N-terminal deuterium labeling (Cys-d_3Cys). (A) DNA sequence and the corresponding model peptide used in this experiment. The consecutive cysteine residues to be modified by the cyclodehydratase PatD are underlined. N-terminal ^{Ac}F stands for *N*-acetyl phenylalanine, which is incorporated into the model peptide instead of methionine in order to prevent side oxidation at thioether of methionine. (B-E) MALDI-TOF-MS spectra of reaction products, (B) translation product, (C) cyclodehydration product by PatD, (D) oxidation product by hydrogen peroxide and (E) acid-mediated hydrolysis product. (F) Summary of the oxidation reaction with the N-terminally deuterium labeled substrate peptide based on the MALDI-TOF-MS spectra.

Substrate scope of the oxidation reaction for the in vitro synthesis of thiazole-containing peptides

In order to investigate substrate scope of the oxidation method for the synthesis of thiazole-containing peptides, model peptides were designed, where all proteinogenic amino acids except for Cys, Ser, or Thr were placed at the position N-terminally adjacent to the two consecutive cysteines (in other words Phe (F) in the model peptide in the previous experiments was mutated into 17 kinds of proteinogenic amino acids, **Figure 2.11A**). Using these model peptides, the oxidation reaction was performed (**Figure 2.11B**).

After translation at 37°C for 30 min and a subsequent cyclodehydration at 25°C for 16 h, MALDI-TOF-MS detected major peaks corresponding to the desired peptides containing two consecutive thiazolines in the cases of Ala (A), Tyr (Y), Leu (L), Ile (I) and Met (M) (**Figure 2.11C**). Inefficient cyclodehydration was observed with other 12 amino acids (data not shown) and model peptides with these amino acids were not tested in the following modifications. The resulting cyclodehydration products containing two consecutive thiazolines were incubated with hydrogen peroxide and subsequently hydrolyzed by TFA (**Figure 2.11C**). In all tested cases, acid resistant peaks were observed after acid-mediated hydrolysis, demonstrating wide substrate scope of this oxidation method. (Note that in the case of methionine, oxidation proceeded at side chain thioether judged by MALDI-TOF-MS spectra showing increase of molecular mass by 16 Da upon the oxidation.)

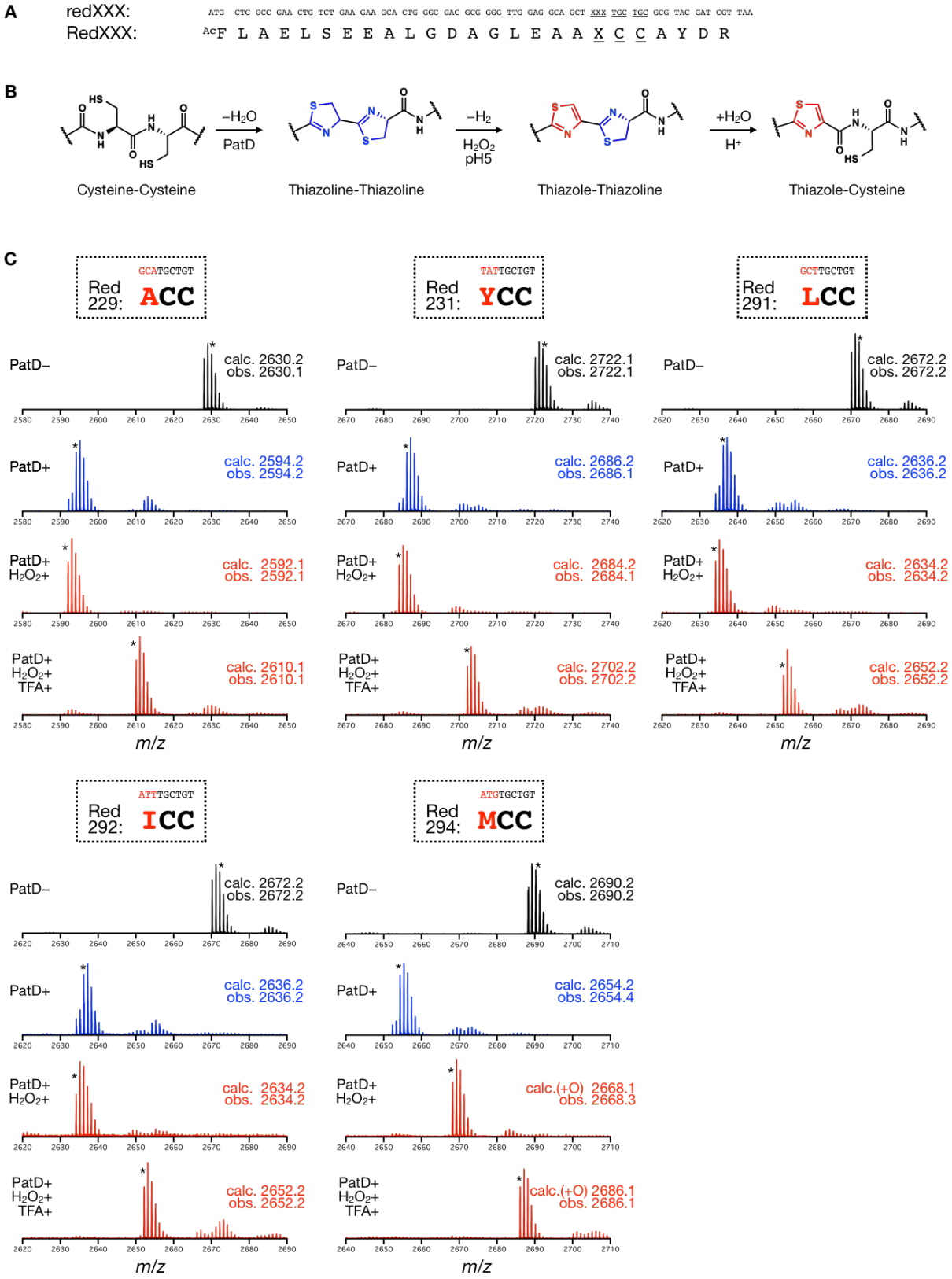

Figure 2.11 Investigation of substrate scope of the oxidation reaction for the *in vitro* synthesis of thiazole-containing peptides. (**Continued**)

Figure 2.11 (**Continued**) (A) DNA sequence and the corresponding model peptide used in this experiment. The consecutive cysteine residues to be modified by the cyclodehydratase PatD as well as the mutated residue are underlined. N-terminal ^{Ac}F stands for *N*-acetyl phenylalanine, which is incorporated into the model peptide instead of methionine in order to prevent side oxidation at thioether of methionine. (B) Reaction scheme of the oxidation reaction. (C) MALDI-TOF-MS spectra of reaction products, translation products, cyclodehydration products, oxidation products and hydrolysis products. The monoisotopic peaks are labeled with asterisk (*). In translation products, peaks corresponding to the peptides with free thiols are labeled. In the case of methionine, labeled peaks in the oxidation product and hydrolysis product are corresponding to the peptide with thiazole-thiazoline and thiazole-cysteine, respectively, with sulfoxide at side chain of methionine.

Oxidation of three consecutive thiazolines

Multiple consecutive azoles are sometimes found in peptidic natural products as exemplified by telomestatin and plantazolicin (**Figure 1.1 and 1.3**). These natural products prompted the synthesis of multiple consecutive thiazoles by the oxidation method developed here. For this purpose, model peptide containing three consecutive cysteines was designed (**Figure 2.12A**) and by using this model peptide, the oxidation reaction was performed. MALDI-TOF-MS detected peaks corresponding to the desired products (**Figure 2.12B-E**) Especially, upon the oxidation by hydrogen peroxide, peak shift corresponding to the loss of four hydrogen atoms was observed (**Figure 2.12C and D**), and after TFA-mediated hydrolysis, acid resistant peak was observed (**Figure 2.12 E**) suggesting the formation of two thiazoles in peptidic backbone. In addition, by using site-specific deuterium labeling by means of genetic code reprogramming as mentioned above, thiazole-thiazole-thiazoline structure was confirmed. These results demonstrated the synthesis of natural product-like two consecutive thiazolines in peptidic backbone.

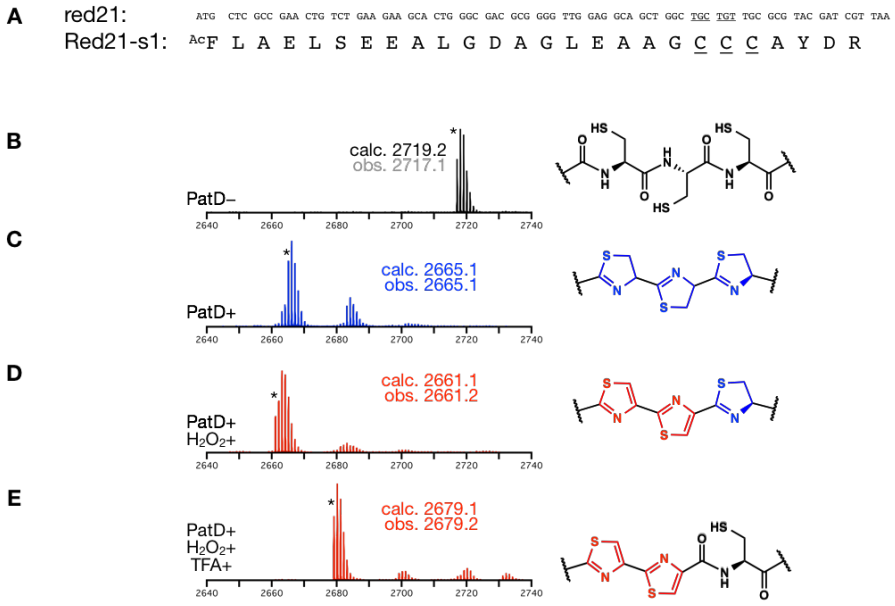

Figure 2.12 The synthesis of thiazole-thiazole-thiazoline structure by the oxidation method. (A) DNA sequence and the corresponding model peptide used in this experiment. The consecutive cysteine residues to be modified by the cyclodehydratase PatD are underlined. N-terminal ^{Ac}F stands for *N*-acetyl phenylalanine, which is incorporated into the model peptide instead of methionine in order to prevent side oxidation at thioether of methionine. (B-E) MALDI-TOF-MS spectra of reaction products, (B) translation product, (C) cyclodehydration product by PatD, (D) oxidation product and (E) hydrolysis product. The monoisotopic peaks are labeled with asterisk (*). In translation product (B), the peak corresponding to the peptide containing intramolecular disulfide is labeled.

Discussion

Proposed mechanism of the oxidation reaction

Based on the results in the site-selective deuterium labeling assay, proposed mechanism for the oxidation reaction is shown in **Figure 2.13**. After translation of a peptide containing two consecutive cysteines and subsequent cyclodehydration by PatD, the resulting two consecutive thiazolines in peptidic backbone are isomerized (tautomerized) into the structure 3, and the N-terminal heterocycle in the structure 3 was selectively oxidized by hydrogen peroxide to provide thiazole-thiazoline structure 4. The proposed mechanism can rationalize the importance of the assistance by C-terminal thiazoline for the oxidation of N-terminal thiazoline.

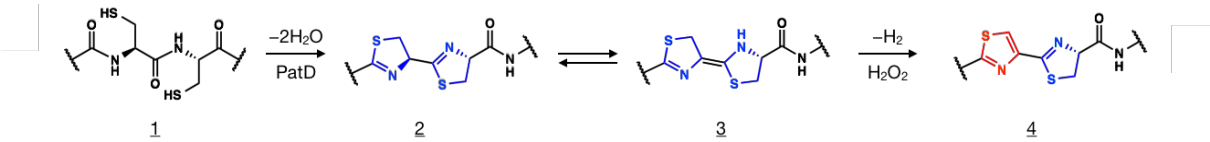

Figure 2.13 Proposed mechanism for the oxidation reaction.

Conjugated π electron system of thiazole-thiazoline structure

For acid-mediated hydrolysis of the thiazole-thiazoline structure, in the oxidation product by hydrogen peroxide, relatively harsh conditions were required compared to hydrolysis of the two consecutive thiazolines structure (See supporting results). These results suggested that the thiazole and thiazoline are forming conjugated π electron system in peptidic backbone and it was a first indication of oxidation at N-terminal thiazoline since oxidation at C-terminal thiazoline would not provide stabilized thiazoline structure. Such a planer conjugated π electron system would be hard to incorporate into peptidic backbone just by the polymerization of proteinogenic/non-proteinogenic amino acids. It suggests the utility of the cyclodehydration-oxidation method for the development of novel bioactive peptides by exploring new chemical space, which was previously almost inaccessible by the conventional peptide library construction methods.

Reports on spontaneous oxidation of two consecutive thiazolines in natural products

The oxidation reaction developed in the present study was originated from the oxidation-prone property of the two consecutive thiazolines. There are actually several reports on the oxidation of two consecutive thiazolines (**Figure 2.14**). S. Carmeli *et. al.* reported the isolation and structural determination of Mirabazoles[126] and Tantazoles[127]. In these reports, they argued that thiazoline adjacent to another thiazoline in Mirabazole A and Tantazole A underwent oxidation during isolation and purification, to form thiazole-containing analogs, Didehydromirabazole A and Didehydrotantazole A. They suggested these oxidized products would be artifacts since they isolated only unoxidized Tantazole A by faster workup and storage of all chromatographic fractions under argon at −196°C, and also they detected only unoxidized Mirabazole A by "careful" HPLC analysis of crude algal extract. Though in these reports C-terminal thiazolines to help the oxidation are α-methyl thiazolines, oxidation would take place by the similar mechanism to the oxidation reaction proposed in the present study.

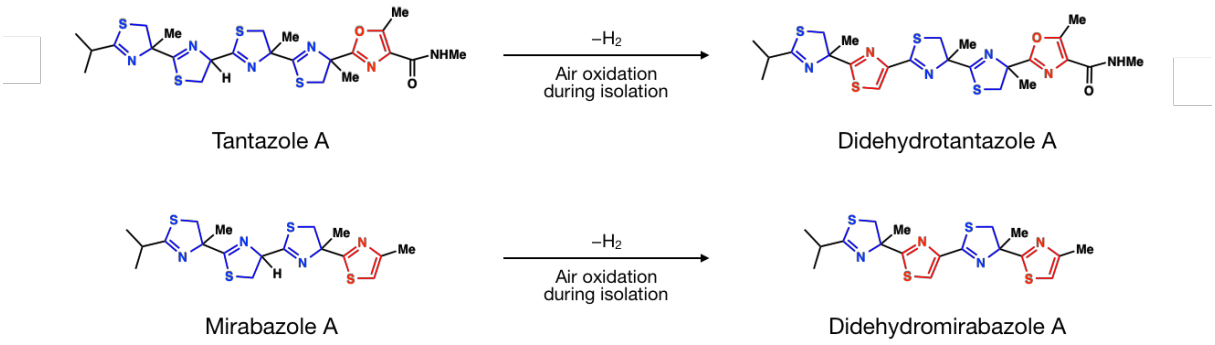

Figure 2.14 Reported spontaneous oxidation reaction of two consecutive thiazolines in peptidicc natural products, Mirabazole A and Tantazole A.

Spontaneous oxidation of consecutive thiazolines in organic synthesis

There are multiple methods for organic synthesis of thiazoline moieties. [128] In some of the method, the synthesis of consecutive thiazolines was attempted. In all the cases, however, the attempts resulted in the isolation of oxidized thiazole-thiazoline structure as major product instead of two consecutive thiazolines[129-132]. To the best of my knowledge, only one literature is available, which reported intermediate of the oxidation reaction (**Figure 2.15**). In the literature, after the attempt at second thiazoline ring formation for construction of the consecutive thiazolines, the authors observed structure (7), which is an oxidized structure of an isomer (6) derived from the desired consecutive thiazolines (5), as a minor product and the thiazole-thiazoline (8) structure as a major product. The yield of consecutive heterocycles was 57% without any optimization. It would be possible that the similar mechanism of the oxidation on sulfur atom at N-terminal thiazoline as described in the literature, proceeded in the oxidation reaction developed in the present studies. The absence of the intermediate sulfoxide would be rationalized by rapid conversion after the oxidation at sulfer atom in the aqueous solvent or during MALDI-TOF-MS analysis, since the conversion of the compound (7) into compound (8) during chromatography isolation was reported in the literature.

These reports are consistent with the observations in the present study but it would be still worth noting that, to the best of my knowledge, the structure before oxidation (two consecutive thiazolines or its isomer) and direct evidence of isomerization/tautomerization of the two consecutive thiazolines were first detected in the present study. In addition, requirement of chemical oxidation was demonstrated in order to detect the oxidized product containing thiazole-thiazoline moiety as a major peak by MALDI-TOF-MS analysis.

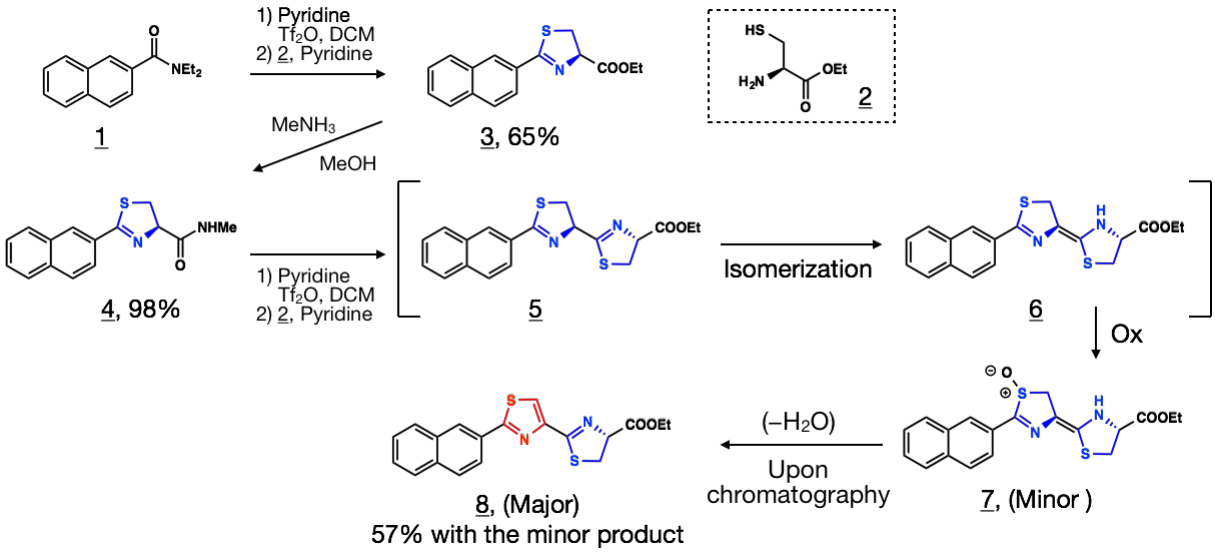

Figure 2.15 A reported oxidation of two consecutive thiazolines. An attempt to apply a thiazoline forming reaction to yield two consecutive thiazolines resulted in the formation of thiazole-thiazoline structure.[129]

Oxidation of azolines in peptidic backbone in biosynthesis of natural products

There are many peptidic natural products with fused heterocyclic structures and for the biosynthetic pathways for the peptidic natural products, both NRPS and RiPPs pathway are involved. In both the biosynthetic pathways, enzymatic oxidation is assumed, however, it might be possible that the isolated structures are air-oxidized product and original natural products have non-oxidized structures as the observations by S. Carmeli *et. al.* as mentioned above. And it might be also possible that assistance for the oxidation of an azoline by an adjacent heterocycle plays an important role for oxidation of heterocycles in peptidic natural product biosynthesis. Along with this context, capability of oxazolines to be oxidized and to exhibit assistance for the oxidation on an adjacent azolines would be of interest. Since the preparation of fused oxazolines, which is one of the required precursor structures for the investigation of the chemical properties of oxazolines, by chemical approach would be difficult as exemplified by a report, in which synthesis of fused oxazolines was attempted but resulted in the formation of dehydroalanine (**Figure 2.16**), enzymatic approach would enable the synthesis of fused oxazolines structure. These investigations would provide new insights into understanding of biosynthetic pathways of azole-containing peptides.

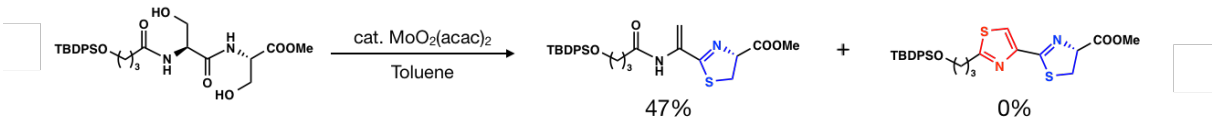

Figure 2.16 A report on an attempt at synthesis of consecutive oxazolines and an undesired dehydration to form dehydroalanine residue instead of consecutive oxazoilines.

Significance of site-selective deuterium labeling method by means of genetic code reprogramming

Recently, biosynthesis of peptidic natural products by RiPPs pathway is getting more and more interest as the subject of biology and biotechnology. Post-translational modification enzymes involved in RiPPs pathway often modify multiple residues in substrate peptides and this promiscuity is the reason, which makes these enzymes of great interest, but this promiscuous characteristics sometimes make it difficult to analyze enzymatic modification reactions since the substrate peptides are relatively large to be analyzed by conventional structural analysis methods without any labeling. To overcome these problems, recently deuterium labeling strategy has been often employed. In these reports, authors prepared deuterium-labeled substrate peptides by using solid-phase peptide synthesis (SPPS). Although SPPS can achieve desired site-selective labeling of peptides with deuterium, it has several disadvantages that Fmoc-protected deuterium labeled amino acids are relatively expensive compared to non-protected analogs and all the substrate peptides must be synthesized and purified every peptides of interest. Another strategy to prepare deuterium labeled peptides is overexpression of recombinant protein (peptides) by *E. coli*. Although this method does not require Fmoc-protected deuterium labeled amino acids, this method cannot label the peptides with deuterium in a site selective manner. To the contrary, in the present study, site-selective deuterium labeling method of substrate peptides was developed. By means of genetic code reprogramming, deuterated cysteine (d_3Cys) as well as canonical cysteine were incorporated into several peptides. This method enabled site-selective deuterium labeling by using relatively inexpensive, non-protected deuterated amino acids. This method can offer facile method for the

preparation of mutant substrate peptides containing designated position for deuterium labeling, which would be of great use for the mutagenesis study of many post-translational modification enzymes in the future studies.

Isotopic effect in oxidation of deuterated thiazoline

In the present study, site-selective deuterium labeling was employed to determine hydrogen, which is involved in the oxidation reaction. Thus, slower reaction, or isotopic effect was expected. The reaction rate can be qualitatively compared by comparing the peak intensity ratio in MALDI-TOF-MS spectra after the acid-mediated hydrolysis between the peaks corresponding to the "partial hydrolysis" and "complete hydrolysis" (**Figure 2.17**). Deuterium labeling at C-terminal thiazoline made the oxidation slower. Since deuteriums at C-terminal cysteine should not directly involved in the oxidation reaction, this slower oxidation should be attributed to higher concentration of deuterated cysteine (d_3Cys) which is added into cell-free translation mixture to prevent cross incorporation of deuterated cysteine and canonical cysteine (See supplemental results for the detail). On the other hand, much slower oxidation was indicated by N-terminal deuterium labeling in the presence of the same concentration of deuterated cysteine. These results were consistent with the expected isotopic effect.

Reaction scheme	MALDI-TOF-MS spectra	Yield	Reaction conditions
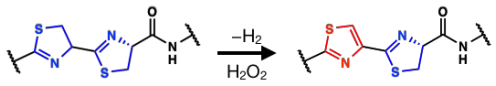	Figure 2.5	+++	• ca. 0.25 mM Cys
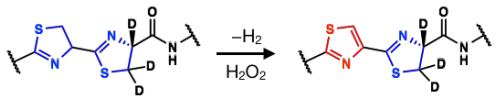	Figure 2.9	++	• ca. 2.5 mM d_3Cys
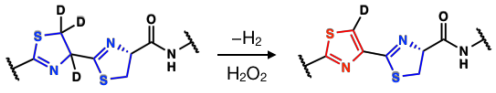	Figure 2.10	+	• ca. 2.5 mM d_3Cys • Isotopic effect

Figure 2.17 The effect of the amount of free (deuterated) cysteine in the reaction mixture and deuterium labeling against the yield of the oxidation product. For each reaction scheme, the corresponding MALDI-TOF-MS spectra, the yield of the oxidation product and the reaction conditions are listed. The yields are evaluated qualitatively by the ratio between corresponding to the "complete hydrolysis" and "the partial hydrolysis" in MALDI-TOF-MS spectra shown in the listed figures.

Compatibility of chemical oxidation of thiazoline by hydrogen peroxide with molecular evolution methods such as mRNA display method.

Previously, a hydrogen peroxide-mediated peptide modification reaction was reported installing dehydroalanine residue from a non-proteinogenic amino acid, selenolysine, which can be ribosomally incorporated into peptides.[133] The modification method led to *in vitro* selection of functional lanthionine peptides, which is characterized by a macrocyclic structure closed by thioether bond derived from michael addition of Cys to dehydroalanine residue. [134] In the *in vitro* selection, lanthionine peptide library was constructed by using the macrocyclization strategy and isolated active lanthionine peptides, demonstrating the compatibility of hydrogen peroxide with mRNA display method. Thus, the combination of molecular evolution methods such as mRNA display method and the oxidation method for the synthesis of thiazole-containing peptides described in this chapter would enable the construction of peptide libraries with unique structural scaffold and lead to the development of novel bioactive peptides.

Conclusion

In the present study, *in vitro* synthetic method of thiazole-containing peptides was developed by integrating a cell-free translation system, a post-translational cyclodehydratase PatD, and chemical oxidation reaction by hydrogen peroxide. The oxidation protocol was originated from a serendipitous observation that one of the two consecutive thiazolines was oxidized during MALDI-TOF-MS analysis suggesting oxidation-prone character of the two consecutive thiazolines and hydrogen peroxide was found to efficiently oxidize the two consecutive thiazollines into conjugated thiazole-thiazoline structure in peptidic backbone.

In order to investigate the site selectivity of the oxidation reaction, in this study, a deuterium labeling method of substrate peptides was developed by means of flexizyme-mediated genetic code reprogramming method. This deuterium labeling method enabled the synthesis of precursor peptides site-selectively labeled with deuteriums. The major advantages of this method are the use of non-protected deuterated amino acids instead of Fmoc-protected ones unlike SPPS, and site selective introduction of deuteriums unlike recombinant peptide/protein synthesis. The site selective labeling method would be advantageous in monitoring post-translational enzymatic reactions. By using the labeling method, it was revealed that the oxidation proceeded at upstream thiazoline by assistance from C-terminally adjacent thiazoline.

Moreover, the oxidation method was successfully applied to the synthesis of various peptides with backbone thiazole-thiazoline structure and thiazole-thiazole-thiazoline structure demonstrating versatility of the oxidation method. The *in vitro* synthetic method of thiazole-containing peptides, combined with molecular evolution methods, would make it possible to construct peptide libraries with natural product-like backbone aromatic rings, which would be advantageous for the peptide drug development.

Supplemental results

Genetic code reprogramming for the site-selective incorporation of deuterated cysteine (d_3Cys) and canonical cysteine into a single peptide

In the present study, genetic code reprograming method was applied for site-selective incorporation of deuterium-labeled cysteine (d_3Cys) as well as canonical cysteine. In order to achieve customized ribosomal synthesis of site-selectively labeled peptides under the reprogrammed genetic code shown in **Figure S2.1A**, externally aminoacylated Cys-tRNA$^{AsnE2}_{CCA}$ and d_3Cys were added into cell-free translation mixture, and instead canonical Cys and Trp were removed from the cell-free translation mixture. In detail, concentration of each component was adjusted based on the following considerations. For the introduction of "biologically indistinguishable" amino acids such as deuterated cysteine (d_3Cys) and canonical cysteine by means of genetic code reprogramming, cross contamination should be suppressed as much as possible. Potential cause of such cross contamination is hydrolysis of externally aminoacylated Cys-tRNA in the translation mixture before or during translation reaction. In the customized translation system, d_3Cys is aminoacylated on Cys-tRNA, which will decode cysteine codon (UGU and UGC), but this reaction would be in competition with the same reaction with canonical cysteine, which is potencially derived from hydrolysis of pre-acylated Cys-tRNA$^{AsnE2}_{CCA}$. In order to suppress the undesired competitive translation, concentrations of each component were adjusted as 10 mM for d_3Cys and at most 50 μM for Cys-tRNA$^{AsnE2}_{CCA}$. Since Cys, potencial cause of the cross contamination would be 50 μM at most (In this estimation, aminoacylation reaction by flexizyme in quantitative yield, purification of Cys-tRNA in quantitative yield by ethanol precipitation, and undesired hydrolysis in quantitative yield are assumed.), whereas d_3Cys was added at 10 mM, 200 times higher concentration than canonical Cys, providing higher chance to yield site-selectively labeled peptides.

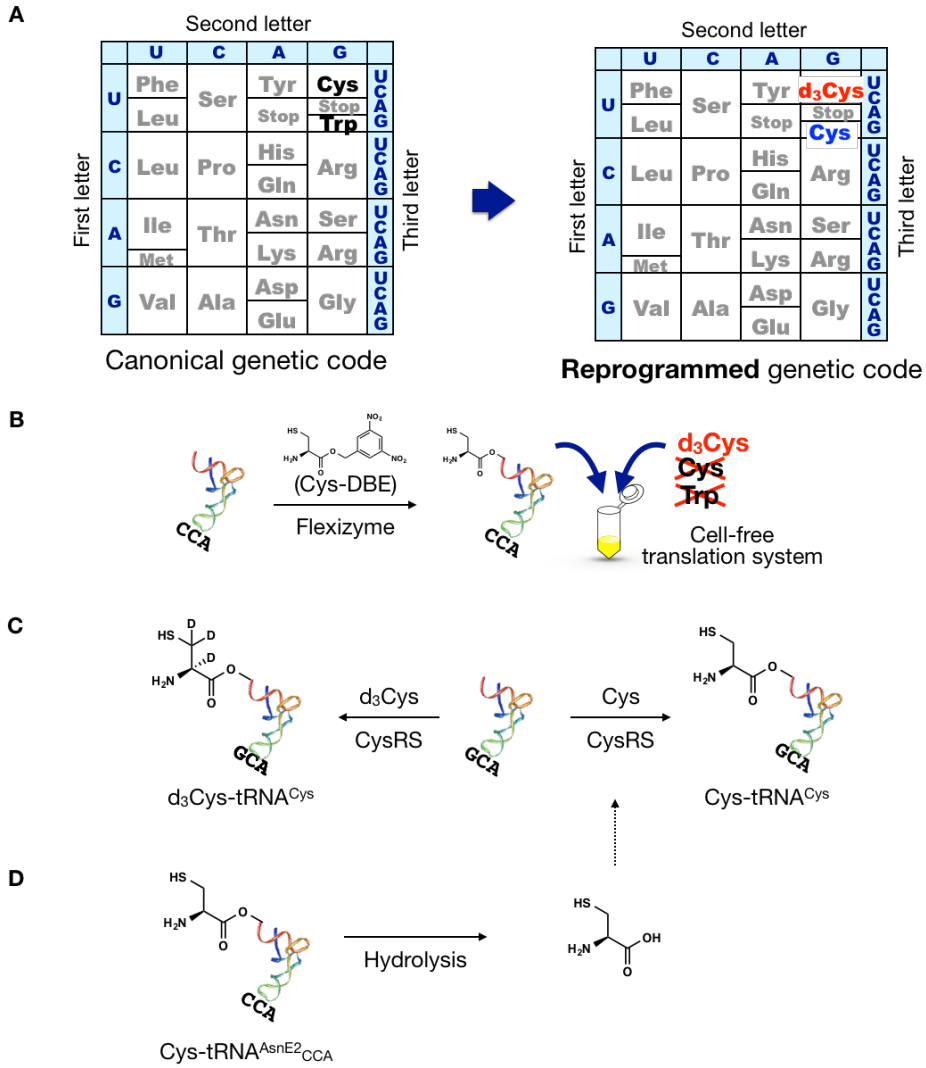

Figure S2.1 Genetic code reprogramming for site-selective incorporation of d_3Cys and canonical cysteine. (A) Schematic illustration of reprogrammed genetic code. Genetic code was reprogrammed by substitutions of Cys and Trp to d_3Cys and Cys, respectively. (B) Schematic illustration of genetic code reprogramming. $tRNA^{AsnE2}_{CCA}$ was aminoacylated externally by means of flexizyme with canonical cysteine and added into translation mixture together with d_3Cys. And instead, Trp and canonical Cys were removed from the translation mixture. Concentrations of each component were set based on the considerations discussed in the text. (C) Desired aminoacylation of $tRNA^{Cys}$ by d_3Cys catalyzed by cysteinyl tRNA synthetase (CysRS) in cell-free translation system and undesired aminoacylation of the $tRNA^{Cys}$ by canonical cysteine, which is potentially liberated from Cys-$tRNA^{AsnE2}_{CCA}$ by hydrolysis (D).

Then, two model peptides containing d_3Cys and Cys (discussed in the main text) were analyzed by MALDI-TOF-MS analysis after reduction of the translation products by DTT to reduce intramolecular disulfide bond formation (**Figure S2.2**). In each case, MALDI-TOF-MS detected major peak corresponding to the model peptide containing a single d_3Cys and canonical Cys as well as almost completed reduction of the intramolecular disulfide bond by 0.5 M DTT.

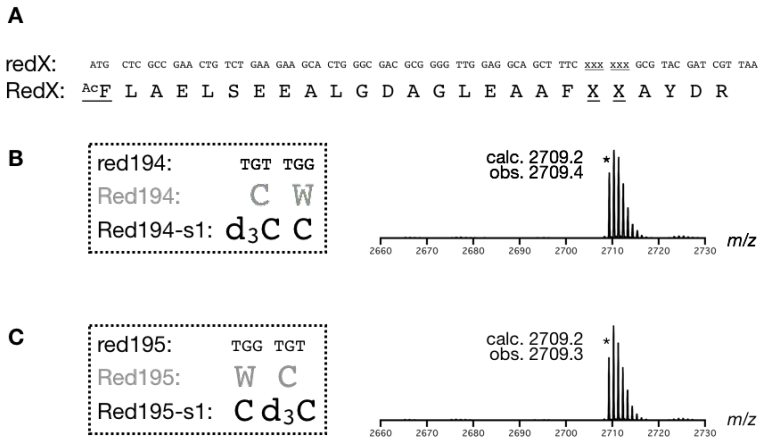

Figure S2.2 Site-specific incorporation of deuterated cysteine (d_3Cys) and canonical Cys. (A) General sequence of model DNA encoding model peptides. ^{Ac}F stands for *N*-acetyl phenylalanine incorporated instead of methionine in order to prevent side oxidation at side chain thioether. (B) MALDI-TOF-MS spectra of the translation product under the reprogramed genetic code after the incubation with DTT. Sequences of model DNA, original peptide sequence, and peptide sequence supposed to be expressed under the reprogrammed genetic code shown in **Figure S2.1** are also shown.

And the resulting peptide was further analyzed by MS/MS (**Figure S2.3**). Series of fragment peaks corresponded to the designated site-selective incorporation of d_3Cys and canonical Cys without any detectable fragment peaks corresponding to the cross contamination product confirming the construction of the customized translation system under the reprogramed genetic code, which assign deuterated Cys (d_3Cys) and Cys in a site-specific manner.

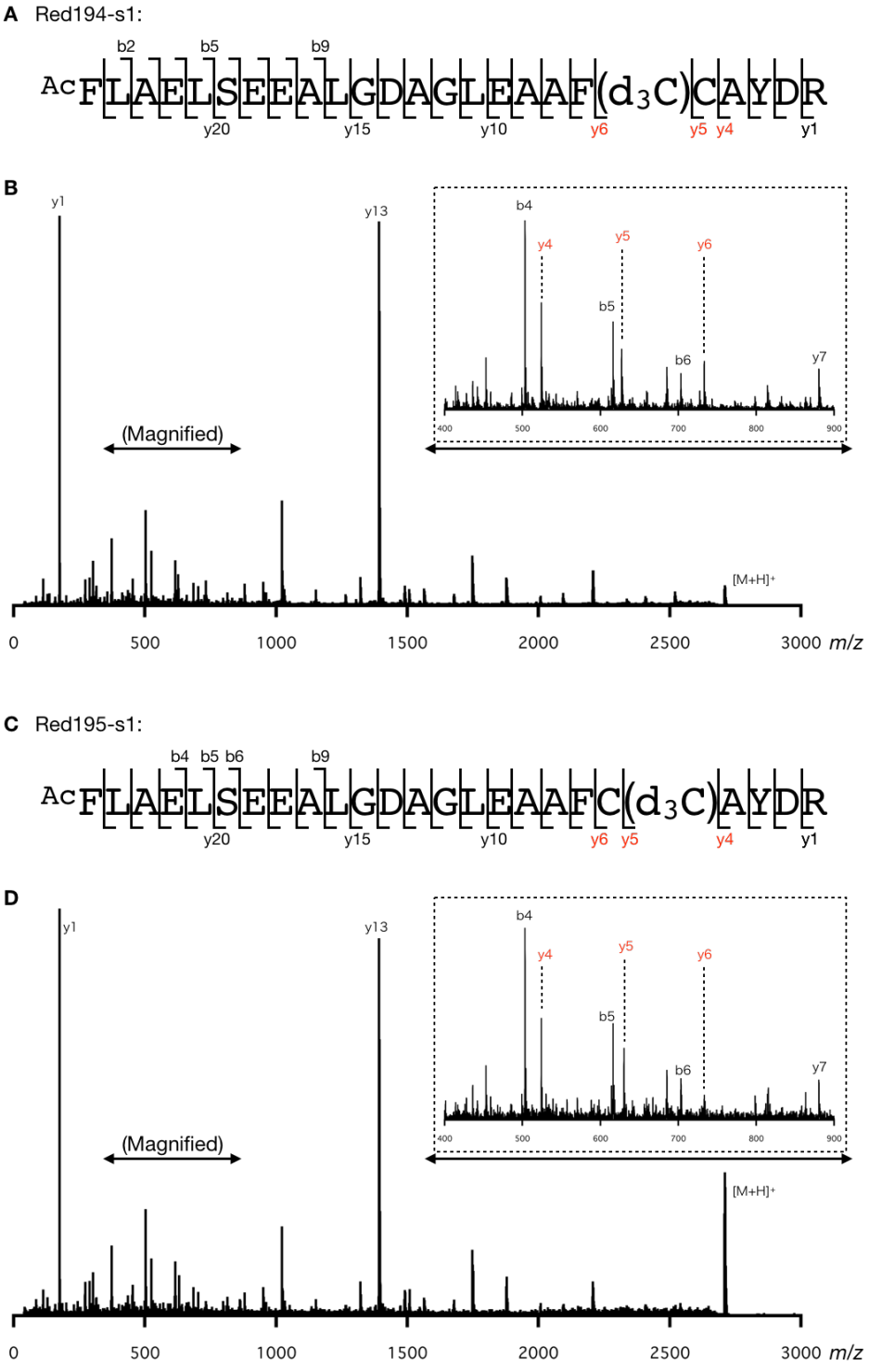

Figure S2.3 MS/MS analysis of the site-specific incorporation of deuterated Cys and canonical Cys. (A, C) Summary of the MS/MS analysis. Detected b ions and y ions are displayed. (B, D) MS/MS spectra of translation products of the customized cell-free translation system.

Materials and methods

All the chemical reagents were purchased from Cambridge Isotope Laboratories, Kanto Chemical, Nacalai Tasque, Sigma-Aldrich Japan, Tokyo Chemical Industry, Wako Pure Chemical Industries, or Watanabe Chemical Industry. All the chemical reagents were used without further purification. All the DNA oligomers were purchased from Eurofins Genomics.

N-acetyl phenyl alanine cyanomethyl ester (AcPhe-CME)

AcPhe-CME was synthesized as previously described.

The cyclodehydratase PatD

The purification of PatD was reported in a literature from our laboratory[97]. In brief, the N-terminally His_{10}-tagged cyclodehyddratase PatD was overexpressed in BL21(DE3) pLysS cells transformed with *patD*/pET16b and purified by Ni-NTA column. The concentration of PatD was determined based on UV-absorbance[135].

DNA oligomers

Ini1-1G-5'.F49:

GTAATACGACTCACTATAGGCGGGGTGGAGCAGCCTGGTAGCTCGTCGG

Ini cat.R44: GAACCGACGATCTTCGGGTTATGAGCCCGACGAGCTACCAGGCT

T7ex5.F22: GGCGTAATACGACTCACTATAG

Ini-3'.R38: TGGTTGCGGGGGCCGGATTTGAACCGACGATCTTCGGG

Ini-3'.R20: TGGTTGCGGGGGCCGGATTT

EnAsn-5'.F49:

GTAATACGACTCACTATAGGCTCTGTAGTTCAGTCGGTAGAACGGCGGA

EnAsn CCA.R43: GAACCAGTGACATACGGACUCCAAATCCGCCGTTCTACCGACT

EnAsn-3'.R38: TGGCGGCTCTGACTGGACTCGAACCAGTGACATACGGA

EnAsn-3'.R20 TGGCGGCTCTGACTGGACTC

PatE-pre-lon b.F47:

GGCGTAATACGACTCACTATAGGGTTAACTTTAACAAGGAGAAAAAC

T7EX5.F22: GGCGTAATACGACTCACTATAG

KYred14 a.F53:

GGTTAACTTTAACAAGGAGAAAAACATGCTCGCCGAACTGTCTGAAGAAGCAC

KYred14 a.R49:

GAAAGCTGCCTCCAACCCCGCGTCGCCCAGTGCTTCTTCAGACAGTTCG

KYred14(2) b.R44: CGAAGCTTAACGATCGTACGCACAGCAGAAAGCTGCCTCCAACC

KYred15 b.R47: CGAAGCTTAACGATCGTACGCGCACGCGCAGAAAGCTGCCTCCAACC

KYred18 a.R45: GCTGCCTCCAACCCCGCGTCGCCCAGTGCTTCTTCAGACAGTTCG

KYred18 c.R20: CGAAGCTTAACGATCGTACG

KYred21 b.R49:

CGAAGCTTAACGATCGTACGCGCAACAGCAGCCAGCTGCCTCCAACCCC

red194 b.R46: CGAAGCTTAACGATCGTACGCCCAACAAAAAGCTGCCTCCAACCCC

red195 b.R46: CGAAGCTTAACGATCGTACGCACACCAAAAAGCTGCCTCCAACCCC

red229 b.R46: CGAAGCTTAACGATCGTACGCACAGCATGCAGCTGCCTCCAACCCC

red231 b.R46: CGAAGCTTAACGATCGTACGCACAGCAATAAGCTGCCTCCAACCCC

red291 b.R46: CGAAGCTTAACGATCGTACGCACAGCACAGAGCTGCCTCCAACCCC

red292 b.R46: CGAAGCTTAACGATCGTACGCACAGCAAATAGCTGCCTCCAACCCC

red294 b.R46: CGAAGCTTAACGATCGTACGCACAGCACATAGCTGCCTCCAACCCC

DNA templates

DNA templates coding precursor peptides were prepared using primer extension followed by multistep PCR reactions. For the information of primer sets corresponding to teach DNA template, see the **Table 2.1** below. The polymerase reaction mixture for both extension and PCR reaction contains: 10 mM Tris·HCl (pH 9.0), 50 mM KCl, 2.5 mM $MgCl_2$, 0.25 mM dNTPs, 0.1% (v/v) Triton X-100, and Taq DNA polymerase.

In primer extension, appropriate forward and reverse primers (1 μM each) were mixed in the polymerase reaction mixture. The primer extension reaction was performed in a 100 μl scale, by denaturing (95°C for 1 min), followed by 5 cycles of annealing (50°C for 1 min) and extension (72°C for 1 min). The primer extension reaction product was 200-fold diluted by the polymerase reaction mixture and amplified using the appropriate forward and reverse primers (0.5 μM each) with a 100 μl scale, by 5 cycles of denaturing (95°C for 40 s), annealing (50°C for 40 s), and extension (72°C for 40 s). The resulting PCR mixture was again 200-fold diluted by the polymerase reaction mixture and amplified using the appropriate forward and reverse primers (0.5 μM each) in a 200 μl scale, by 12 cycles of denaturing (95°C for 40 s), annealing (50°C for 40 s), and extension (72°C for 40 s). For some DNA templates, the extension products were directly amplified in the conditions of final PCR. The resulting DNA was purified by phenol/chloroform extraction and ethanol precipitation and then dissolved in 20 μl of water and directly used for *in vitro* translation reaction.

Table 2.1 DNA oligomers for the preparation of DNA templates for translation.

	Primer extension		1st PCR		Final PCR	
	Forward	Reverse	Forward	Reverse	Forward	Reverse
red14(2)	KYred14 a.F53	KYred14 a.R49	PatE-pre-Ion b.F47	KYred14(2) b.R44	T7EX5.F22	KYred14(2) b.R44
red15	KYred14 a.F53	KYred14 a.R49	PatE-pre-Ion b.F47	KYred15 b.R47	T7EX5.F22	KYred15 b.R47
red21	KYred14 a.F53	KYred18 a.R45	PatE-pre-Ion b.F47	KYred21 b.R49	T7EX5.F22	KYred18 c.R20
red194	KYred14 a.F53	KYred18 a.R45	PatE-pre-Ion b.F47	red194 b.R46	T7EX5.F22	KYred18 c.R20
red195	KYred14 a.F53	KYred18 a.R45	PatE-pre-Ion b.F47	red195 b.R46	T7EX5.F22	KYred18 c.R20
red229	KYred14 a.F53	KYred18 a.R45	PatE-pre-Ion b.F47	red229 b.R46	T7EX5.F22	KYred18 c.R20
red231	KYred14 a.F53	KYred18 a.R45	PatE-pre-Ion b.F47	red231 b.R46	T7EX5.F22	KYred18 c.R20
red291	KYred14 a.F53	KYred18 a.R45	PatE-pre-Ion b.F47	red291 b.R46	T7EX5.F22	KYred18 c.R20
red292	KYred14 a.F53	KYred18 a.R45	PatE-pre-Ion b.F47	red292 b.R46	T7EX5.F22	KYred18 c.R20
red294	KYred14 a.F53	KYred18 a.R45	PatE-pre-Ion b.F47	red294 b.R46	T7EX5.F22	KYred18 c.R20

tRNA$^{fMet}_{CAU}$ and tRNA$^{AsnE2}_{CCA}$

DNA templates coding tRNAs were prepared using primer extension followed by multistep PCR reactions. For the information of primer sets corresponding to each DNA template of tRNA, see the **Table 2.2.** The polymerase reaction mixture for both extension and PCR reaction

contains: 10 mM Tris·HCl (pH 9.0), 50 mM KCl, 2.5 mM $MgCl_2$, 0.25 mM dNTPs, 0.1% (v/v) Triton X-100, and Taq DNA polymerase.

In primer extension, appropriate forward and reverse primers (1 μM each, see) were mixed in the polymerase reaction mixture. The primer extension reaction was performed in a 10 μl scale, by denaturing (95°C for 1 min), followed by 5 cycles of annealing (50°C for 1 min) and extension (72°C for 1 min). The primer extension reaction product was 20-fold diluted by the polymerase reaction mixture and amplified using the appropriate forward and reverse primers (0.5 μM each see) with a 200 μl scale, by 5 cycles of denaturing (95°C for 40 s), annealing (50°C for 40 s), and extension (72°C for 40 s). The resulting PCR mixture was again 200-fold diluted by the polymerase reaction mixture and amplified using the appropriate forward and reverse primers (0.5 μM each) in a 1000 μl scale for the following 1000 μl scale *in vitro* transcription, by 12 cycles of denaturing (95°C for 40 s), annealing (50°C for 40 s), and extension (72°C for 40 s). The resulting DNA was purified by phenol/chloroform extraction and ethanol precipitation and then dissolved in 100 μl of water and directly used for the following *in vitro* transcription.

The PCR product was used for *in vitro* transcription reaction. Transcription reaction mixture contains: 40 mM Tris·HCl (pH 8.0), 1 mM spermidine, 0.01% (v/v) Triton X-100, 10 mM DTT, 23 mM $MgCl_2$, 5 mM NTPs, 1.125% (v/v) of 2M KOH, 10 mM GMP, 10% (v/v) PCR product and 2% (v/v) T7 RNA polymerase.

Table 2.2 DNA oligomers for the preparation of tRNAs

	Primer extension		1st PCR		Final PCR	
	Forward	Reverse	Forward	Reverse	Forward	Reverse
tRNA fMet CAU	Ini1-1G-5'.F49	Ini cat.R44	T7ex5.F22	Ini-3'.R38	T7ex5.F22	Ini-3'.R20
tRNA AsnE2 CCA	EnAsn-5'.F49	EnAsn CCA.R43	T7ex5.F22	EnAsn-3'.R38	T7ex5.F22	EnAsn-3'.R20

Flexizymes (general procedures for eFx and dFx)

DNA templates coding tRNAs were prepared using primer extension followed by multistep PCR reactions. For the information of primer sets corresponding to each DNA template of

flexizymes, see the **Table 2.3.** The polymerase reaction mixture for both extension and PCR reaction contains: 10 mM Tris·HCl (pH 9.0), 50 mM KCl, 2.5 mM $MgCl_2$, 0.25 mM dNTPs, 0.1% (v/v) Triton X-100, and Taq DNA polymerase.

In primer extension, appropriate forward and reverse primers (1 μM each) were mixed in the polymerase reaction mixture. The primer extension reaction was performed in a 100 μl scale, by denaturing (95°C for 1 min), followed by 5 cycles of annealing (50°C for 1 min) and extension (72°C for 1 min). The primer extension reaction product was 200-fold diluted by the polymerase reaction mixture and amplified using the appropriate forward and reverse primers (0.5 μM each) in a 1000 μl scale for the following 1000 μl scale *in vitro* transcription, by 12 cycles of denaturing (95°C for 40 s), annealing (50°C for 40 s), and extension (72°C for 40 s). The resulting DNA was purified by phenol/chloroform extraction and ethanol precipitation and then dissolved in 100 μl of water and directly used for the following *in vitro* transcription.

The PCR product was used for *in vitro* transcription reaction. Transcription reaction mixture contains: 40 mM Tris·HCl (pH 8.0), 1 mM spermidine, 0.01% (v/v) Triton X-100, 10 mM DTT, 30 mM $MgCl_2$, 5 mM NTPs, 1.5% (v/v) of 2M KOH, 10% (v/v) PCR product and 2% (v/v) T7 RNA polymerase.

Table 2.3 DNA oligomers for the preparation of flexizymes

	Primer extension		Final PCR	
	Forward	Reverse	Forward	Reverse
dFx	Fx5'.F36	dFx.R46	T7ex5.F22	dFx.R19
eFx	Fx5'.F36	eFx.R45	T7ex5.F22	eFx.R18

Ribosomal synthesis of precursor peptides by a cell-free translation system

The cell-free translation system contained all the components required for the ribosomal expression of peptides from template DNAs. The final concentration of each component is listed below; 50 mM HEPES·K (pH 7.6), 100 mM KOAc, 2 mM GTP, 2 mM ATP, 1 mM CTP, 1 mM

UTP, 20 mM creatine phosphate, 12 mM $Mg(OAc)_2$, 2 mM spermidine, 2 mM DTT, 1.5 mg/mL E. coli total tRNA (Roche), 1.2 μM ribosome, 0.6 μM MTF, 2.7 μM IF1, 0.4 μM IF2, 1.5 μM IF3, 30 μM EF-Tu, 30 μM EF-Ts, 0.26 μM EF-G, 0.25 μM RF2, 0.17 μM RF3, 0.5 μM RRF, 4 μg/mL creatine kinase, 3 μg/mL myokinase, 0.1 μM pyrophosphatase, 0.1 μM nucleotide-diphosphatase kinase, 0.1 μM T7 RNA polymerase, 0.73 μM AlaRS, 0.03 μM ArgRS, 0.38 μM AsnRS, 0.13 μM AspRS, 0.02 μM CysRS, 0.06 μM GlnRS, 0.23 μM GluRS, 0.09 μM GlyRS, 0.02 μM HisRS, 0.4 μM IleRS, 0.04 μM LeuRS, 0.11 μM LysRS, 0.03 μM MetRS, 0.68 μM PheRS, 0.16 μM ProRS, 0.04 μM SerRS, 0.09 μM ThrRS, 0.03 μM TrpRS, 0.02 μM TyrRS, 0.02 μM ValRS, 500 μM each proteinogenic amino acids, and 100 μM 10-HCO-H_4folate.

The translation reaction was performed at 37°C for 30 min typically at 2 μL scale, in the presence of 0.2 μL of DNA template. For the synthesis of peptides containing non-proteinogenic amino acids, the following procedures were adopted.

Aminoacylation of tRNA by activated amino acids by means of flexyzyme

As general procedures, 42 μM of tRNA and 42 μM of flexizyme, (eFx or dFx) was heated at 95°C for 2 min in the presence of 83 mM HEPES·K (pH 7.5) and gradually cooled at 25°C for 5 min. 33% vol. of 600 mM $MgCl_2$ was added to the mixture, and the reaction mixture was further incubated at 25°C for 5 min. After cooling the mixture on ice, the 25% vol. of activated amino acid in DMSO was added and the reaction was performed for several hours (typically 2–24 h). After the incubation, the aminoacylation was quenched by the addition of 400% vol. of 0.3 M NaOAc (pH 5.2). After ethanol precipitation in acidic conditions, pellet was washed twice with 70% ethanol containing 0.1 M NaOAc (pH5.2) and once with 70% ethanol, and the resulting pellet was dissolved in 1 mM NaOAc just before adding into translation mixture.

In the specific cases in this chapter, the conditions, $tRNA^{fMet}_{CAU}$–eFx (on ice, 2 h) and $tRNA^{AsnE2}_{CCA}$–dFx (on ice, 6 h) were used for Ac-Phe-CME and Cys-DBE, respectively.

Ribosomal synthesis of peptides containing non-proteinogenic structures by a customized cell-free translation system

In the customized cell-free translation mixture, aminoacyl tRNA prepared by flexizyme was typically added into the system at 50 μM based on the amount of total tRNA, regardless of aminoacylation efficiency. And instead, corresponding amino acid was removed from the system.

Methionine as well as 10-HCO-H_4folate and tryptophan were removed from the translation system for the incorporation of acetyl phenylalanine and cysteine, respectively. In addition, for the incorporation of deuterated cysteine (d_3Cys), d_3Cys was externally added at concentrations mentioned in the supporting results.

Post-translational modification reaction with the cyclodehydratase PatD

To the translation mixture, was added 100% vol. of a cyclodehydration mixture (12 μM PatD, 90 mM HEPES·K (pH 8.4), 15 mM DTT, and 1 mM ATP), and the resulting mixture was incubated at 25°C for 16 h. Final concentration of each component is; 50% translation mixture, 6 μM PatD, 45 mM HEPES·K (pH 8.4), 7.5 mM DTT, and 0.5 mM ATP.

Post-translational modification with hydrogen peroxide

To the cyclodehydratoin mixture, was added 100% vol. of an oxidation mixture [200 mM hydrogen peroxide in 1 M NaOAc buffer (pH 5).] The resulting oxidation mixture was incubated at 42°C for 1 h. Final concentration of each component is; 50% dehydration mixture, 100 mM H_2O_2, 0.5 M NaOAc buffer (pH 5). In the substrate scope experiments, f.c. 250 mM H_2O_2 was used.

Hydrolysis assay in acidic conditions

To the reaction mixture (either a dehydration product or a oxidation product), was added 100% vol. of 4% (v/v) trifluoroacetic acid (TFA) in water and the resulting mixture containing 50% of original reaction mixture and 2% of trifluoroacetic acid, was incubated at 42°C for 30 min or at 60°C for 2 h. (Stronger acidic conditions were necessary for the complete peak shift, which was another indication of the oxidation at N-terminal thiazoline.)

MALDI-TOF-MS and MALDI-TOF -MS/MS

The translation mixture, cyclodehydration product, oxidation product, or acid-hydrolysis product was desalted through solid phase extraction (SPE) column (C-Tip C18; Nikkyo Technos), which was equilibrated with elution-solution (80% acetonitrile and 0.5% acetic acid in H_2O) and then with wash-solution (4% acetonitrile and 0.5% acetic acid in H_2O), prior to the sample injection. After the sample injection the column was washed twice with wash-solution, and eluted with matrix-solution (elution-solution containing half-saturated matrix). MALDI-TOF-MS was carried out on an ultrafleXtreme (Bruker Daltonics) externally calibrated with peptide calibration standard II (Bruker Daltonics), in reflector mode.

MALDI-TOF-MS/MS was carried out on an ultrafleXtreme (Bruker Daltonics) and the MS/MS spectra were analyzed on flexAnalysis (Bruker Daltonics) manually.

Chapter 3 Development of *in vitro* synthetic method of Ψ[CH_2NH]-containing peptides

Introduction

In nature, there are many peptidic natural products containing backbone heterocyclic structures such as azolines and azoles, which is the focus of the chapter 2 of this thesis. These heterocyclic structures endow the peptides with fascinating characteristics for peptide drug development, such as structural rigidity, peptidase resistance, conjugated π electron system for interactions with nucleic acids or metal ions[125]. Recently, high membrane permeability was also reported for azoline and azole-containing peptides[15].

On the other hand, albeit it is relatively rare, peptidic natural products with backbone azolidines are also found in nature (**Figure 3.1**). For example, quite recently, macrocyclic peptide, lugdunin was isolated from *S. lugdunensis* and revealed to exhibit strong anti-MRSA activity[136], making the peptidic natural product as a fascinating drug candidate of great interest based on the continuous emergence of MRSA. For the biosynthesis of lugdunin, NRPS mediated biosynthesis was proposed and the thiazolidine formation was attributed to spontaneous ring closure between N-terminal cysteine and C-terminal aldehyde, which is introduced by reductase, involved in the NRPS[136].

Other examples for azolidine-containing peptidic natural products are yersiniabactin[137] and pyochelin[138], isolated from *Y. pestis* and *P. aeruginosa*, respectively, and both exhibiting siderophore activity. In their biosynthesis, thiazolidine formations by reduction of peptidic thiazolines by specific reductases are demonstrated [139] [140].

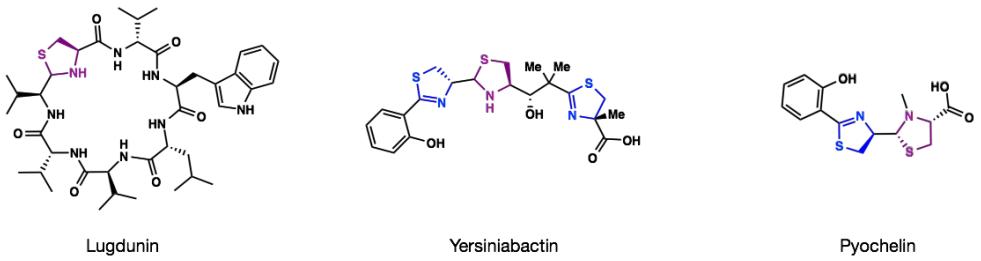

Figure 3.1 Examples of peptidic natural products with backbone azolidine moieties.

Although thiazolidine-containing peptides would be good candidates for the development of novel bioactive peptides, to the best of my knowledge, no post-translational reductase involved in RiPPs mediated biosynthetic pathways was reported, making it hard to approach *in vitro* synthesis of azolidine-containing peptides just by reconstitution of biosynthetic enzymes. Based on the previous study described in chapter 2, in which integration of enzymatic and chemical modification reactions enabled the synthesis of thiazole-containing peptides, it was envisioned that the approach integrating chemical and enzymatic modification reactions would also be applied for *in vitro* synthesis of thiazolidine-containing peptides (**Figure 3.2**).

In the present study, in order to expand structural diversity, which is accessible by *in vitro* translation and subsequent post-translational modification reactions, a cell-free translation system, post-translational cyclodehydratase, and chemical reduction by sodium cyanoborohydride were combined to achieve *in vitro* synthesis of thiazolidine-containing peptides.

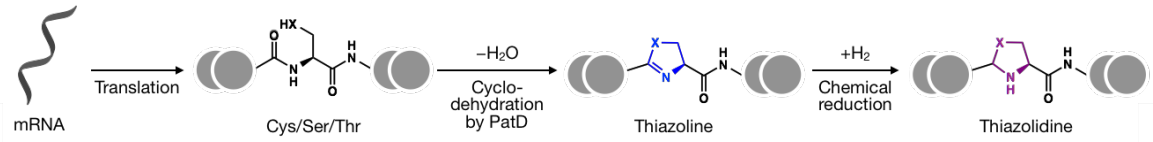

Figure 3.2 Schematic illustration of the concept of *in vitro* synthesis of thiazoldine-containing peptides by the integration of enzymatic and chemical post-translational modification reactions

Results

Chemical reduction of enzymatically synthesized thiazoline-containing peptides.

First, a model template DNA encoding a model peptide containing N-terminal truncated leader sequence and a single cysteine to be modified by the cyclodehydratase PatD, was designed (**Figure 3.3A**) and incubated with translation mixture in 37°C for 30 min, and the resulting translation product was desalted with C18 column and directly analyzed by Matrix-assisted laser desorption/ionization time-of-flight mass spectrometry (MALDI-TOF-MS). MALDI-TOF-MS detected a major peak corresponding to the designated model precursor peptide containing a single cysteine (**Figure 3.3C**). Next, a model template DNA was incubated with translation mixture in the presence of the cyclodehydratase PatD and incubated at 37°C for 1 h, MALDI-TOF-MS detected a major peak corresponding to the peptide containing a single thiazoline derived from cysteine, suggesting highly efficient cyclodehydration catalyzed by PatD (**Figure 3.3D**).

Then, the resulting translation-dehydration product was further incubated with sodium cyanoborohydride in acidic conditions (pH 5), MALDI-TOF-MS detected a peak shift corresponding to the increase in molecular mass by 2 Da, corresponding to the formation of thiazolidine (**Figure 3.3E**). Intriguingly, prolonged incubation with sodium cyanoborohydride in pH 5 resulted in a further increase of molecular mass by 2 Da (in total 4 Da from the thiazoline-containing peptide, **Figure 3.3F**). It was hypothesized that the reduction product, with molecular mass larger than the starting thiazoline-containing peptide by 4 Da in total, was the peptide containing $\Psi[CH_2NH]$-containing peptide. (Note that for a symbol $\Psi[X]$, Ψ stands for the introduction of peptidomimetic structures followed by detailed structures in brackets. It is often used to denote peptidomimetic structures. $\Psi[CH_2NH]$ stands for the substitution of amide bonds by amino methyl moieties, which is so called reduced amide.)

In order to test the hypothesis, first the reduction product was analyzed by MS/MS analysis and a series of fragment peaks consistent with the formation of $\Psi[CH_2NH]$ were detected (**Figure 3.4**). Next, in order to further confirm the formation of $\Psi[CH_2NH]$ structure, alkylation of free thiol by 2-iodoacetamide was attempted. After the alkylation reaction, MALDI-TOF-MS showed almost complete peak shift corresponding to the addition of 2-iodoacetamide on free thiol

supporting the formation of Ψ[CH_2NH] structure (**Figure 3.5**).

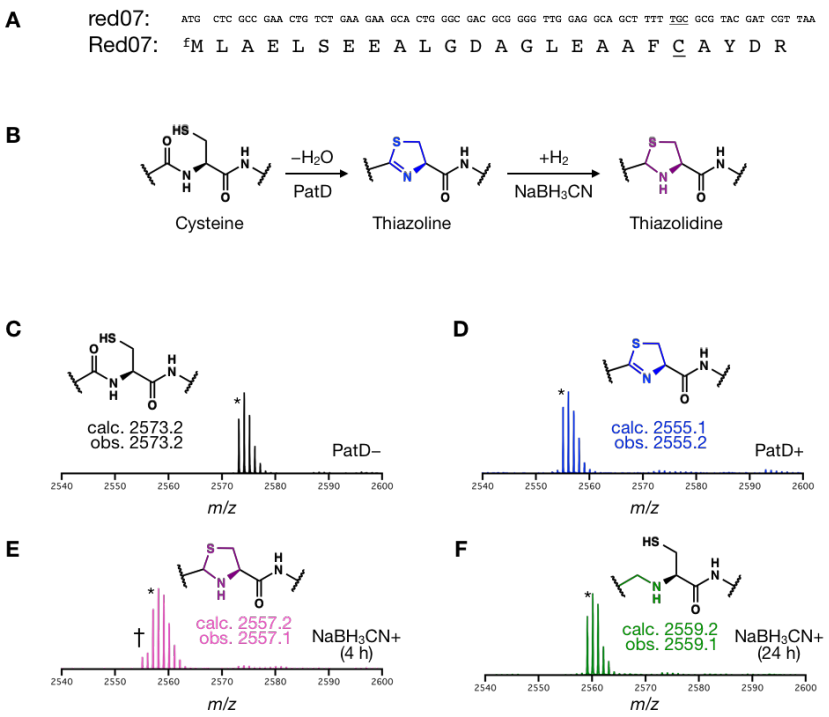

Figure 3.3 Chemical reduction of enzymatically expressed peptide containing thiazoline moiety. (A) DNA sequence and the corresponding model peptide used in this experiment containing single cysteine aligned with N-terminal truncated leader peptide. The cysteine to be modified is underlined. N-terminal ^{f}M stands for *N*-formyl methionine. (B) Reaction scheme of the chemical reduction for the synthesis of thiazolidine-containing peptides. Thiazoline moiety, which was introduced into a ribosomally expressed precursor peptide was incubated with sodium cyanoborohydride in order to convert thiazoline into thiazolidine moiety. (C-F) MALDI-TOF-MS spectra of reaction products, (C) translation product, (D) cyclodehydration product by PatD, (E, F) reduction product by sodium cyanoborohydride at 25°C for 4 h (E) and 24 h (F).

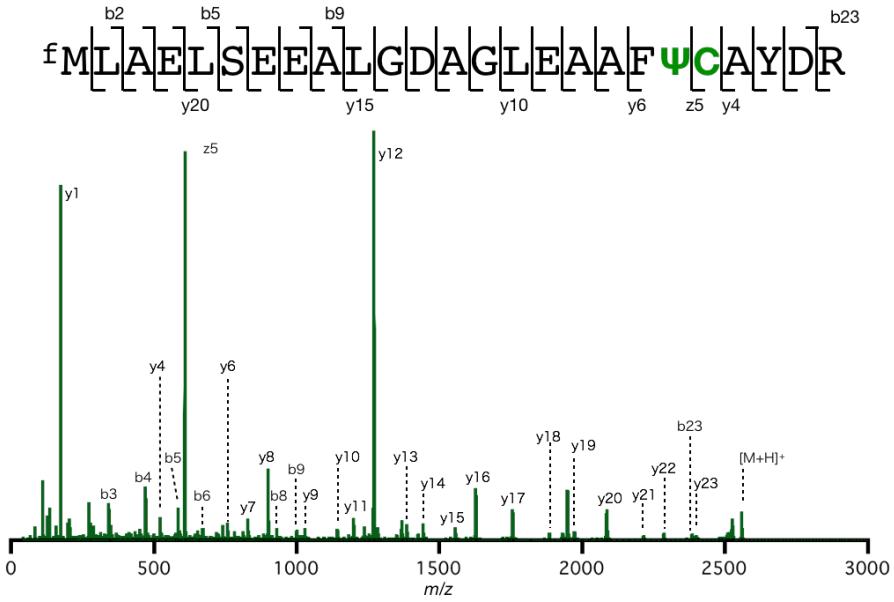

Figure 3.4 MS/MS analysis of the reduction product. The fragment peak z5 is further discussed in supplemental results.

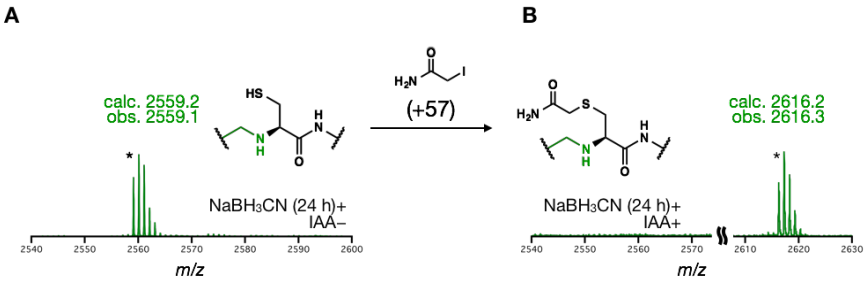

Figure 3.5 Detection of free thiol by 2-iodoacetamide (IAA). Reaction scheme and MALDI-TOF-MS spectra of reaction products, (A) reduction product by sodium cyanoborohydride and (B) alkylation product by 2-iodoacetamide.

Based on these results, proposed mechanism for the formation of Ψ[CH_2NH] is shown in **Figure 3.6**. The cyclodehydration by PatD coupled with translation installed thiazoline moiety (2) derived from cysteine residue (1) into the model peptide. The resulting thiazoline (2) was reduced by sodium cyanoborohydride yielding thiazolidine moiety (3), which is further reduced by sodium cyanoborohydride after tautomerization into imine intermediate (4) yielding the Ψ[CH_2NH] structure (5).

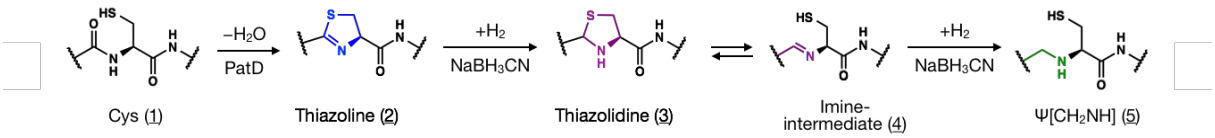

Figure 3.6 Proposed mechanism for the formation of Ψ[CH_2NH] structure from enzymatically expressed thiazoline-containing peptides.

Model reactions for the formation of Ψ[CH_2NH]-containing peptides

In order to test this hypothesis, next model compounds were synthesized and used for model reactions (**Figure 3.7**). First, a model compound (1) was incubated with sodium cyanoborohydride in deuterated buffer and the reaction mixture was monitored by ^{1}H-NMR. ^{1}H-NMR spectrum suggested the formation of Ψ[CH_2NH], which was also confirmed by HR-ESI-MS. Since, in the model reaction, the formation of intermediates, thiazolidine or imine intermediates were not clearly observed, a model compound (2) was also synthesized and incubated in the same reaction conditions and monitored by ^{1}H-NMR. ^{1}H-NMR spectrum as well as HR-ESI-MS confirmed the formation of Ψ[CH_2NH] structure (3), supporting the proposed mechanism of the two-step reduction by sodium cyanoborohydride for Ψ[CH_2NH] structure formation starting from thiazoline via thiazolidine (**Figure 3.6**). [See supporting results, including control experiments and model reactions using sodium cyanoborodeuteride ($NaBD_3CN$)].

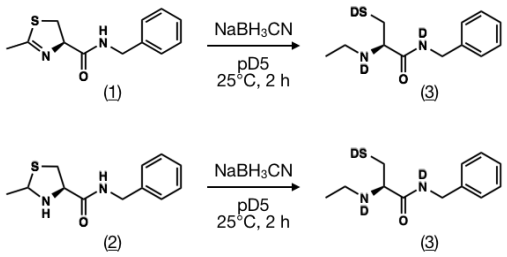

Figure 3.7 Model reactions for the formation of Ψ[CH_2NH] structure. The starting compounds were incubated with sodium cyanoborohydride in deuterated buffer (pD 5) and the reaction mixture was monitored by ^{1}H-NMR and ESI-MS. See supporting results for the detail.

Substrate scope of the reduction for the synthesis of Ψ[CH_2NH]-containing peptides

In order to investigate substrate scope of the reduction method for the synthesis of Ψ[CH_2NH]-containing peptides, model peptides were designed and prepared (**Figure 3.8A and 3.9A**). All proteinogenic amino acids except for Cys, Ser, or Thr were placed at the position N-terminally adjacent to cysteine (in other words Phe (F) in the model peptide in the previous experiments was mutated into 17 kinds of proteinogenic amino acids). After dehydration-coupled translation at 37°C for 1 h, MALDI-TOF-MS detected major peaks corresponding to the desired thiazoline-containing peptides in all cases showing extremely high substrate tolerance and catalytic efficiency of the cyclodehydratase PatD (**Figure 3.8B and 3.9B**). Subsequently, the resulting thiazoline-containing peptides were incubated with sodium cyanoborohydride at pH 5 and MALDI-TOF-MS of the reduction product showed peak shifts to different extents depending on the mutated amino acids (**Figure 3.8B and 3.9B**).

In the cases of [Gly (G), Asp (D), Glu (E), Lys (K), Arg (R), Gln (Q), Met (M), Trp (W), Ala (A), Leu (L) and Tyr (Y)], major peaks corresponding to the Ψ[CH_2NH]-containing peptides were observed after reduction for 24 hours with tiny peak corresponding to the starting thiazoline-containing peptides and intermediate thiazolidine-containing peptides. In the cases of Asn (N), His (H) and Pro (P), peak shifts were relatively slow. In the cases of Val (V) and Ile (I), the reduction was much slower and peaks corresponding to the starting thiazoline-containing peptides

can be observed even after 48 h reduction probably due to steric hindrance by β-blanched side chains. Nonetheless, the peaks corresponding to the Ψ[CH_2NH]-containing peptides were observed as major peaks even in the cases of Val (V) and Ile (I).

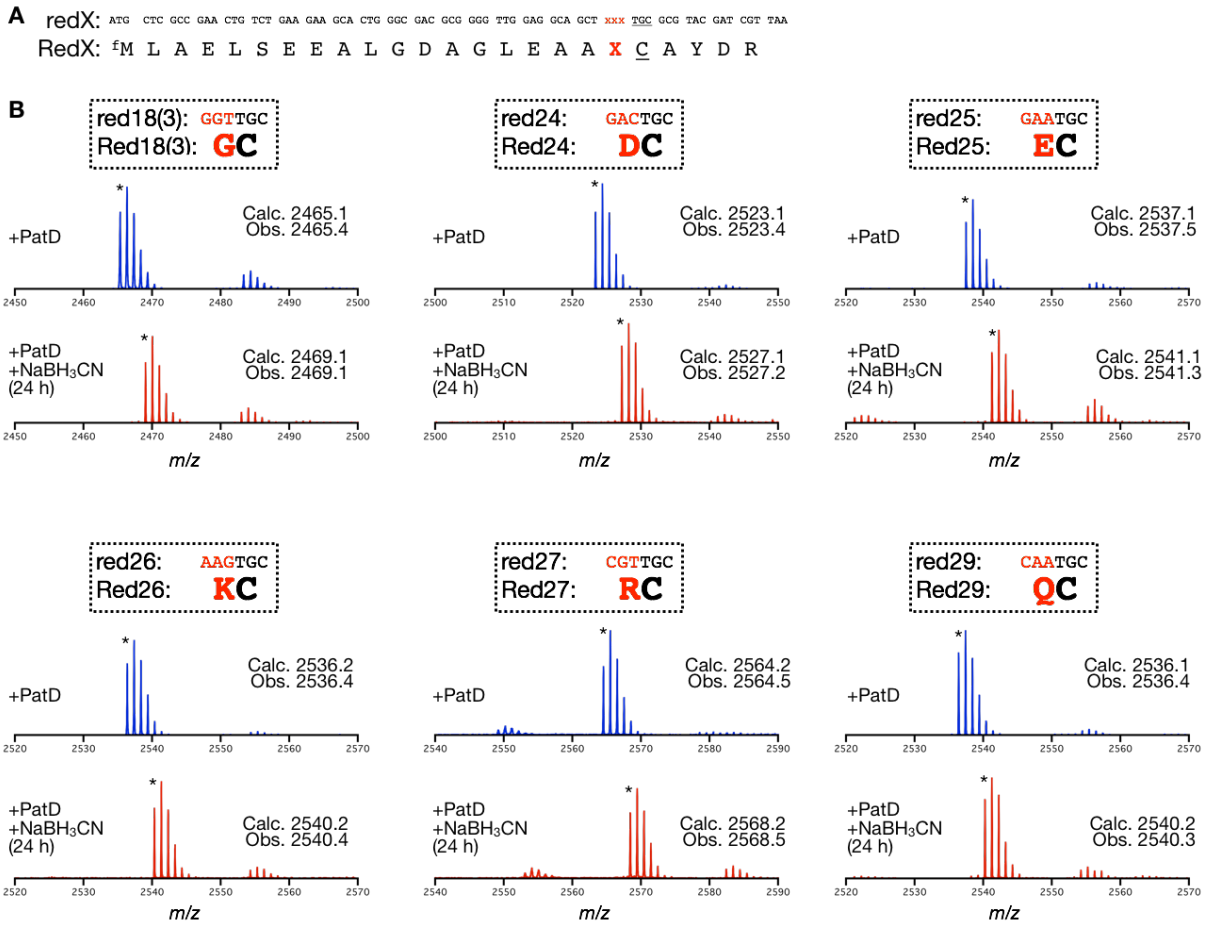

Figure 3.8 Substrate scope for the reduction method. **(Continued)**

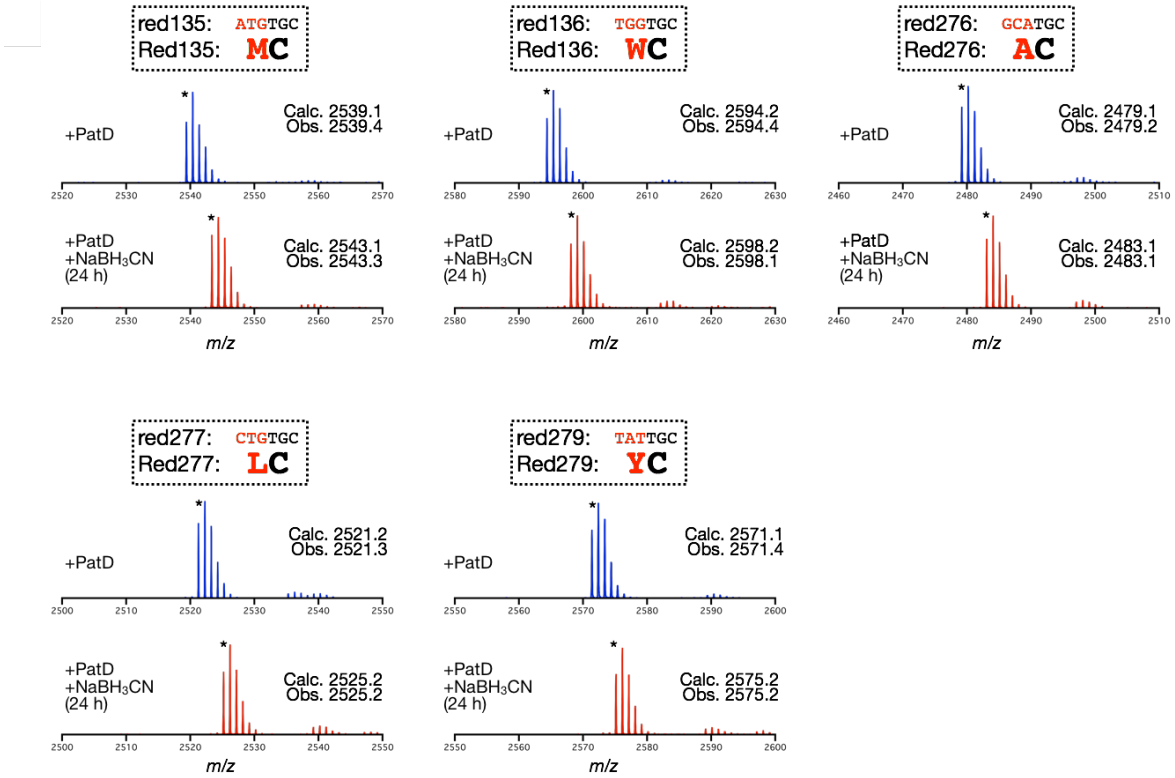

Figure 3.8 (Continued) Substrate scope for the reduction method. (A) Mutant precursor peptides with XC sequences, where X was Gly (G), Asp (D), Glu (E), Lys (K), Arg (R), Gln (Q), Met (M), Trp (W), Ala (A), Leu (L), or Tyr (Y) were used. (B) MALDI-TOF-MS spectra of reaction products before and after the reduction. In these conditions, peaks corresponding to the thiazoline-containing peptides were replaced by peaks corresponding to the Ψ[CH_2NH]-containing peptides after 24 hours. Monoisotopic peaks are labeled with asterisk (*)

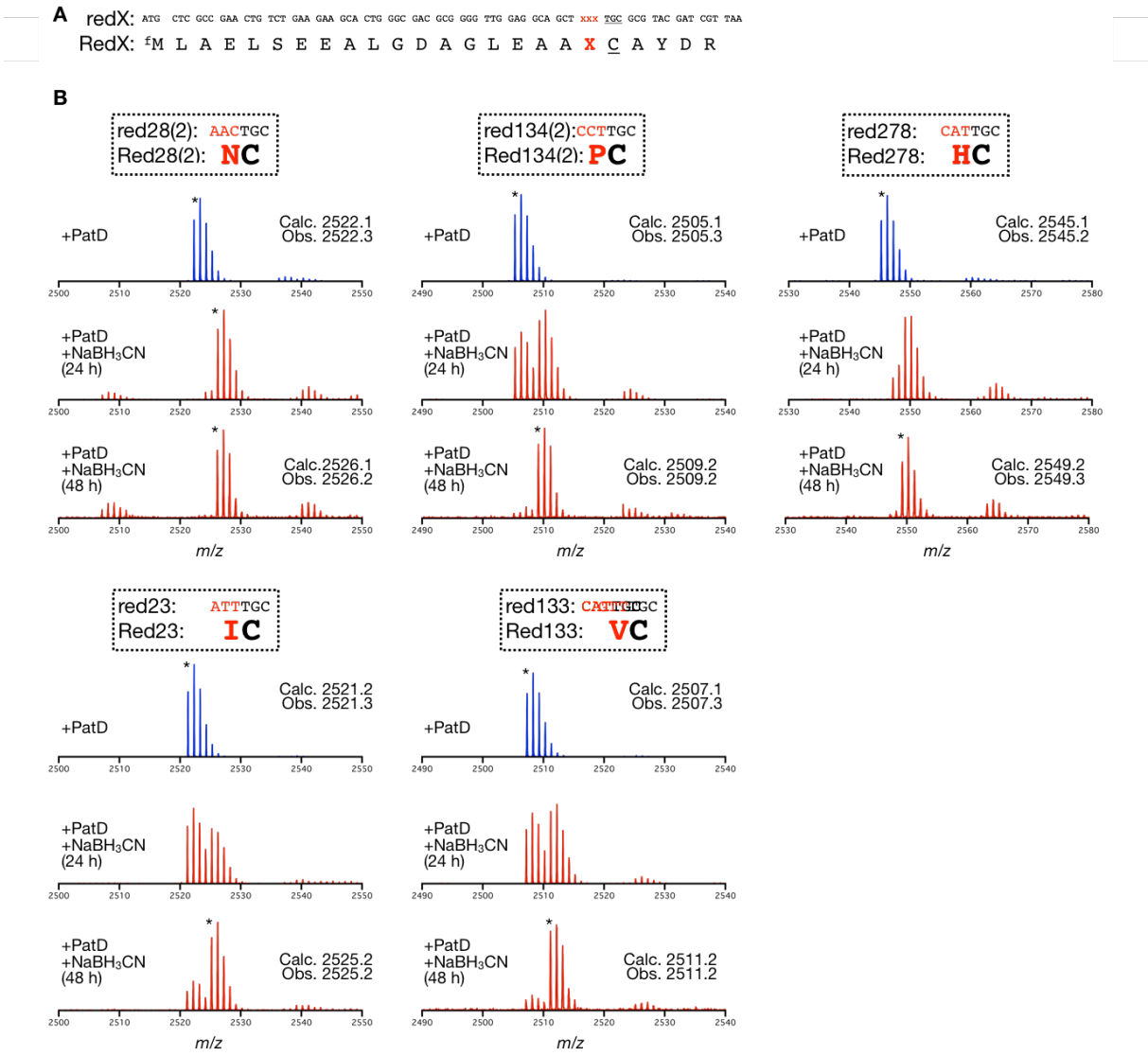

Figure 3.9 Substrate scope for the reduction method. (A) Mutant precursor peptides with XC sequences, where X was Ile (I), Asn (N), Pro (P), Val (V), or His (H). (B) MALDI-TOF-MS spectra of reaction products before and after the reduction. In these conditions, reduction proceed relatively slower, and additional incubation for another 24 hours was required to detect peaks corresponding to the Ψ[CH_2NH]-containing peptides as major peaks. Monoisotopic peaks are labeled with asterisk (*)

Desulfurization reaction for the synthesis of various Ψ[CH_2NH]-containing peotides.

Since the reduction method developed here requires C-terminal cysteine residue adjacent to amide bond to be reduced, substrate scope at C-terminal amino acid residue is limited only to cysteine. To expand substrate scope of the reduction method, desulfurization reaction was next attempted to convert Ψ[CH_2NH]Cys into Ψ[CH_2NH]Ala (**Figure 3.10**). For this purpose, selective desulfurization of thiol in non-protected peptidic scaffold was required, which is actually well investigated in the studies of chemical protein synthesis by native chemical ligation [141].

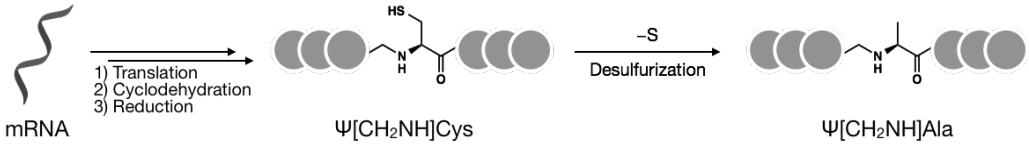

Figure 3.10 Schematic illustration of *in vitro* synthesis of various Ψ[CH_2NH]-containing peptides from non-protected peptide bearing Ψ[CH_2NH] structure via desulfurization reaction.

Short introduction for native chemical ligation and applications of non-proteinogenic amino acids combined with desulfurization reaction.

In the reaction of native chemical ligation[142], typically non-protected peptide thioester and non-protected peptide bearing N-terminal cysteine are ligated by thioester exchange and a subsequent *S* to *N* acyl shift resulting in peptide linked by newly synthesized amide bond, just before the cysteine residue (**Figure 3.11**). Native chemical ligation has been enabled synthesis of longer peptides/proteins, which is hard to synthesize by conventional solid phase peptide synthesis (SPPS), the synthesis of highly decorated proteins with non-proteinogenic structures, and mirror-image proteins composed of D-amino acids, which are hard to synthesize by translation reaction.[143].

One of the most significant technical break-through for the prosperity of native chemical ligation methodology nowadays was the development of desulfurization reaction, which enabled ligation at cysteine-less sequences, exemplified by ligation at Ala (**Figure 3.11**). Native chemical

ligation at cysteine-less sequences paved the way for the general strategy of the chemical synthesis of proteins.

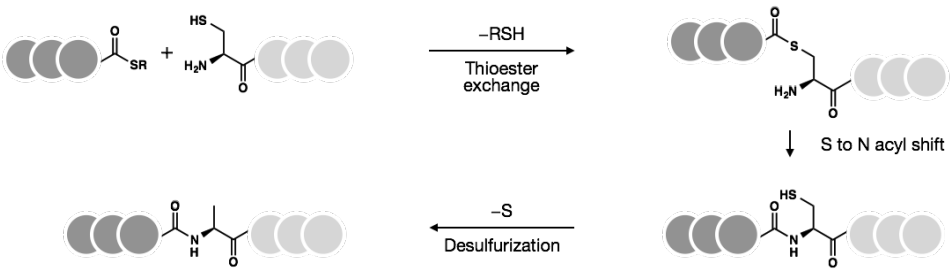

Figure 3.11 Native chemical ligation with non-protected peptides containing C-terminal thioester and non-protected peptides containing N-terminal cysteine, and a subsequent desulfurization reaction for the formal ligation at alanine instead of cysteine.

Historically, Raney nickel-mediated desulfurization to convert cysteine residue into alanine residue was first demonstrated in 2001[144] and in that report, thiol-containing amino acids were suggested that can potentially be used at the ligation site in protein synthesis. Afterwards, organic synthesis of β-thiol containing phenylalanine was reported and applied for native chemical ligation[145]. Following these earlier reports, several groups reported native chemical ligation using thiol-containing proteinogenic amino acid analogs, including analogs of Val[146, 147], Lys[148, 149], Thr[150], Leu[151], Pro[152], Gln[153], Arg [154], Asp[155], Glu[156], Trp[157] and Asn[158]. Along with the development of thiol-containing amino acids, several desulfurization reaction conditions were also reported following the desulfurization reaction mentioned above. The radical mediated desulfurization[146, 159] are now widely performed for chemical protein synthesis and reaction mechanism of the reaction is shown in **Figure 3.12**

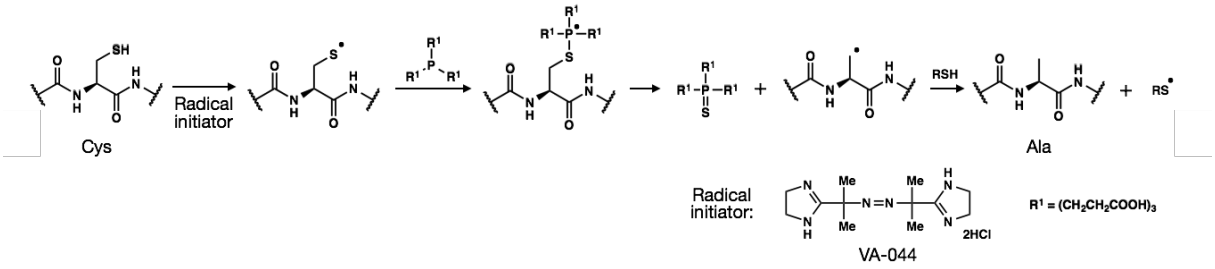

Figure 3.12 Reaction mechanism for the radical mediated desulfurization, where RSH stands for additional thiol in the reaction mixture such as cysteine as well as cysteine residue in peptides or proteins, dithiothreitol (DTT), 2-mercaptoethanol, and glutathione. The desulfurization reaction using 2,2'-Azobis[2-(2-imidazolin-2-yl)propane] dihydrochloride (VA-044), TCEP, and glutathione as radical initiator, phosphine, and additional thiol, respectively, was applied for the synthesis of Ψ[CH_2NH]Ala-containing peptide.

Desulfurization for conversion of Ψ[CH$_2$NH]Cys into Ψ[CH$_2$NH]Ala.

In order to convert Ψ[CH$_2$NH]Cys structure into Ψ[CH$_2$NH]Ala structure, the radical mediated desulfurization reaction was applied. After cyclodehydration-coupled translation, and subsequent reduction by sodium cyanoborohydride, the buffer exchange was performed by gel filtration and to the filtrate containing the reduction product added VA-044, glutathione, and TCEP and incubated at 60°C for 30 min. MALDI-TOF-MS detected peak shift corresponding to the desired desulfurization from Ψ[CH$_2$NH]Cys structure to Ψ[CH$_2$NH]Ala structure (**Figure 3.13**) demonstrating further expansion of substrate scope of this cyclodehydration-reduction protocol for the synthesis of various Ψ[CH$_2$NH]-containing peptides.

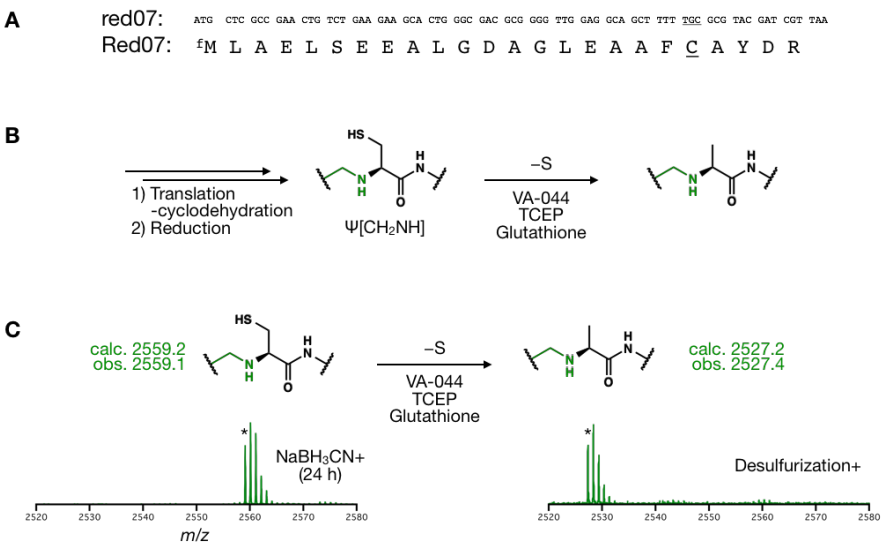

Figure 3.13 Conversion of Ψ[CH$_2$NH]Cys into Ψ[CH$_2$NH]Ala by radical-mediated desulfurization reaction. (A) DNA sequence and the corresponding model peptide used in this experiment composed of N-terminal truncated leader peptide and a single cysteine to be modified by the cyclodehydratase PatD (underlined). N-terminal ^{f}M stands for *N*-formyl methionine. (B) Reaction scheme for the synthesis of Ψ[CH$_2$NH]-containing peptides by cyclodehydration-coupled translation, reduction and desulfurization reaction. (C) MALDI-TOF-MS spectra of the reaction products before and after desulfurization.

Discussion

Substrate scope of the synthetic method of Ψ[CH_2NH]-containing peptides

In the present study, *in vitro* synthetic method of Ψ[CH_2NH]-containing peptides was developed. Integration of a cell-free translation and enzymatic cyclodehydration and chemical reduction enabled template dependent synthesis of a wide variety of Ψ[CH_2NH]-containing peptides with all the tested 17 kinds of N-terminally adjacent amino acids and C-terminally adjacent Cys and Ala residues by further integration of the radical mediated desulfurization reaction. As mentioned above, β-thiol-containing proteinogenic amino acid analogs would enable further expansion of substrate scope of this reduction protocol. This approach would require (i) ribosomal incorporation of such non-proteinogenic amino acids, (ii) substrate tolerance by the cyclodehydratase PatD and (iii) the reduction by sodium cyanoborohydride. For the first issue (i), genetic code reprogramming method has been already developed and would be applicable to such non-proteinogenic amino acid derivatives. For the second issue (ii), since PatD can modify both serine and threonine, substitutions at β-position may be tolerated. Post-translational modification reactions of non-proteinogenic amino acid residues containing β-substituted Cys/Ser/Thr analogs are now underway (data not shown).

Reported bioactive Ψ[CH_2NH]-containing peptides.

Ψ[CH_2NH] structure, which was unexpectedly the target of the synthetic method developed here is one of the most well-studied peptidomimetic structures.[160] There have actually been studied many peptidomimetic structures in order to develop bioactive peptides based on previously characterized peptide ligand of bioactive peptides. In many cases, canonical linear peptide containing only proteinogenic aminoacids are labile in a biological conditions making it difficult to keep the peptide *in vivo* at effective concentration, and thus improvement of pharmacological properties of the peptides are desired. In other cases, peptidases/proteases are targets of interest for drug development and the peptide bond to be cleaved by the enzymes are good target for modifications to inhibit catalytic activities of peptidases/proteases. In such contexts, amide bond is modified by a wide variety of "peptidomimetic structures".

Very early application of peptidomimetic Ψ[CH_2NH] structure was reported in that the

introduction of Ψ[CH_2NH] structure into substrate peptide of a targeted protease, renine improved IC_{50} by 1600-fold.[161] Following the drastic improvement just by introduction of a single substitution into peptidic scaffold, a lot of bioactive peptides based on the Ψ[CH_2NH] structure were designed such as antibacterial peptides with improved stability[162] or greater bacterial selectivity [163] and peptidyl prolyl isomerase inhibitors mimicking twisted-amide transition state[164]. In addition, structural analysis of Ψ[CH_2NH]-containing peptides was also reported[165]. In these reports, the introduction of Ψ[CH_2NH] structure affected protease resistance, the extent of mimicry of intermediate in the enzymatic reaction on the original substrate peptides, net charge of the peptide, and intra molecular hydrogen-bonding pattern to alter global conformation of the peptide.

Although the introduction of Ψ[CH_2NH] structure into peptidic backbone can modulate properties of peptides, bioactive peptides are often designed based on known substrate peptides, in which the substitution of amide bonds are introduced and *de novo* design of novel bioactive peptides has been challenging task. The reduction method developed here, can generate Ψ[CH_2NH]-containing peptides in a template dependent manner and in mild conditions in water, which would enable the construction of Ψ[CH_2NH]-containing peptide library with huge diversity. Based on these properties, the reduction method, combined with molecular evolution methods, would enable the *de novo* development of novel bioactive peptides against any proteins of interest even with proteins with non-peptide substrates.

Reported synthetic methods of Ψ[CH_2NH]-containing peptides

Based on a serendipitous observation that thiazoline can be converted into Ψ[CH_2NH] structure by two-step reduction, the present study developed general preparation method of Ψ[CH_2NH]-containing peptides. In general, for the preparation of Ψ[CH_2NH]-containing peptides there are multiple choice of methods[166] including (i) preparation of a Ψ[CH_2NH]-containing building block, equivalent to dipeptide, (ii) solid phase reductive amination by using aminoaldehyde as a building block and (iii) aziridine-mediated ligation method, which was recently reported.[167] Although all of the methods can prepare desired Ψ[CH_2NH]-containing peptides, they require instruments and reagents for organic synthesis, and especially in method (ii), which is probably the

most standard method for the introduction of Ψ[CH_2NH] structure, sometimes suffer from dialkylation during reductive amination step, as is seen in general in reductive amination reaction.[166] On the other hand, the reduction method developed here can be conducted with biological reagents and only a single reducing reagent and yield no dialkilation product enabling facile synthesis of Ψ[CH_2NH]-containing peptides.

In general, reduction of amide bond requires harsh conditions and selective reduction of a specific amide bond in a polypeptide scaffold would be very challenging problem. It is strike contrast that the cyclodehydration-reduction protocol developed here is formally equivalent to site-selective reduction of non-protected peptides in water in mild reaction conditions (**Figure 3.14**).

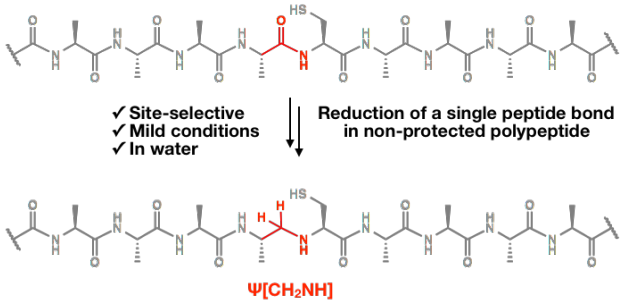

Figure 3.14 The series of reactions for the synthesis of Ψ[CH_2NH]-containing peptides as a formal site-selective amide reduction.

Compatibility of the reduction method with molecular evolution methods

Although the effect of sodium cyanoborohydride ($NaBH_3CN$) against RNA at the optimized conditions in this chapter should be studied, sodium cyanoborohydride has been often used for the modification of RNA[168], suggesting appropriate optimization may lead to moderate reduction conditions, for selective conversion of thiazoline into thiazolidine and Ψ[CH_2NH] structure. In addition, though the effect of radical-mediataed desulfurization reaction against nucleic acids are yet examined, Raney nickel-mediated desulfurization was reportedly compatible for conversion of Cys-tRNA into Ala-tRNA[106], suggesting possibility of the integration of desulfurizaton strategy and mRNA display method. Thus, the combination of molecular evolution methods such as mRNA

display method and the reduction method for the synthesis of thiazolidine- and Ψ[CH_2NH]-containing peptides described in this chapter would enable the construction of peptide libraries with unique structural scaffold and lead to the development of novel bioactive peptides.

Conclusion

In the present study, *in vitro* synthetic method of Ψ[CH_2NH]-containing peptides as well as thiazolidine-containing peptides was developed by integrating a cell-free translation system, a post-translational cyclodehydratase PatD, and chemical reduction reaction by sodium cyanoborohydride. The synthetic method was based on two-step reduction of peptide-embedded thiazoline, which was originally found and characterized by model reactions using ^{1}H-NMR in this study and proved to be applicable to a wide variety of substrate peptide sequences. The reduction method is formally, as a whole, equivalent to site-selective peptide bond reduction in polypeptide scaffold in mild reaction conditions in water, composing the distinctive features of the reaction.

The synthetic method provides general synthetic strategy for the synthesis of Ψ[CH_2NH]-containing peptides, which would enable the construction of Ψ[CH_2NH]-containing peptide library with huge diversity. In contrast to the previous strategies in that the peptidomimetic structures were introduced into already-characterized bioactive peptides, the construction of Ψ[CH_2NH]-containing peptide library would lead to the *de novo* development of novel bioactive peptides.

Supplemental results

Screening of reducing agents

For screening of reaction conditions, several reducing agents such as sodium triacetoxyborohydride, sodium cyanoborohydride, 2-picoline borane, and triazole borane were tested in reactivity as well as solubility in several solvents. Structures, molecular weight, qualitative evaluation of solubility in several solvents are listed in **Figure S3.1**.

			Solubility		
Reductant	**Structure**	**M.W.**	**1 M in water**	**1 M in EtOH**	**1 M in DMSO**
(a) $NaBH_3CN$	-	62.8	Soluble	A little ppt	Soluble
(b) $NaBH(OAc)_3$	-	211.9	Soluble[4]	ppt[4]	A little ppt[4]
(c) Picoline-BH_3 [1]		107.0	ppt	Soluble	Soluble
(d) Triazole-BH_3 [2]		147.0	ppt	ppt	ppt[4]

Figure S3.1 Properties of reducing agents

Then, solution or suspension of each reducing agent was mixed with dehydration product originated from the model precursor peptide containing a single cysteine (**Figure S3.2A**) and incubated at different pH. MALDI-TOF-MS detected peak shift corresponding to the reduction reaction in the cases of sodium cyanoborohydride as well as 2-picoline borane in acidic conditions (**Figure S3.2B-N**). Encouraged by these results, next the reaction time course was monitored by using these two reducing agents. MALDI-TOF-MS detected similar peak shift for sodium cyanoborohydride and 2-picoline borane (**Figure S3.3**). Since sodium cyanoborohydride was soluble in the reaction mixture whereas 2-picoline borane was not, sodium cyanoborohydride was further used for the following chemical reduction experiments.

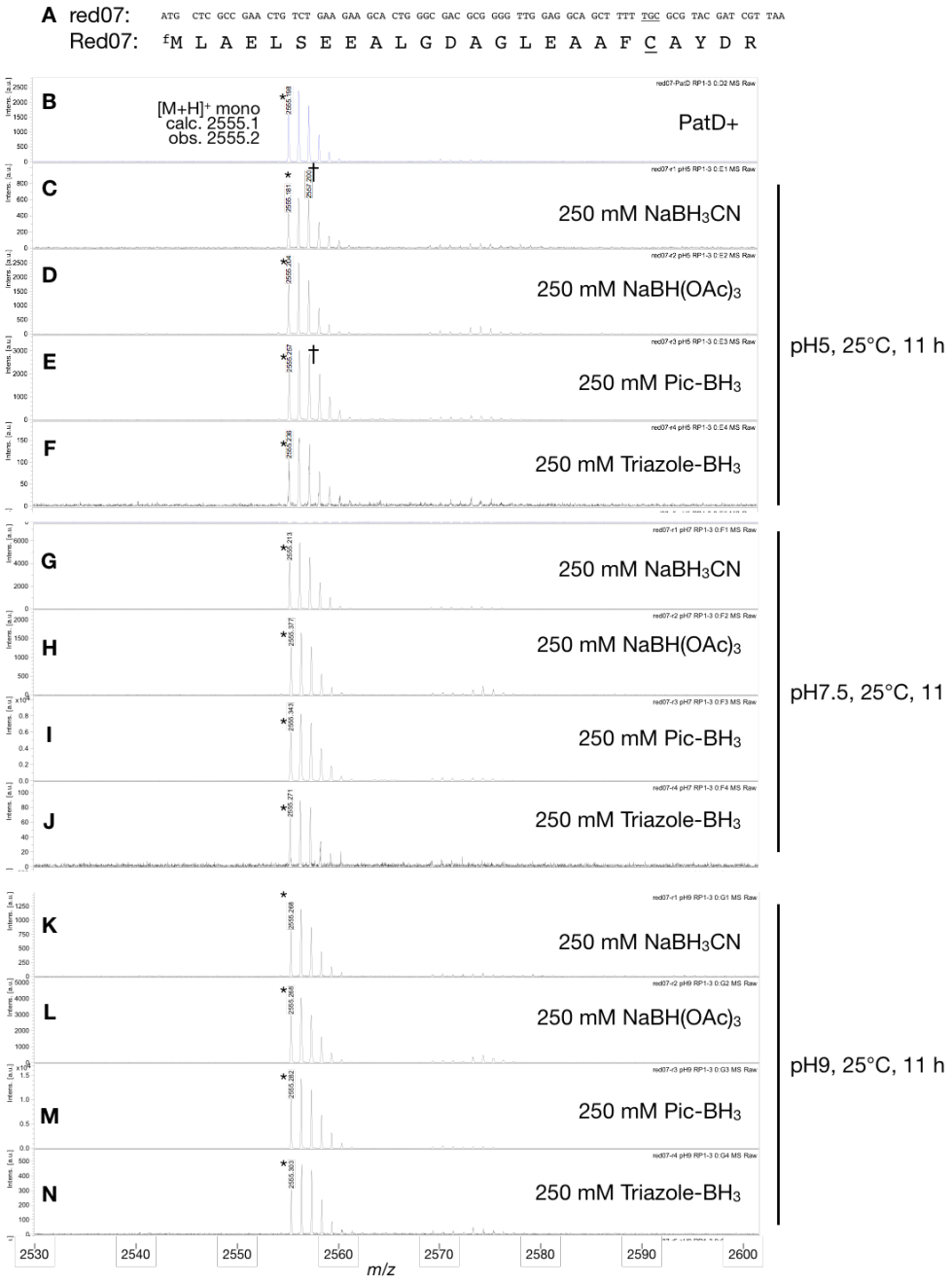

Figure S3.2 Screening of reduction conditions. (A) Sequence of a DNA template and the corresponding model peptide. (B-N) MALDI-TOF-MS spectra of reaction products. The cyclodehydration product of the model peptide (B) and subsequent reduction products with 250 mM reducing agents in different pH at 25°C for 11 h (C-N). Other reaction conditions are indicated besides the spectra.

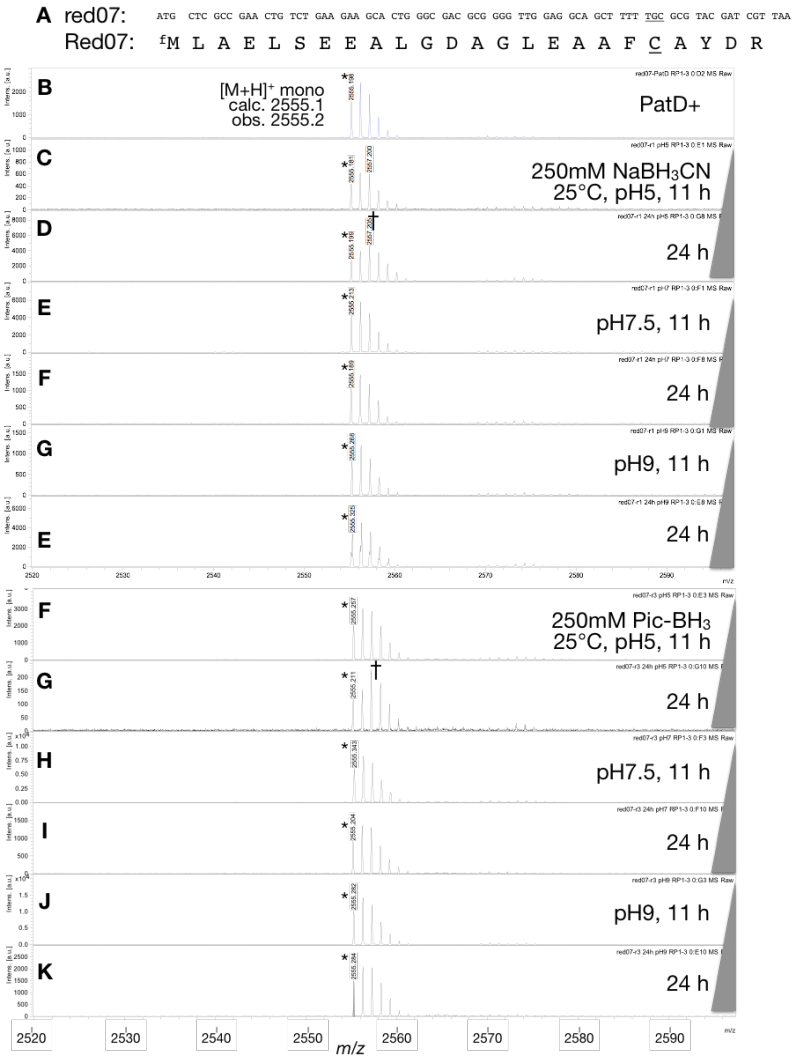

Figure S3.3 Screening of reduction conditions. (A) Sequence of a DNA template and the corresponding model peptide. (B-K) MALDI-TOF-MS spectra of reaction products. The cyclodehydration product (B) and subsequent reduction products with 250 mM reducing agents in different pH at 25°C for 11 h (C-K). Reaction conditions are indicated besides the spectra

Stability of oxazoline in acidic conditions

Since in previous experiments, it was found that azoline moieties, especially oxazoline moiety was susceptible to acid-mediated hydrolysis reaction, here the effect of acetic acid concentration in wash/elution solution as well as matrix solution was tested. Apparent cyclodehydaration efficiency was compared by MALDI-TOF-MS in different concentration of acetic acid in wash/elution solution as well as matrix solution, including 0.5% of acetic acid, which is a standard condition in our laboratory (**Figure S3.4**). There was clear tendency that in the cases of higher concentration of acetic acid, the ratio of unmodified peak was observed, which should be attributed to acceleration of hydrolysis by stronger acidic conditions. Based on the result, in the later experiments, wash/elution and matrix solution without acetic acid was used in some experiments.

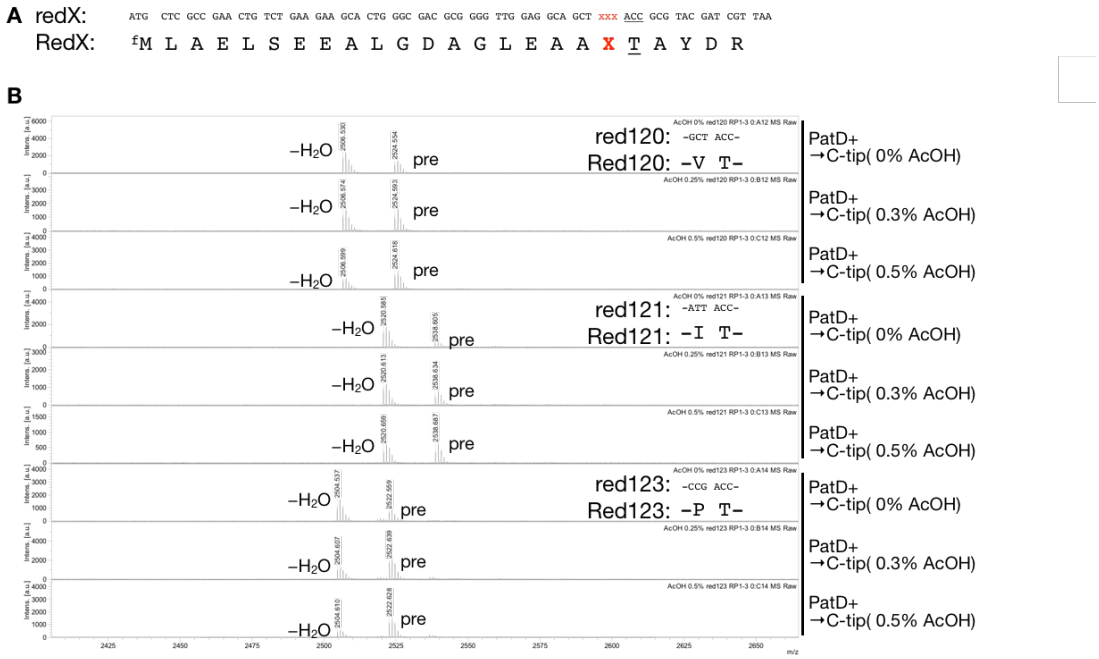

Figure S3.4 Qualitative evaluation of stability of oxazoline moiety in acidic conditions. (A) Sequences of three model DNA templates encoding three different model peptides with XT sequence at C-terminus, where Thr (T) is incorporated to be modified by the cyclodehydratase PatD, which is next to N-terminal adjacent amino acid, X. (B) MALDI-TOF-MS spectra of the dehydration product from each model peptide. The desalting and crystallization procedures were conducted with wash/elution solutions and matirix solution with different concenrations of acetic acid, shown beside the spectra.

Attempt at reduction of oxazoline

As above mentioned, the cyclodehydratase PatD can catalyze oxazoline formation from Ser/Thr residues as well as thiazoline formation from Cys residue. Here, chemical reduction of oxazoline moiety was attempted to test if oxazolidine or Ψ[CH_2NH] can be introduced or not by the chemical reduction of oxazoline moiety by sodium cyanoborohydride.

As described in the previous work, the cyclodehydration efficiency can be summarized as Cys >> Thr > Ser. For the investigation into chemical reduction of oxazolines, truncated N-terminal leader sequence is required because the reduction, which may occur, will give increase of molecular mass at most 4 Da. Or if full length leader peptide is used, monitoring differences between before and after the reaction would be difficult though truncated leader peptide would further decrease the cyclodehydration efficiency of Ser/Thr residues by PatD.

Based on these considerations, first substrate scope of the cyclodehydration efficiency was tested using substrate peptides containing truncated N-terminal leader peptide and mutated region to be modified. Selected proteinogenic amino acids were placed N-terminaly adjacent to Ser/Thr residues and translation product and the cyclodehydration product was monitored by MALDI-TOF-MS (**Figure S3.5 and S3.6**). The mass spectrometry illustrated that Val, Ile, and Pro residues are "good neighbors" as well as that Thr was better residue to be modified compared to Ser residue. The preference for Val, Ile, and Pro was not surprising because these amino acid residues are common in PatE variants, which are found in nature.

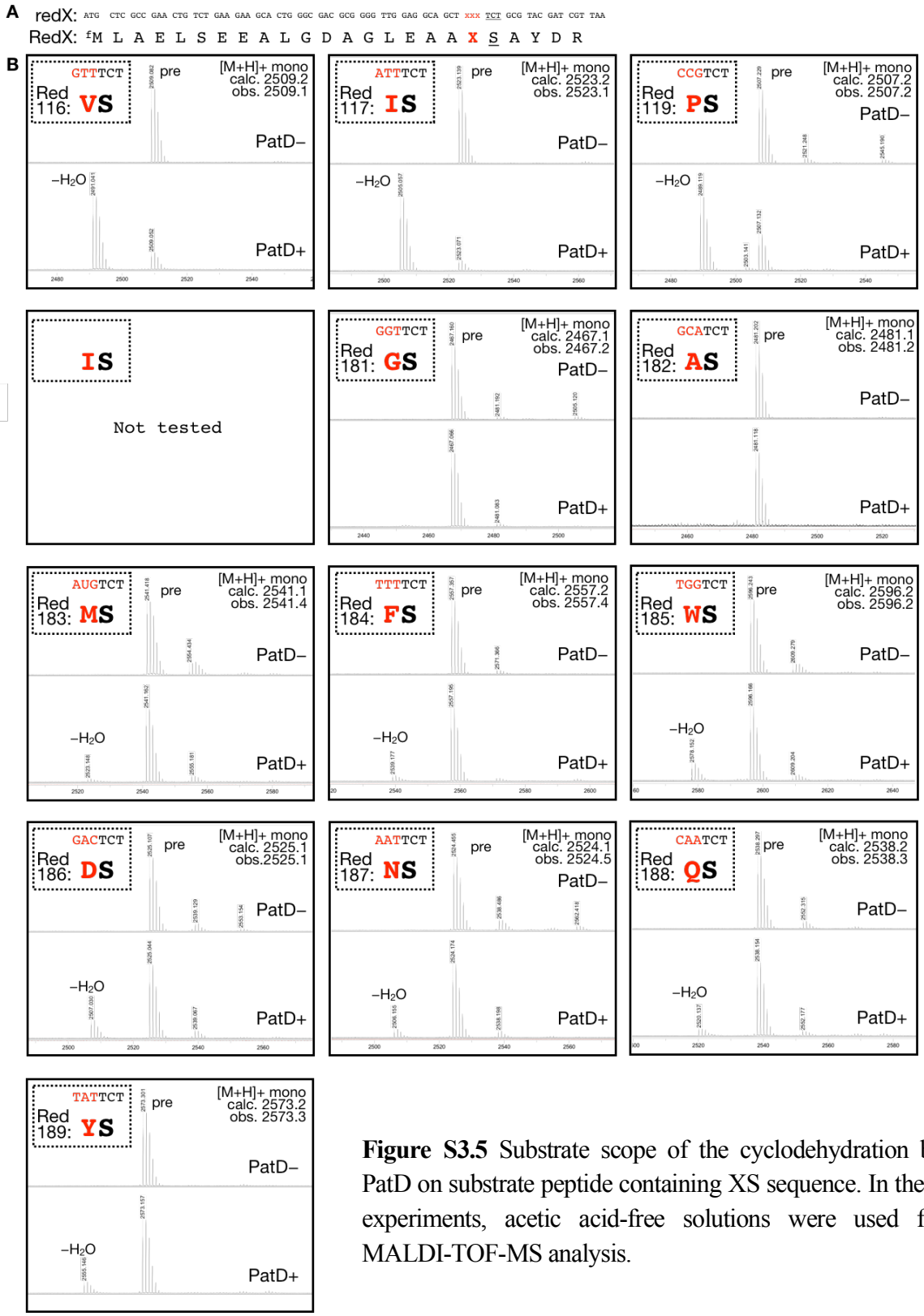

Figure S3.5 Substrate scope of the cyclodehydration by PatD on substrate peptide containing XS sequence. In these experiments, acetic acid-free solutions were used for MALDI-TOF-MS analysis.

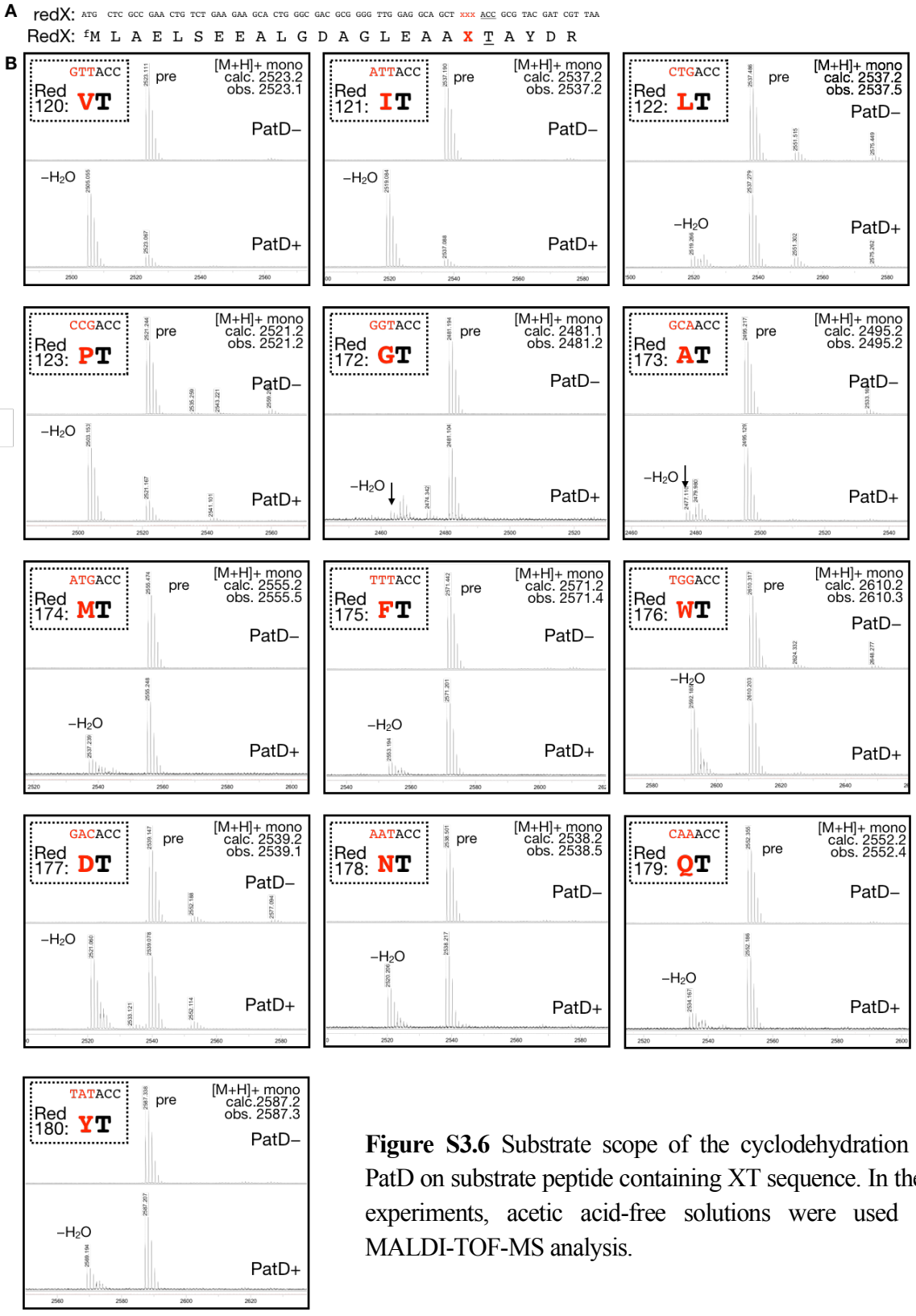

Figure S3.6 Substrate scope of the cyclodehydration by PatD on substrate peptide containing XT sequence. In these experiments, acetic acid-free solutions were used for MALDI-TOF-MS analysis.

Based on the results, the model peptides containing VT, IT, and PT sequences in the region to be modified were further used for the reduction experiments (**Figure S3.7 and S3.8**). The cyclodehydration products were incubated with sodiumcyanoborohydride in acidic conditions (the same conditions to the reduction of thiazoline described in the main text), and MALDI-TOF-MS of the reaction products suggested hydrolysis rather than reduction took place since major peak was corresponding to the starting peptide containing Thr residue. In order to suppress the competiting hydrolysis, the reduction reaction was next attempted in pH 6. Although competing hydrolysis was suppressed, but little significant peak shift was observed corresponding to the reduction reaction. As a short conclusion, for the reduction of oxazoline moiety, other reducing conditions such as reducing agents, solvents and conditions would be required. However, during the attempt at the reduction of oxazoline moieties, mutagenesis analysis provided insights into the substrate tolerance of the cyclodehydratase PatD for substrate peptides containing Ser/Thr residues, which was dismissed in the previous our work.

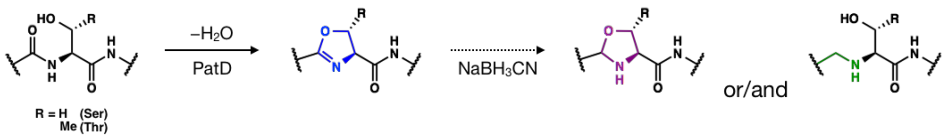

Figure S3.7 Reaction scheme to be tested: Reduction of peptide-embedded oxazoline moiety.

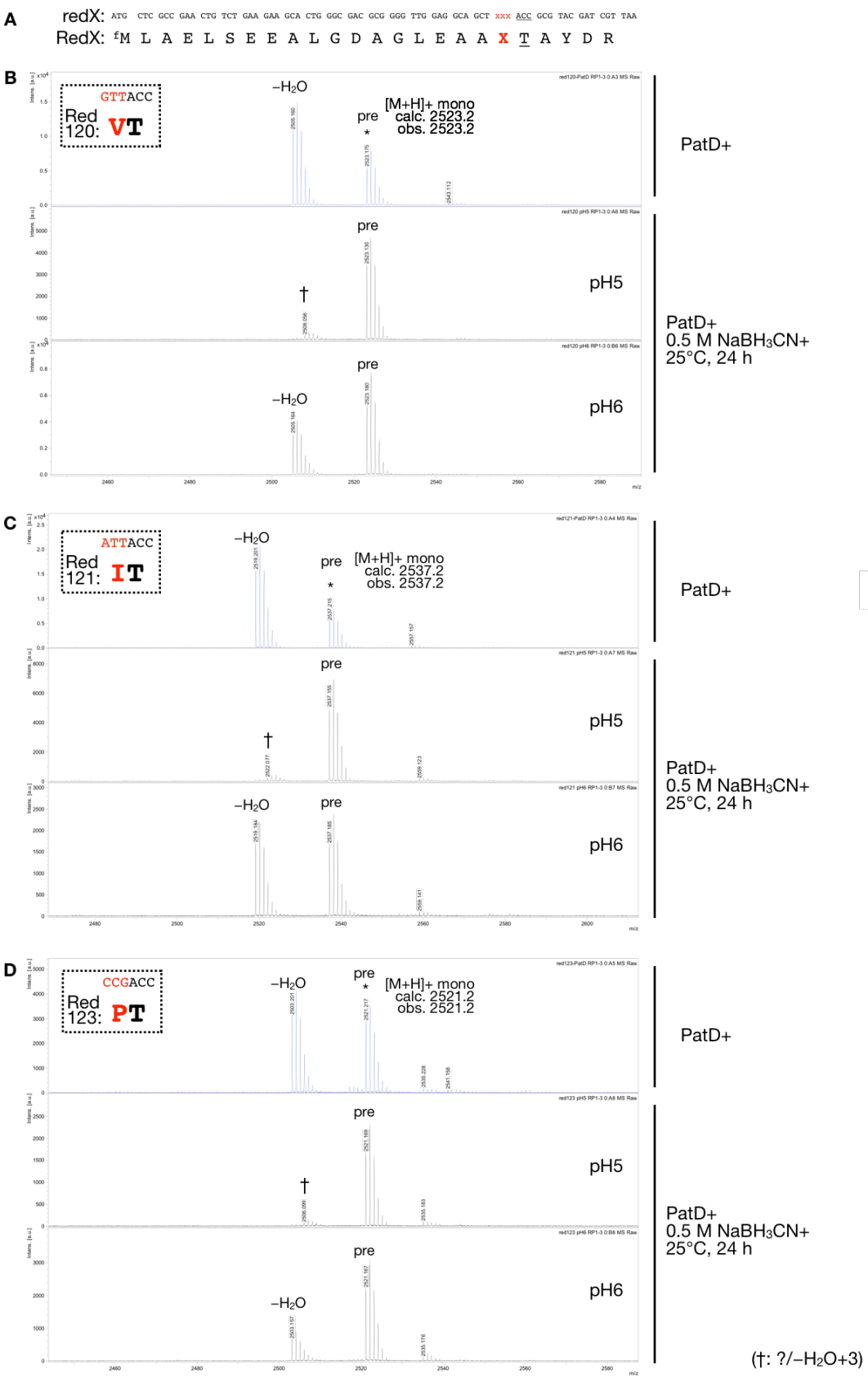
A
redX: ATG CTC GCC GAA CTG TCT GAA GAA GCA CTG GGC GAC GCG GGG TTG GAG GCA GCT xxx ACC GCG TAC GAT CGT TAA
RedX: fM L A E L S E E A L G D A G L E A A X T A Y D R
B
GTTACC
Red 120: VT
−H2O
pre
[M+H]+ mono
calc. 2523.2
obs. 2523.2
PatD+
pH5
†
PatD+
0.5 M NaBH3CN+
25°C, 24 h
pH6
C
ATTACC
Red 121: IT
−H2O
pre
[M+H]+ mono
calc. 2537.2
obs. 2537.2
PatD+
pH5
†
PatD+
0.5 M NaBH3CN+
25°C, 24 h
pH6
D
CCGACC
Red 123: PT
−H2O
pre
[M+H]+ mono
calc. 2521.2
obs. 2521.2
PatD+
pH5
†
PatD+
0.5 M NaBH3CN+
25°C, 24 h
pH6
(†: ?/−H2O+3)

Figure S3.8 Attempt at the reduction of oxazoline-containing peptides (A) The general sequence of DNA templates encoding model peptides containing mutated residue and Thr to be modified, where x and X are mutated position, which is designated in MALDI-TOF-MS spectra below. (B-D) MALDI-TOF-MS spectra of the cyclodehydration and the subsequent reduction products of each model peptides. Reaction conditions are also shown. The DNA sequences and substrate peptide sequences are shown in dashed line.

MS/MS analysis of several mutants of precursor peptide

When the reduction product, which was corresponding to the peptide containing Ψ[CH_2NH] structure, was analyzed by MS/MS analysis, a unidentified fragment peak was observed. (**Figure S3.9**) The unidentified peak was not corresponding to any b or y ions and internal fragment peaks. Based on the molecular mass, it was hypothesized that the structure corresponding to the unidentified peak was C-terminal fragment of the reduction product fragmented at the newly introduced Ψ[CH_2NH] structure: z ion.

To test this hypothesis, two model mutants were designed with a single mutation at either N-terminal or C-terminal region of the Ψ[CH_2NH] structure and the cyclodehydration-reduction products of the mutant peptides were analyzed by MS/MS analysis (**Figure S3.10 and S3.11**). With N-terminal or C-terminal mutations, analogous fragment peaks were observed, supporting the proposed structure for the unidentified peak.

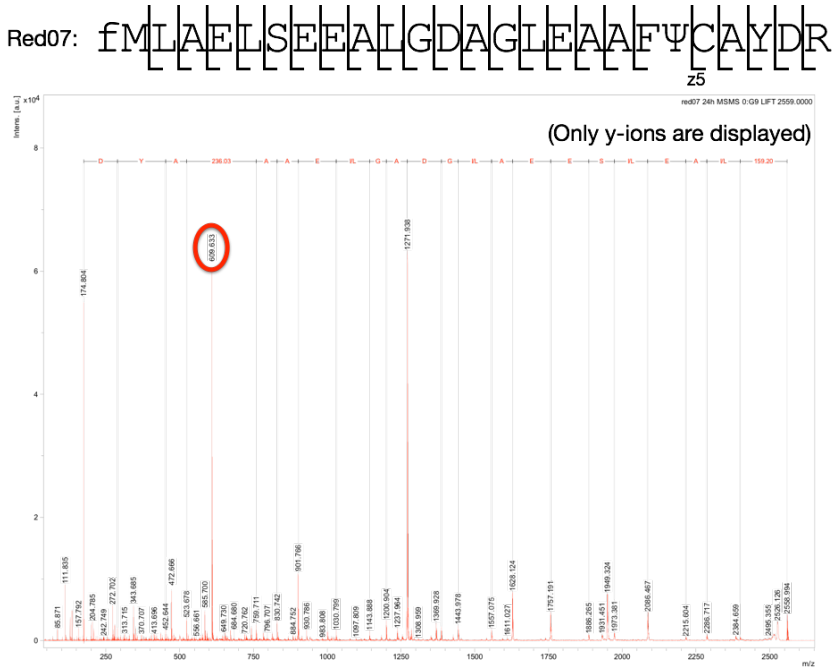

Figure S3.9 MS/MS analysis of cyclodehydration-reduction product with a model peptide containing C-terminal sequence, "FCAYDR." The unidentified fragment peak (*m/z* = 609.6) is highlighted. This is the identical data to **Figure 3.4** placed here for comparison. Proposed structure for the unidentified fragment peak is also presented.

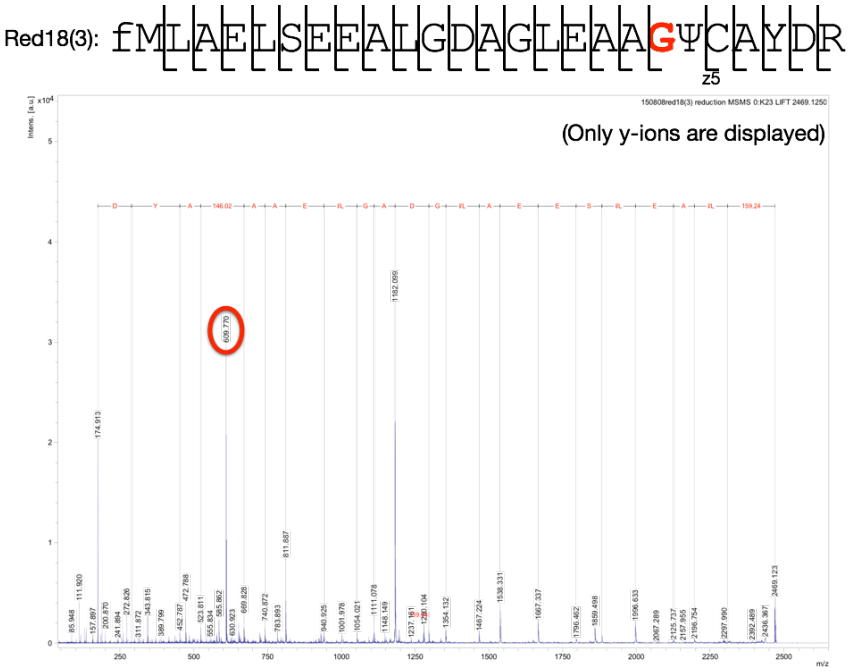

Figure S3.10 MS/MS analysis of cyclodehydration-reduction product with a N-terminal mutated sequence, "GCAYDR", where the Gly (G) was mutated from Phe (F). The unidentified fragment peak (*m/z* = 609.8) is highlighted. Proposed structure for the fragment peak is also presented.

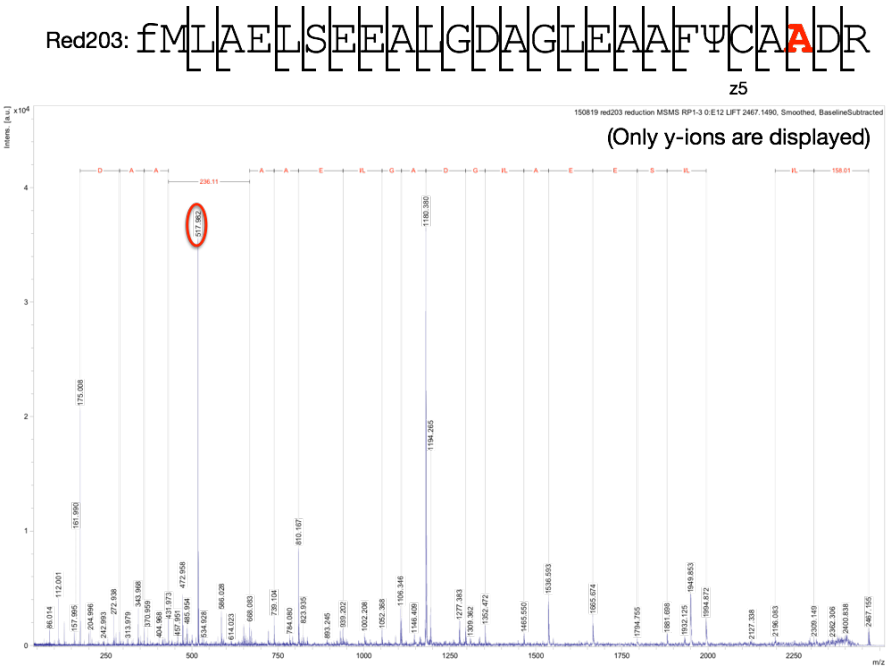

Figure S3.11 MS/MS analysis of cyclodehydration-reduction product with a C-terminal mutated sequence, "FCAADR", where the Ala (A) was mutated from Tyr (Y). The unidentified fragment peak (*m/z* = 518.0) is highlighted. Proposed structure for the fragment peak is also presented.

Starting materials \ Reaction conditions	D_2O 25°C, 2 h	D_2O Buffer (pD 5) 25°C, 2 h	0.5 M $NaBH_3CN$ D_2O Buffer (pD 5) 25°C, 2 h	0.5 M $NaBD_3CN$ D_2O Buffer (pD 5) 25°C, 2 h
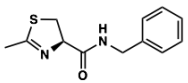 (1)	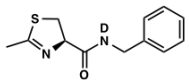 MR 1 (Sample 7)	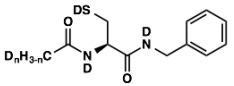 MR 2* (Sample 6)	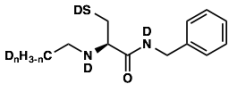 MR 3 (Sample 1)	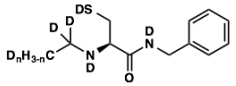 MR 4 (Sample 2)
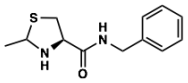 (2)	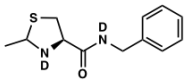 MR 5 (Sample 9)	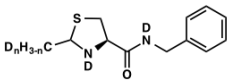 MR 6 (Sample 8)	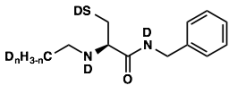 MR 7 (Sample 3)	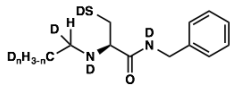 MR 8 (Sample 4)
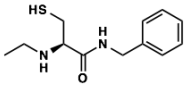 (3)	Not tested	Not tested	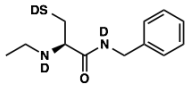 MR 9 (Sample 5-2)	Not tested

Figure S3.12 Summary of the model reactions. Each model compound (1)-(3) was incubated in each reaction condition in NMR tube and the reaction mixture was analyzed by ^{1}H-NMR and ESI-MS for the determination of product structures, and assigned product structures are summarized in this figure. In MR 2, the reaction mixture was incubated for 17 h for the completion of hydrolysis. See the following figures for ^{1}H-NMR charts for each model reaction 1-9 (MR1-9)

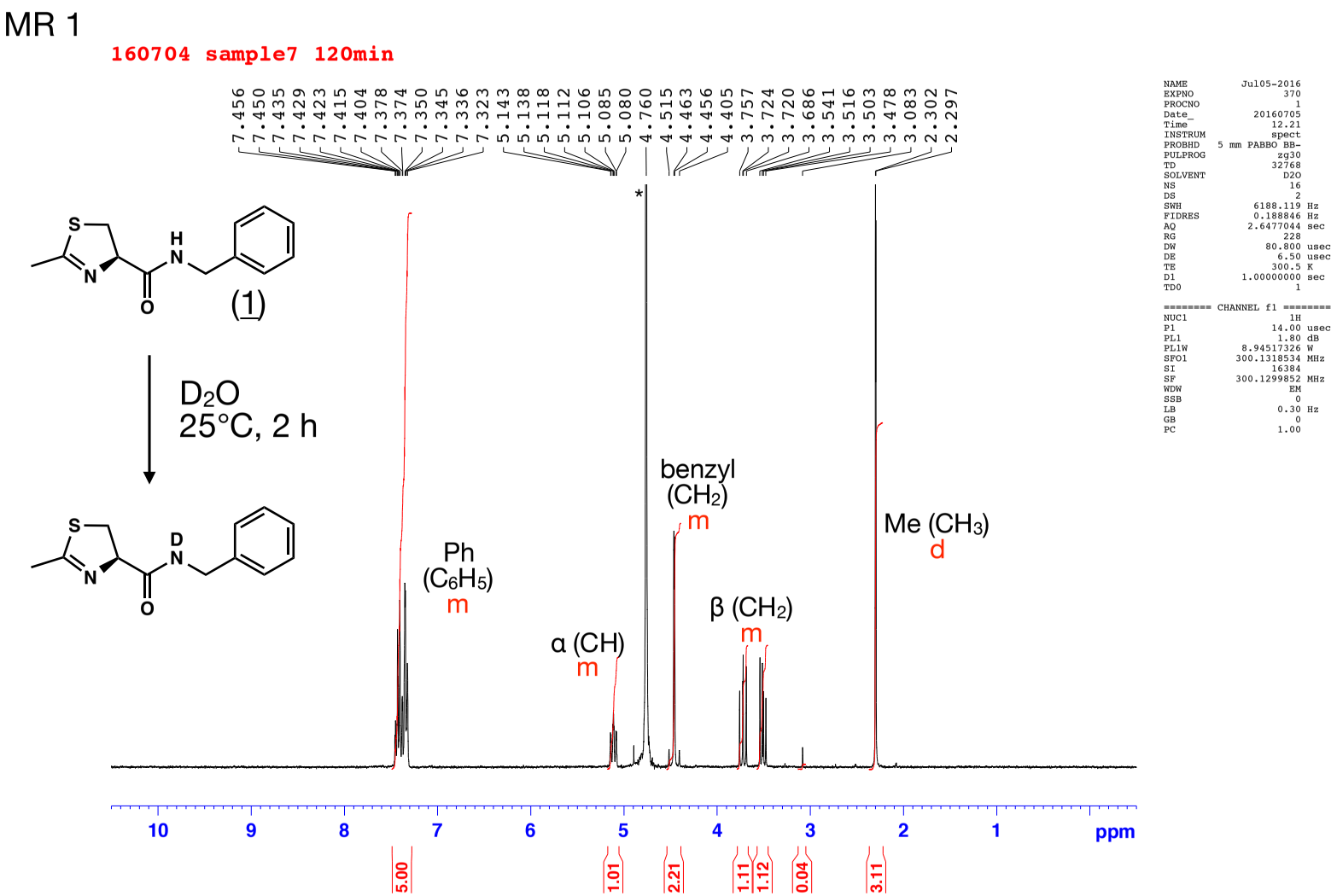

Figure S3.13 1H-NMR chart of the model reaction 1 (MR 1)

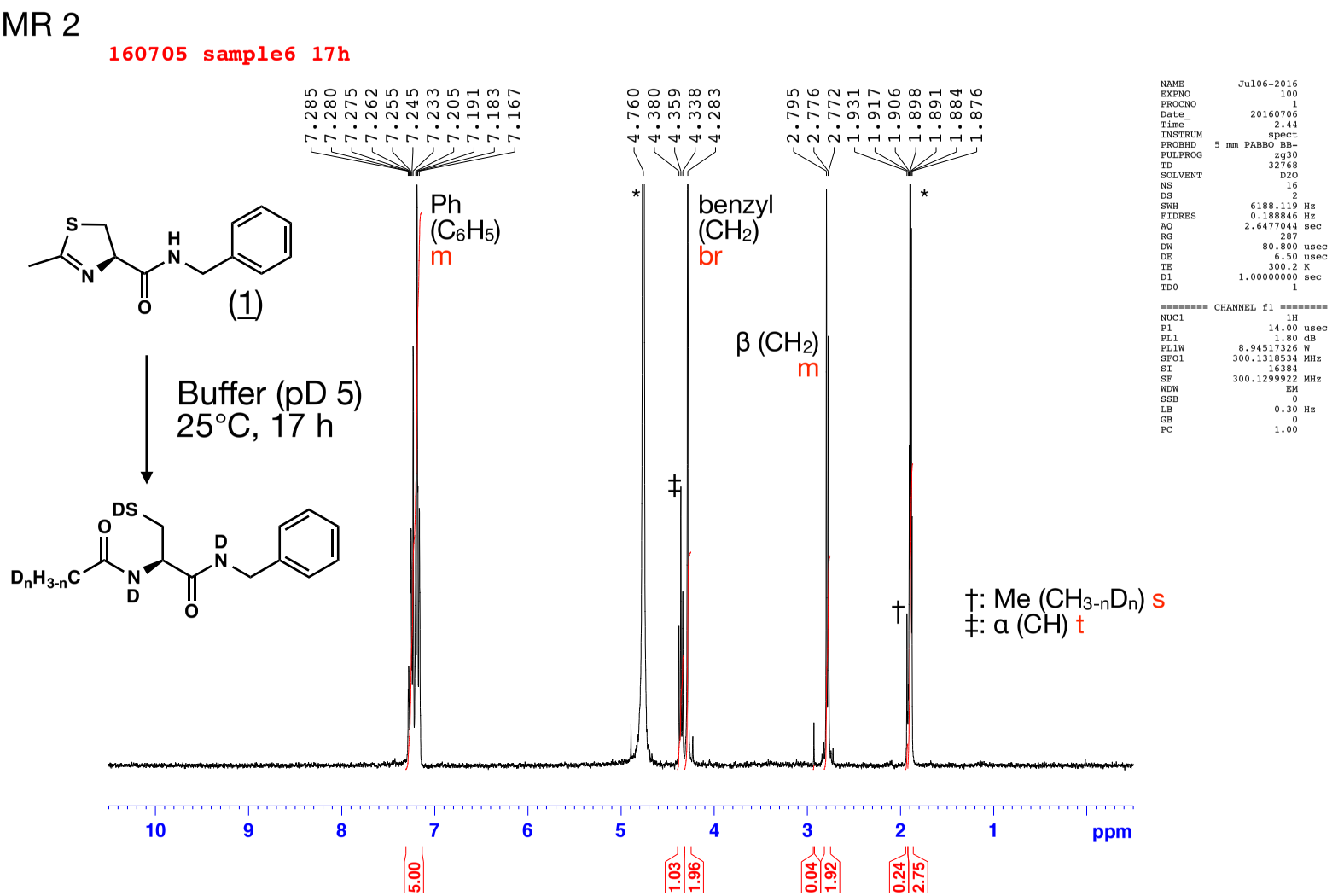

Figure S3.14 1H-NMR chart of the model reaction 2 (MR 2)

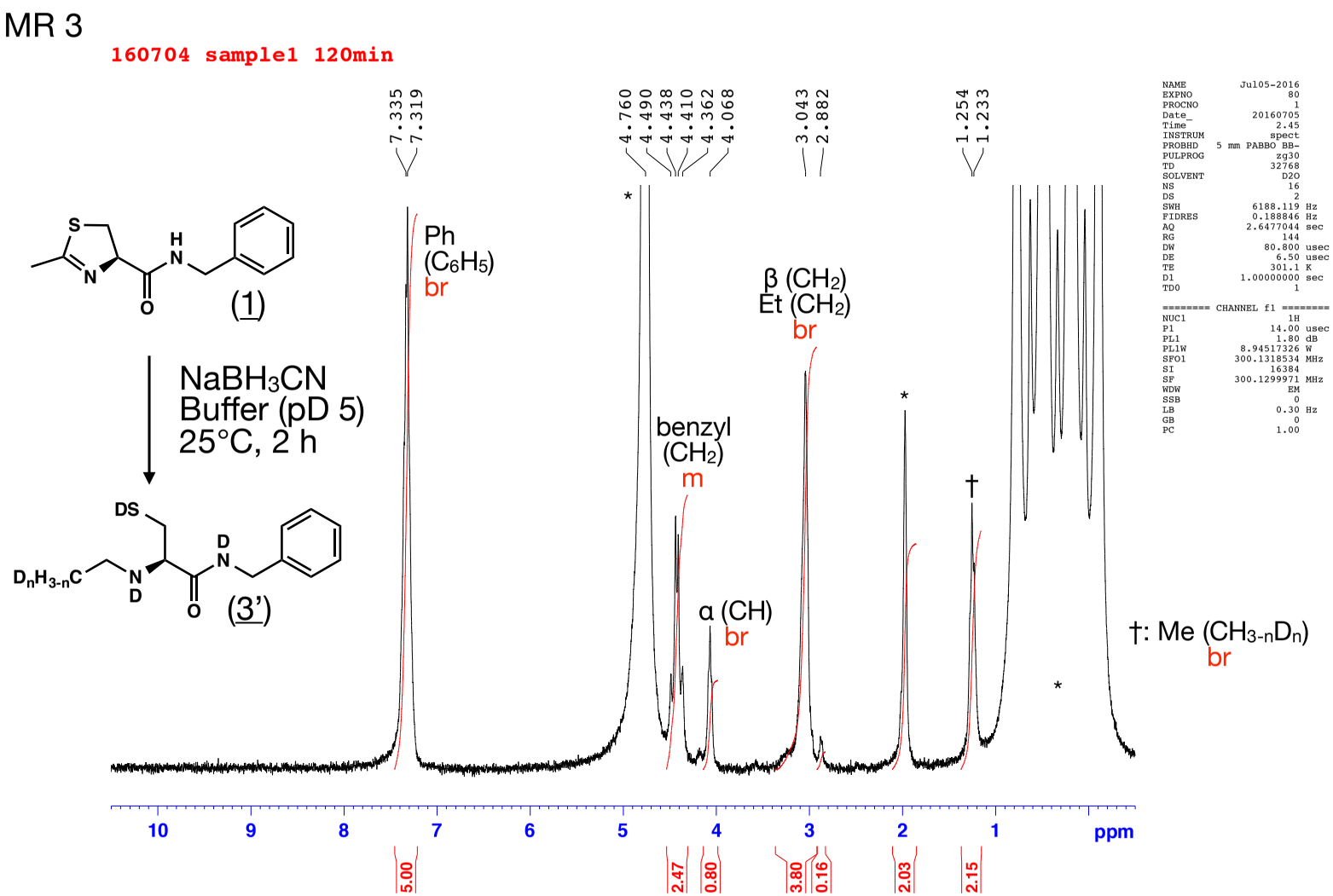

Figure S3.15 1H-NMR chart of the model reaction 3 (MR 3)

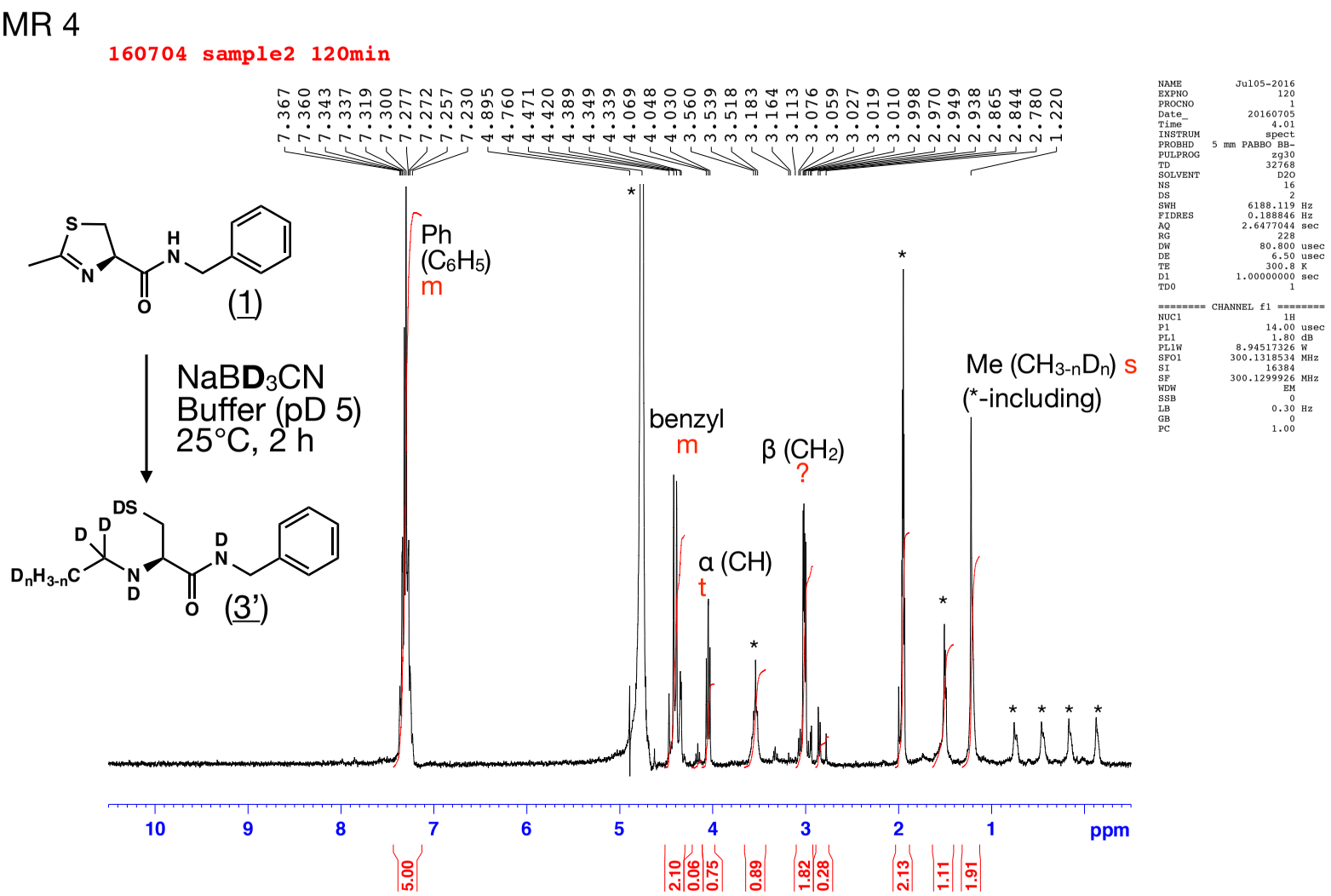

Figure S3.16 1H-NMR chart of the model reaction 4 (MR 4)

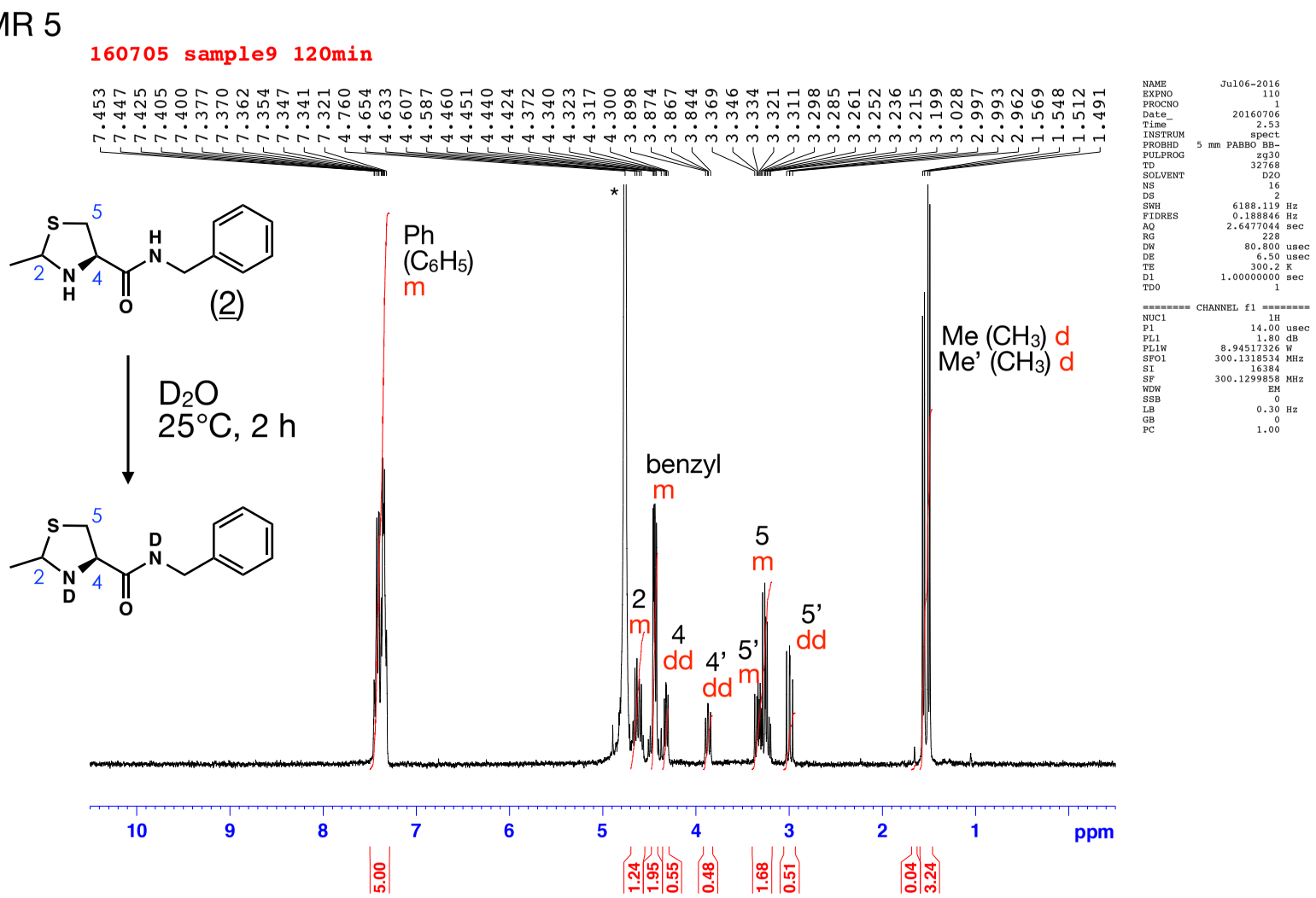

Figure S3.17 1H-NMR chart of the model reaction 5 (MR 5)

MR 6

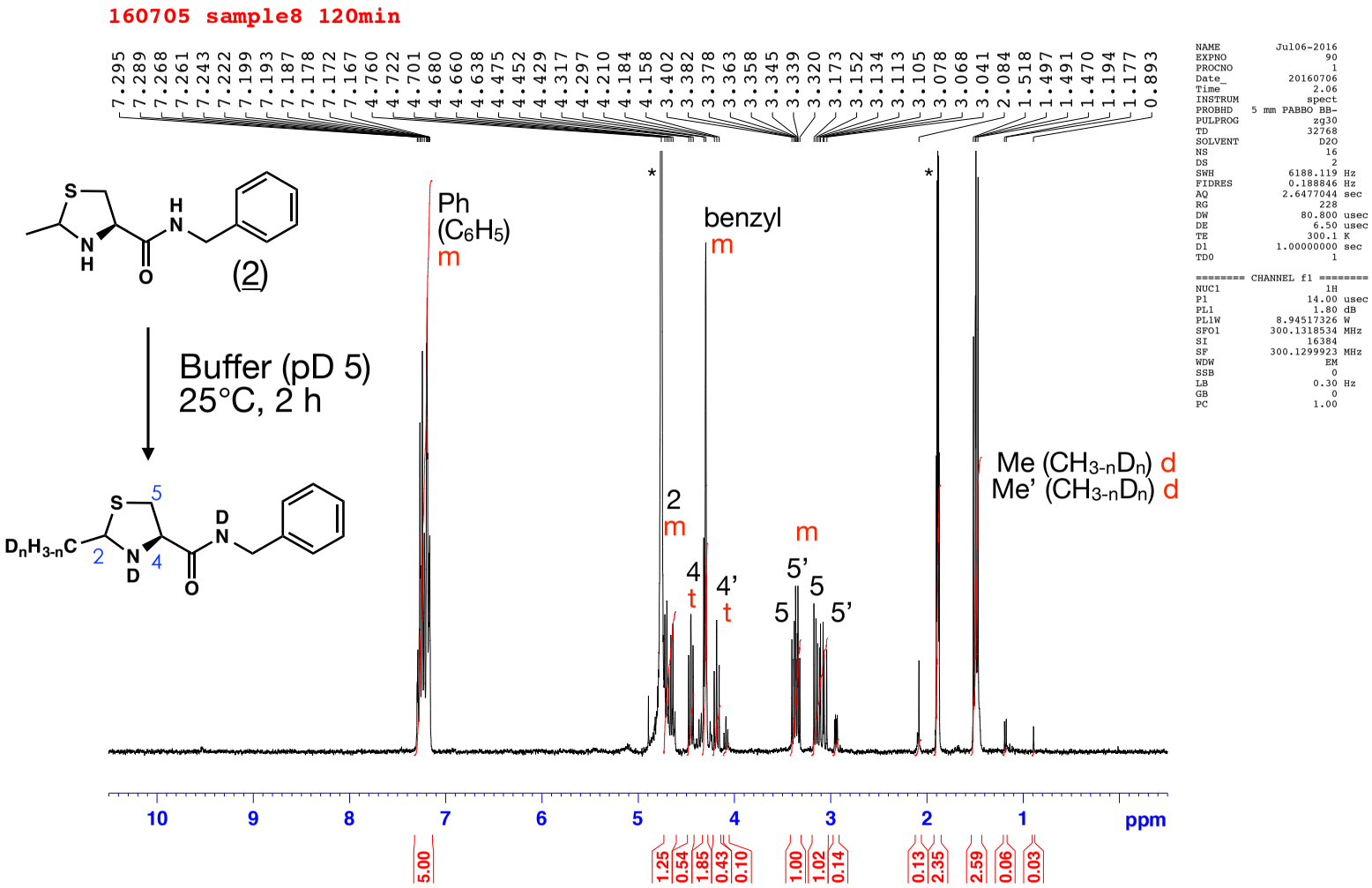

Figure S3.18 1H-NMR chart of the model reaction 6 (MR 6)

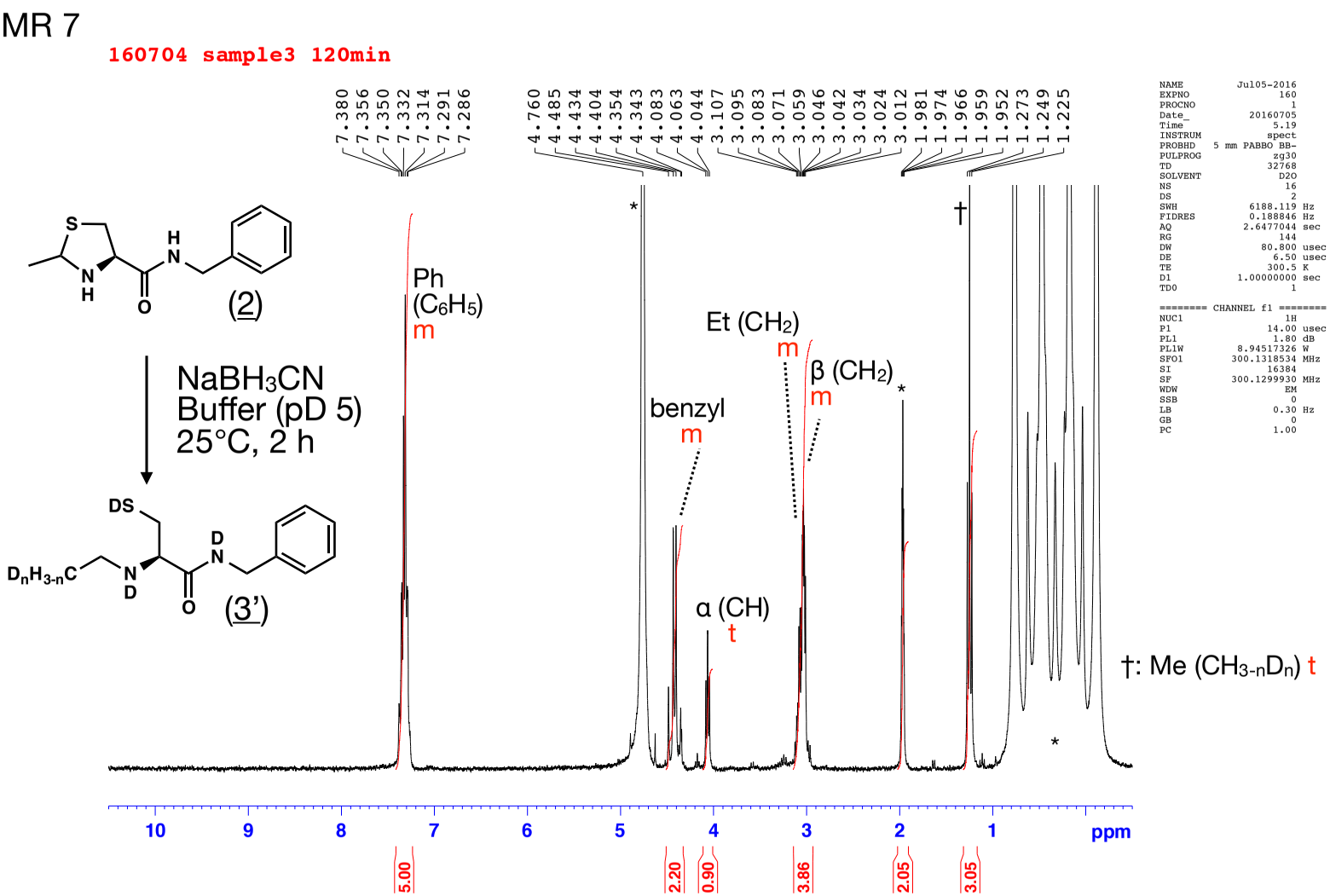

Figure S3.19 1H-NMR chart of the model reaction 7 (MR 7)

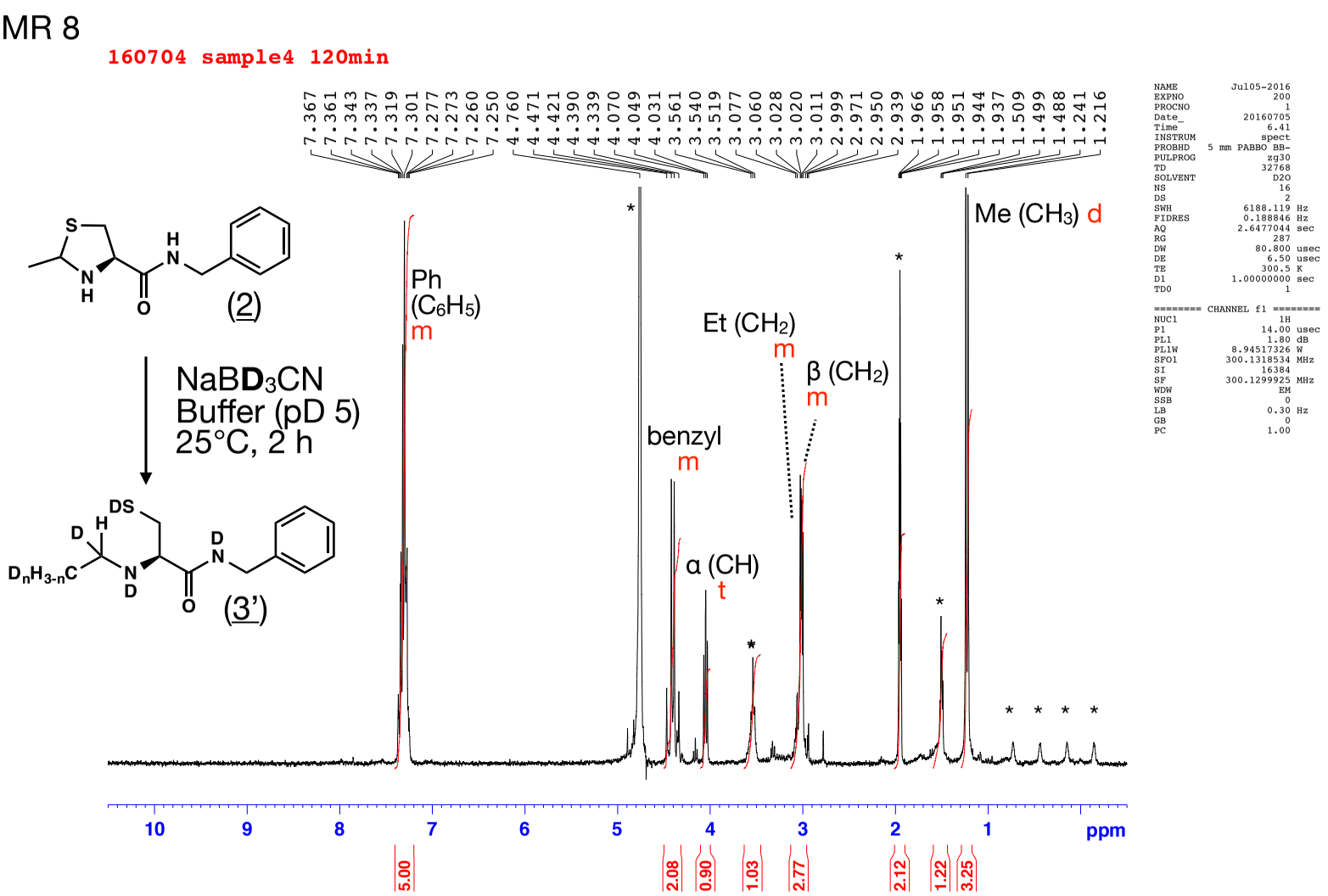

Figure S3.20 1H-NMR chart of the model reaction 8 (MR 8)

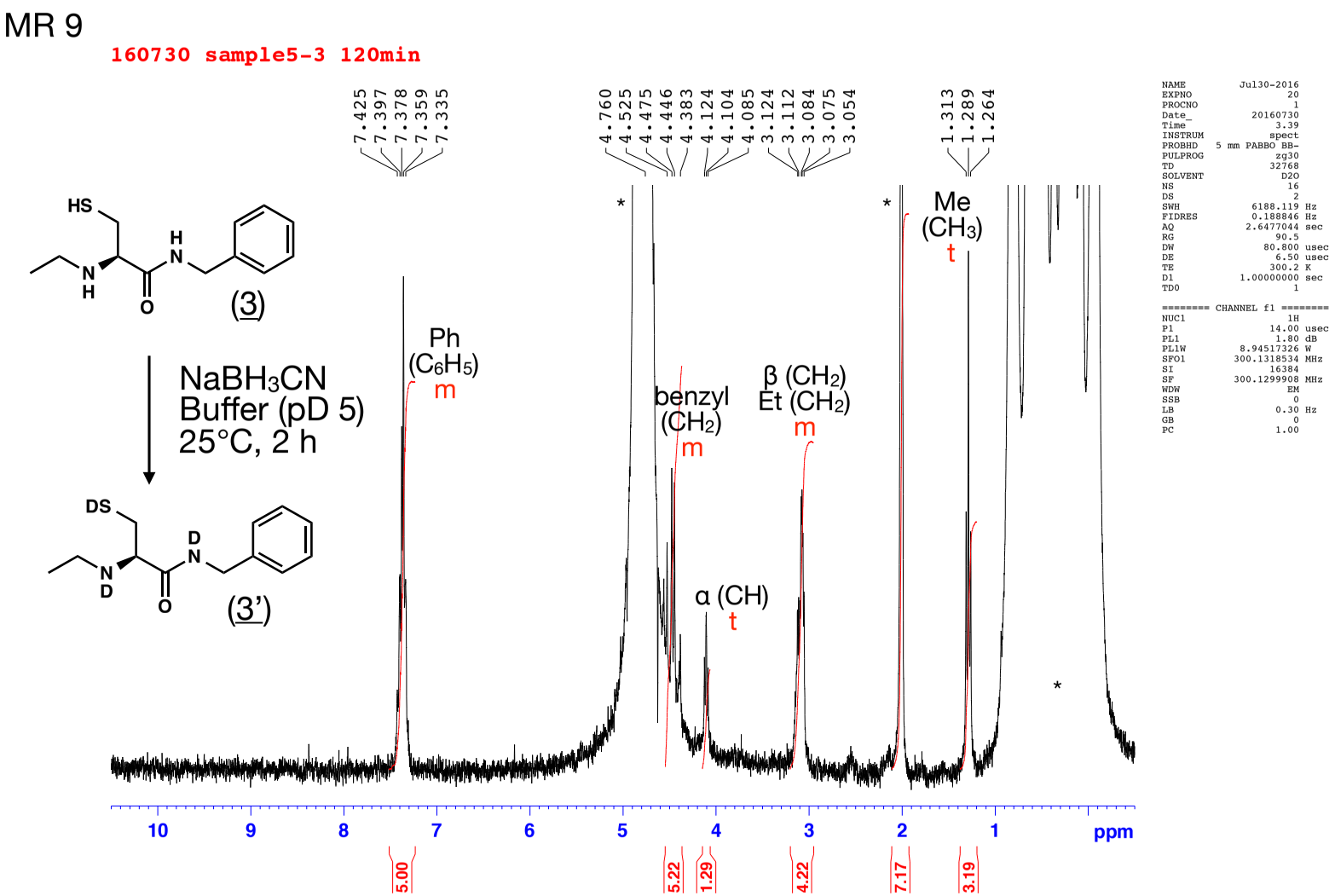

Figure S3.21 1H-NMR chart of the model reaction 9 (MR 9)

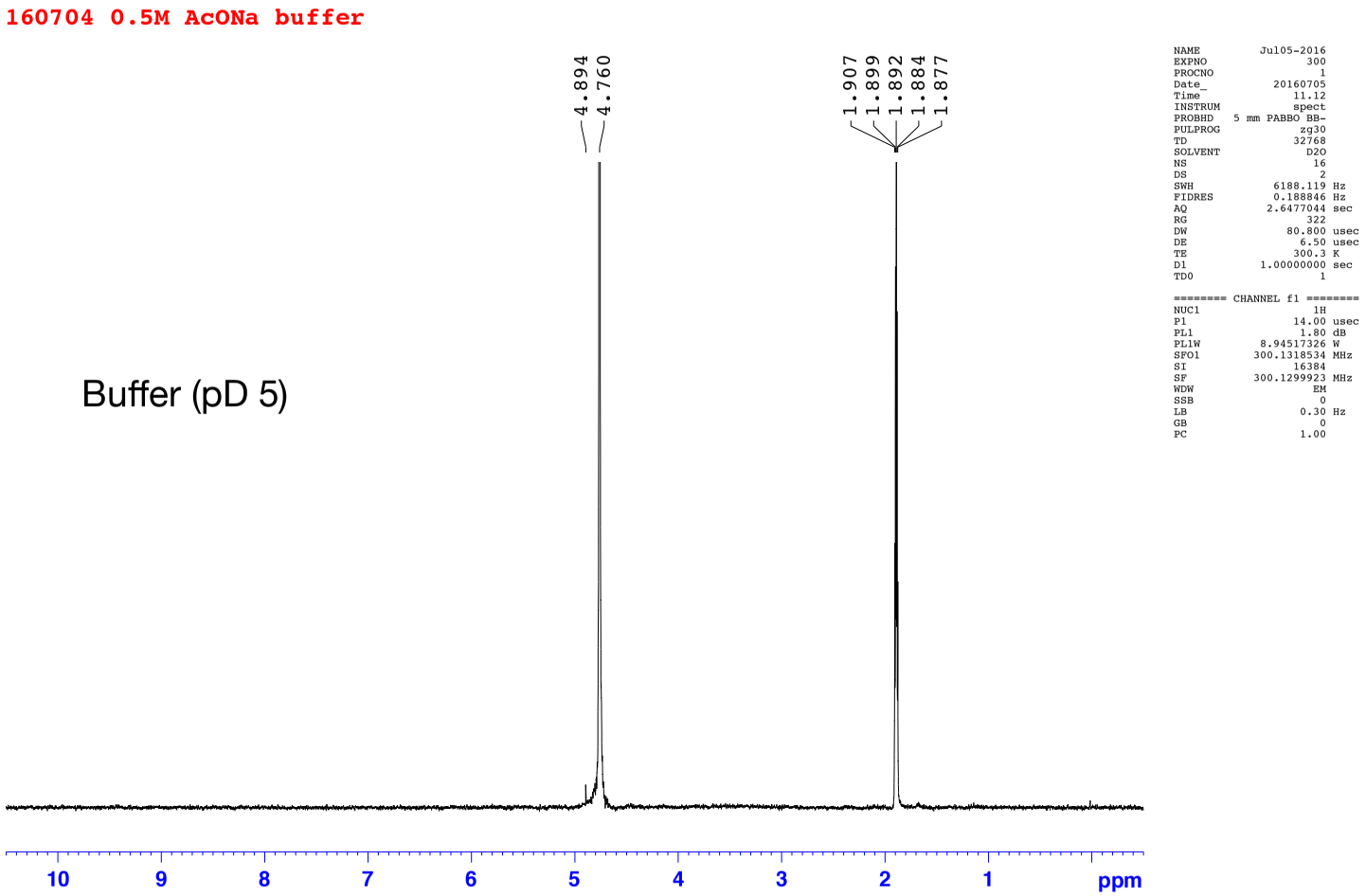

Figure S3.22 1H-NMR chart of the buffer, 0.5 M NaOAc as a control for the model experiments

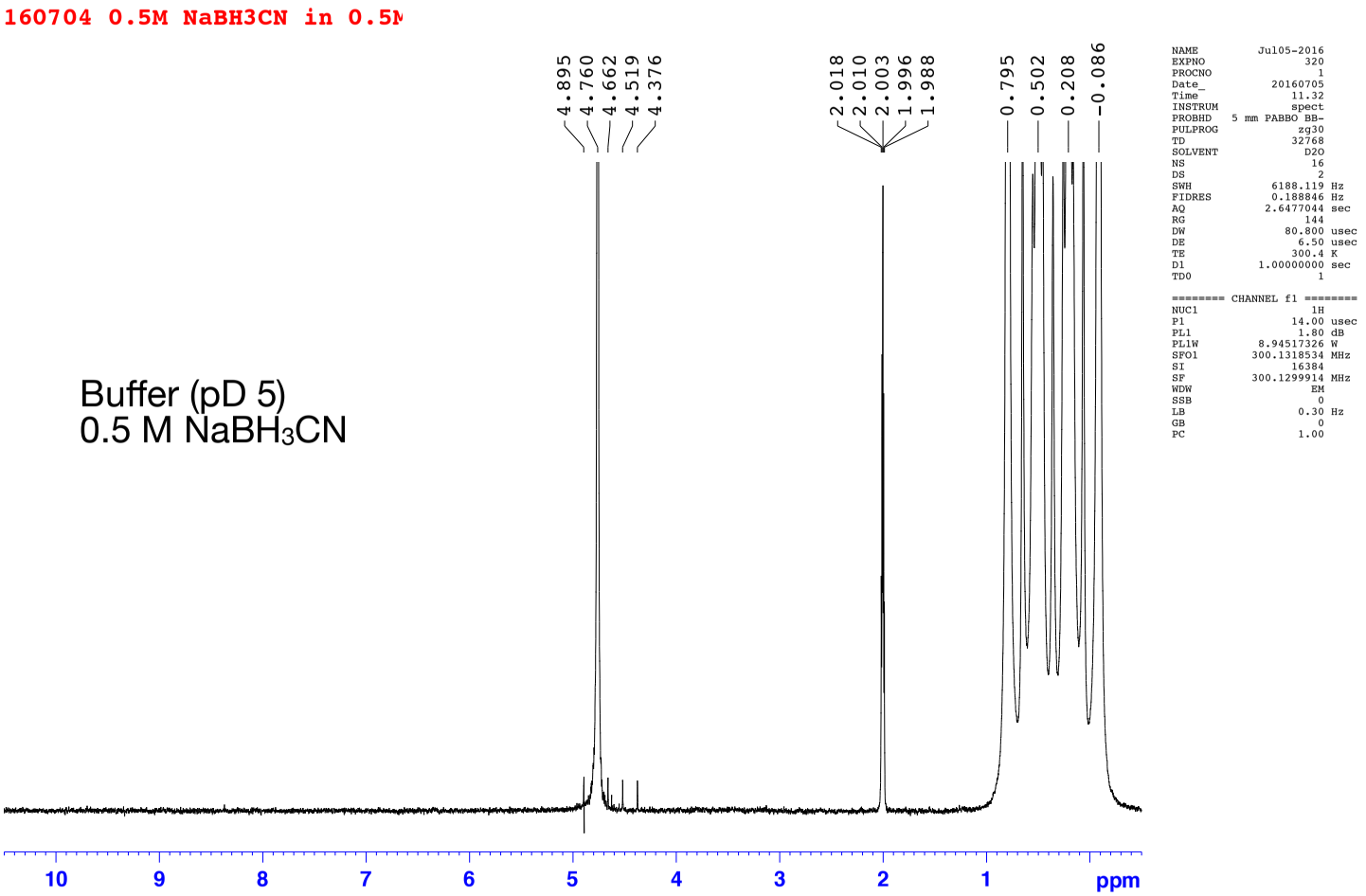

Figure S3.23 1H-NMR chart of 0.5 M $NaBH_3CN$ in the buffer (pD 5) as a control for the model experiments

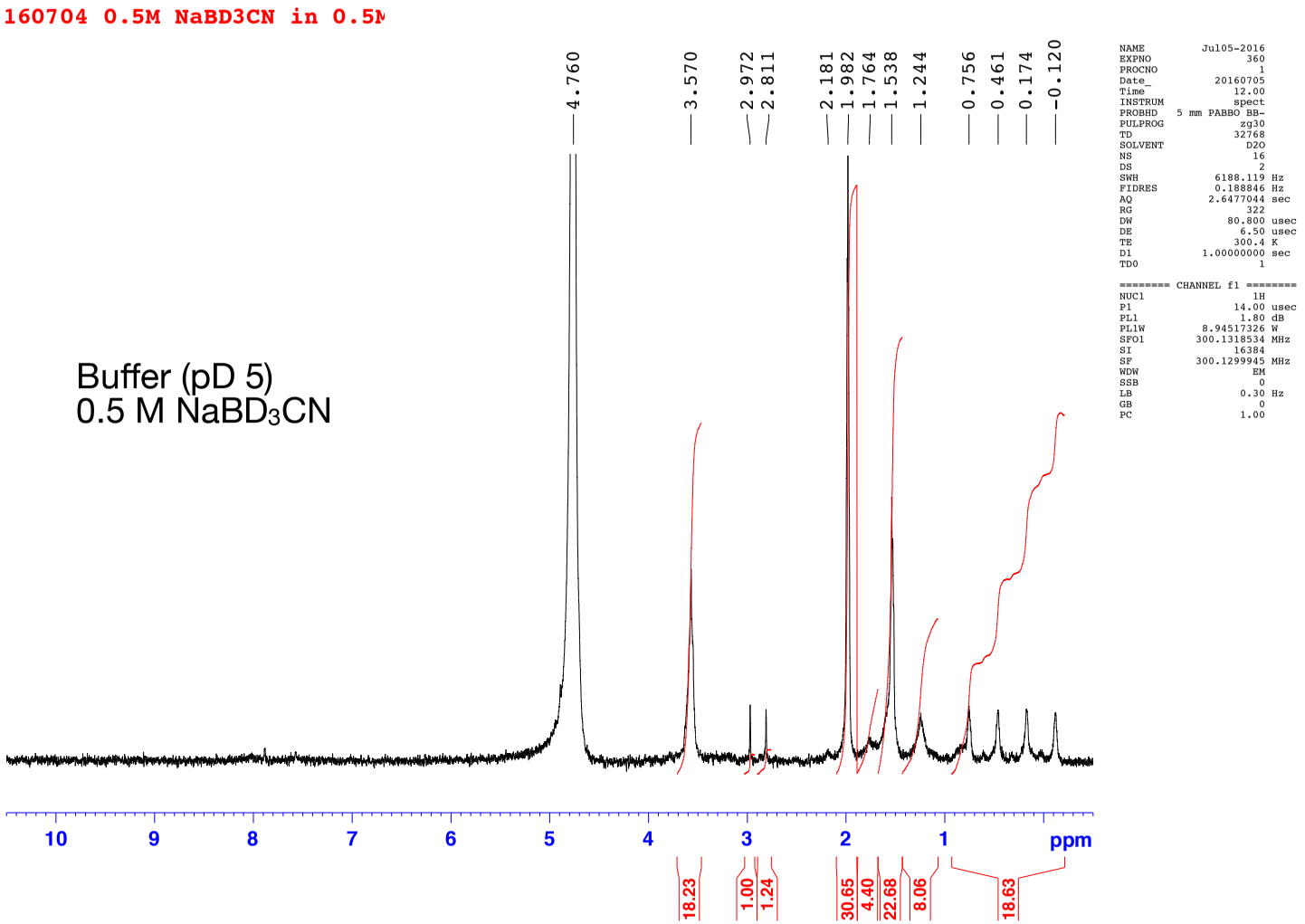

Figure S3.24 1H-NMR chart of 0.5 M $NaBD_3CN$ in the buffer (pD 5) as a control for the model experiments

MR 1

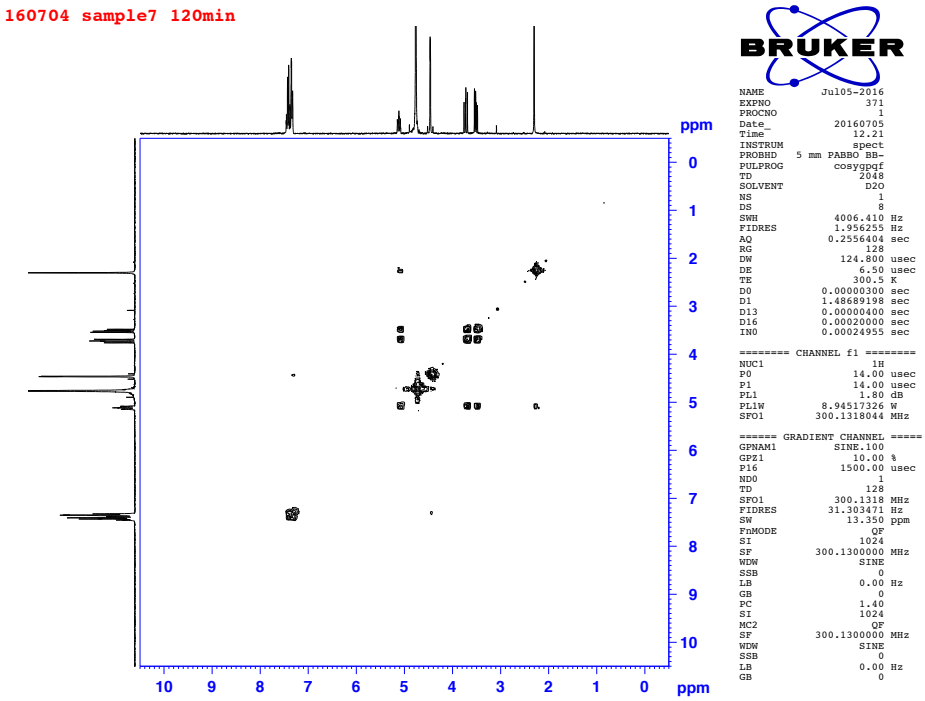

MR 2

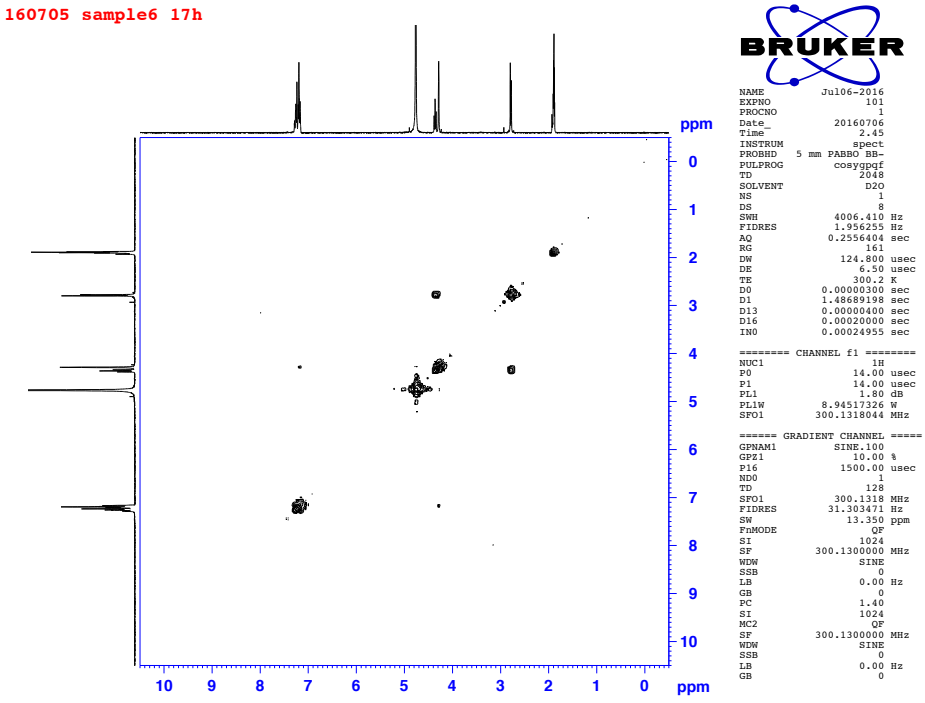

Figure S3.25 H-H COSY spectra of model reactions 1 and 2 (MR 1 and MR 2).

MR 3

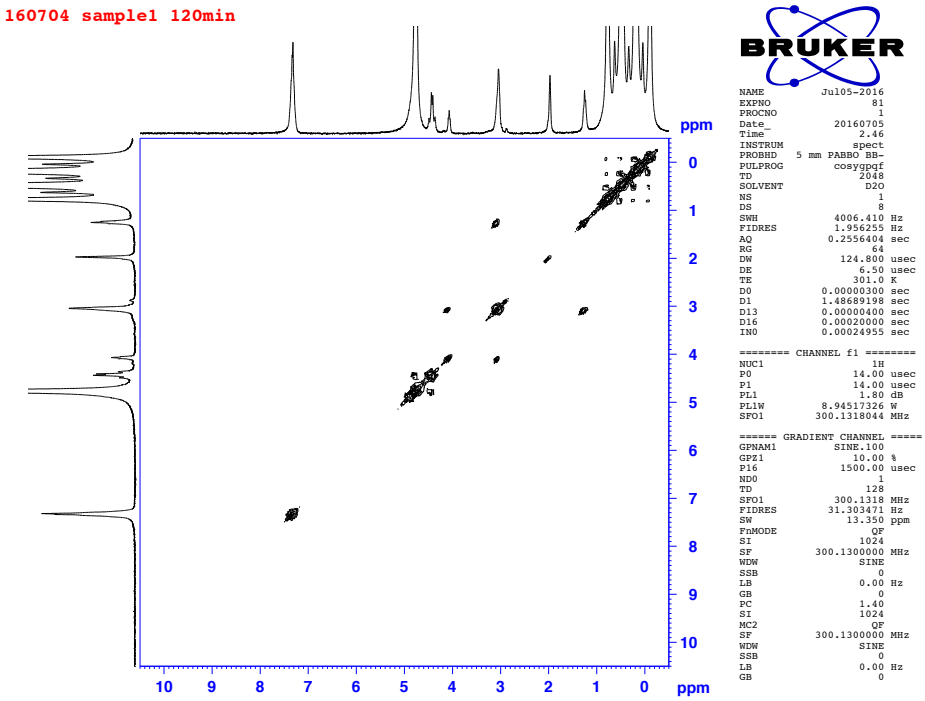

MR 4

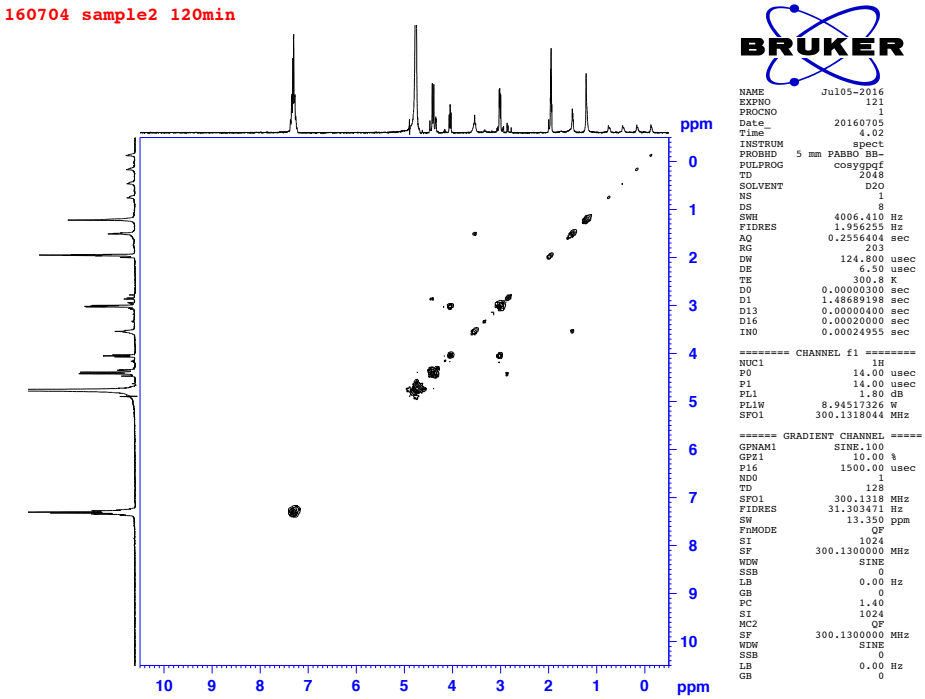

Figure S3.26 H-H COSY spectra of model reactions 3 and 4 (MR 3 and MR 4)

MR 5

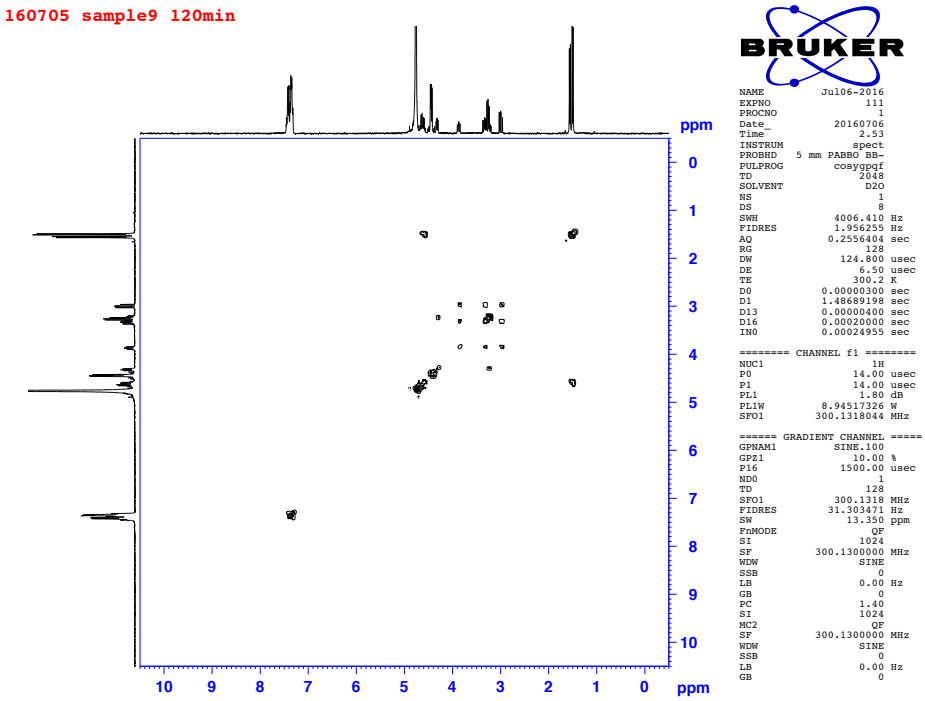

MR 6

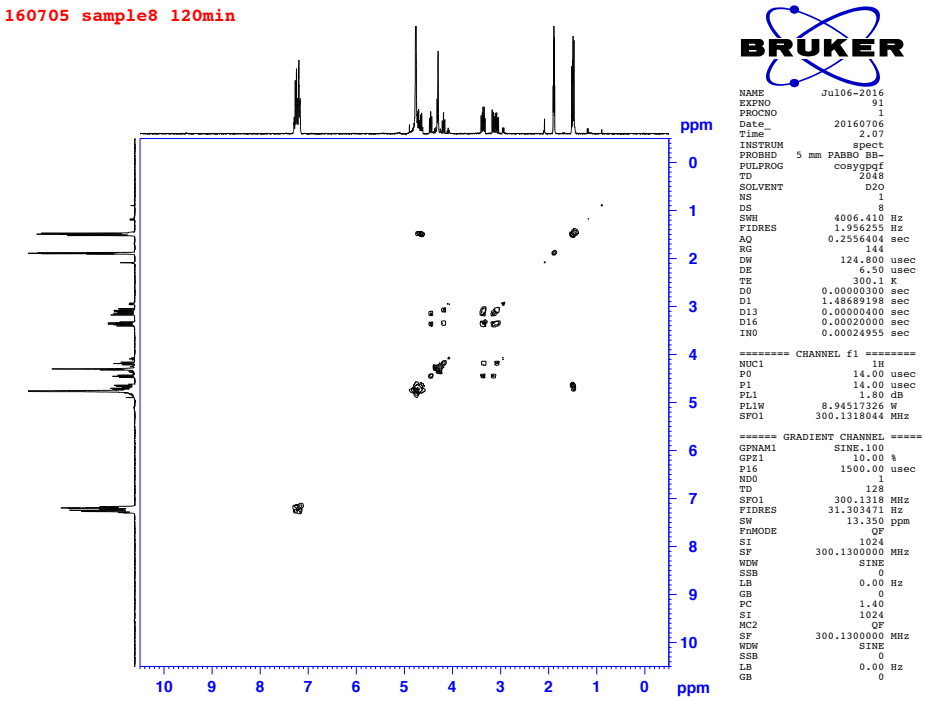

Figure S3.27 H-H COSY spectra of model reactions 5 and 6 (MR 5 and MR 6)

MR 7

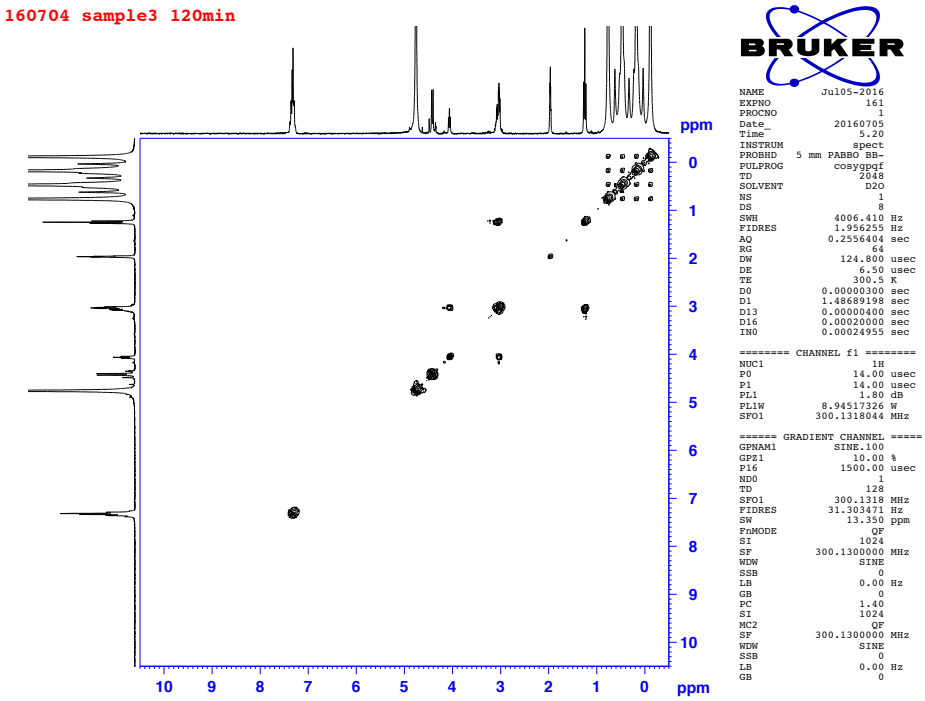

MR 8

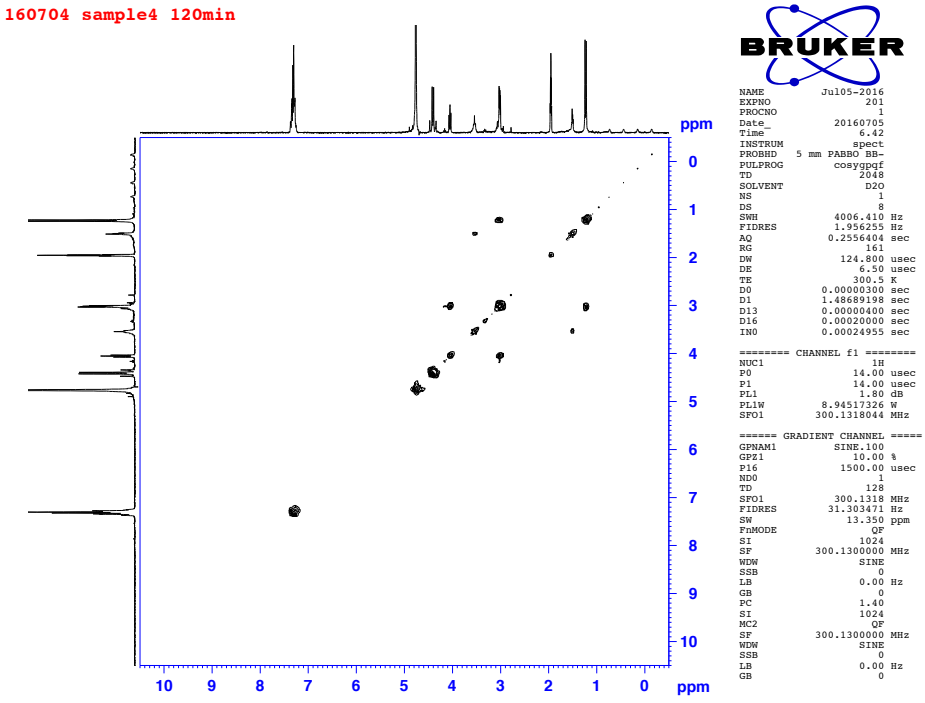

Figure S3.28 H-H COSY spectra of model reactions 7 and 8 (MR 7 and MR 8)

MR 9

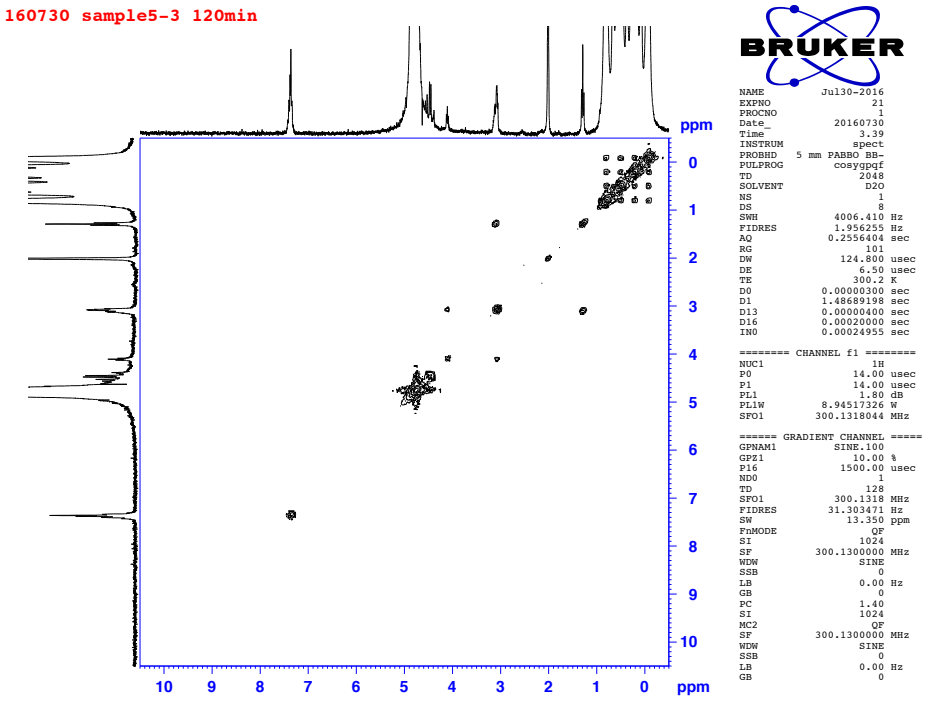

Figure S3.29 H-H COSY spectra of model reactions 9 (MR 9)

Material and methods

All the chemical reagents were purchased from Cambridge Isotope Laboratories, Kanto Chemical, Nacalai Tasque, Sigma-Aldrich Japan, Tokyo Chemical Industry, Wako Pure Chemical Industries, or Watanabe Chemical Industry. All the chemical reagents were used without further purification. All the DNA oligomers were purchased from Eurofins Genomics.

N-acetyl phenyl alanine cyanomethyl ester (AcPhe-CME)

AcPhe-CME was synthesized as previously described.

The cyclodehydratase PatD

The purification of PatD was reported in a literature from our laboratory[97]. In brief, the N-terminally His_{10}-tagged cyclodehyddratase PatD was overexpressed in BL21(DE3) pLysS cells transformed with *patD*/pET16b and purified by Ni-NTA column. The concentration of PatD was determined based on UV-absorbance[135].

DNA oligomers

PatE-pre-lon b.F47:
GGCGTAATACGACTCACTATAGGGTTAACTTTAACAAGGAGAAAAAC
T7EX5.F22: GGCGTAATACGACTCACTATAG
KYred01 a.F44: GGTTAACTTTAACAAGGAGAAAAACATGCTCGCCGAACTGTCTG
KYred01 a.R44: CCAACCCCGCGTCGCCCAGTGCTTCTTCAGACAGTTCGGCGAGC
KYred05 b.R34: GTACGCGCAAAAAGCTGCCTCCAACCCCGCGTCG
KYred07 c.R33: CGAAGCTTAACGATCGTACGCGCAAAAAGCTGC
KYred14 a.F53:
GGTTAACTTTAACAAGGAGAAAAACATGCTCGCCGAACTGTCTGAAGAAGCAC
KYred18 a.R45: GCTGCCTCCAACCCCGCGTCGCCCAGTGCTTCTTCAGACAGTTCG
KYred18 c.R20: CGAAGCTTAACGATCGTACG
KYred18(3) b.R43:CGAAGCTTAACGATCGTACGCGCAACCAGCTGCCTCCAACCCC

KYred23 b.R43: CGAAGCTTAACGATCGTACGCGCAAATAGCTGCCTCCAACCCC

KYred24 b.R43: CGAAGCTTAACGATCGTACGCGCAGTCAGCTGCCTCCAACCCC

KYred25 b.R43: CGAAGCTTAACGATCGTACGCGCATTCAGCTGCCTCCAACCCC

KYred26 b.R43: CGAAGCTTAACGATCGTACGCGCACTTAGCTGCCTCCAACCCC

KYred27 b.R43: CGAAGCTTAACGATCGTACGCGCAACGAGCTGCCTCCAACCCC

KYred28(2) b.R43: CGAAGCTTAACGATCGTACGCGCAGTTAGCTGCCTCCAACCCC

KYred29 b.R43: CGAAGCTTAACGATCGTACGCGCATTGAGCTGCCTCCAACCCC

red99 b.R43: CGAAGCTTAACGATCGTACGCAGATGCAGCTGCCTCCAACCCC

red101 b.R43: CGAAGCTTAACGATCGTACGCAGAAATAGCTGCCTCCAACCCC

red102 b.R43: CGAAGCTTAACGATCGTACGCAGAATAAGCTGCCTCCAACCCC

red103 b.R43: CGAAGCTTAACGATCGTACGCAGAATTAGCTGCCTCCAACCCC

red104 b.R43: CGAAGCTTAACGATCGTACGCAGATTGAGCTGCCTCCAACCCC

red108 b.R43: CGAAGCTTAACGATCGTACGCAGAAACAGCTGCCTCCAACCCC

red111 b.R43: CGAAGCTTAACGATCGTACGCAGACGGAGCTGCCTCCAACCCC

red112 b.R43: CGAAGCTTAACGATCGTACGCGGTAACAGCTGCCTCCAACCCC

red113 b.R43: CGAAGCTTAACGATCGTACGCGGTAATAGCTGCCTCCAACCCC

red114 b.R43: CGAAGCTTAACGATCGTACGCGGTCAGAGCTGCCTCCAACCCC

red115 b.R43: CGAAGCTTAACGATCGTACGCGGTCGGAGCTGCCTCCAACCCC

red115 b.R43: CGAAGCTTAACGATCGTACGCGGTCGGAGCTGCCTCCAACCCC

red133 b.R43: CGAAGCTTAACGATCGTACGCGCAAACAGCTGCCTCCAACCCC

red134(2) b.R43: CGAAGCTTAACGATCGTACGCGCAAGGAGCTGCCTCCAACCCC

red135 b.R43: CGAAGCTTAACGATCGTACGCGCACATAGCTGCCTCCAACCCC

red136 b.R43: CGAAGCTTAACGATCGTACGCGCACCAAGCTGCCTCCAACCCC

red172 b.R43: CGAAGCTTAACGATCGTACGCGGTACCAGCTGCCTCCAACCCC

red173 b.R43: CGAAGCTTAACGATCGTACGCGGTTGCAGCTGCCTCCAACCCC

red174 b.R43: CGAAGCTTAACGATCGTACGCGGTCATAGCTGCCTCCAACCCC

red175 b.R43: CGAAGCTTAACGATCGTACGCGGTAAAAGCTGCCTCCAACCCC

red176 b.R43: CGAAGCTTAACGATCGTACGCGGTCCAAGCTGCCTCCAACCCC

red177 b.R43: CGAAGCTTAACGATCGTACGCGGTGTCAGCTGCCTCCAACCCC

red178 b.R43: CGAAGCTTAACGATCGTACGCGGTATTAGCTGCCTCCAACCCC

red179 b.R43: CGAAGCTTAACGATCGTACGCGGTTTGAGCTGCCTCCAACCCC

red180 b.R43: CGAAGCTTAACGATCGTACGCGGTATAAGCTGCCTCCAACCCC

red181 b.R43: CGAAGCTTAACGATCGTACGCAGAACCAGCTGCCTCCAACCCC

red183 b.R43: CGAAGCTTAACGATCGTACGCAGACATAGCTGCCTCCAACCCC

red184 b.R43: CGAAGCTTAACGATCGTACGCAGAAAAAGCTGCCTCCAACCCC

red185 b.R43: CGAAGCTTAACGATCGTACGCAGACCAAGCTGCCTCCAACCCC

red186 b.R43: CGAAGCTTAACGATCGTACGCAGAGTCAGCTGCCTCCAACCCC

red203 b.R43: CGAAGCTTAACGATCTGCCGCGCAAAAAGCTGCCTCCAACCCC

red276 b.R43: CGAAGCTTAACGATCGTACGCGCATGCAGCTGCCTCCAACCCC

red277 b.R43: CGAAGCTTAACGATCGTACGCGCACAGAGCTGCCTCCAACCCC

red278 b.R43: CGAAGCTTAACGATCGTACGCGCAATGAGCTGCCTCCAACCCC

red279 b.R43: CGAAGCTTAACGATCGTACGCGCAATAAGCTGCCTCCAACCCC

DNA templates

DNA templates coding precursor peptides were prepared using primer extension followed by multistep PCR reactions. For the information of primer sets corresponding to teach DNA template, see the **Table 3.1** below. The polymerase reaction mixture for both extension and PCR reaction contains: 10 mM Tris·HCl (pH 9.0), 50 mM KCl, 2.5 mM $MgCl_2$, 0.25 mM dNTPs, 0.1% (v/v) Triton X-100, and Taq DNA polymerase.

In primer extension, appropriate forward and reverse primers (1 μM each) were mixed in the polymerase reaction mixture. The primer extension reaction was performed in a 100 μl scale, by denaturing (95°C for 1 min), followed by 5 cycles of annealing (50°C for 1 min) and extension (72°C for 1 min). The primer extension reaction product was 200-fold diluted by the polymerase reaction mixture and amplified using the appropriate forward and reverse primers (0.5 μM each) with a 100 μl scale, by 5 cycles of denaturing (95°C for 40 s), annealing (50°C for 40 s), and extension (72°C for 40 s). The resulting PCR mixture was again 200-fold diluted by the polymerase

reaction mixture and amplified using the appropriate forward and reverse primers (0.5 μM each) in a 200 μl scale, by 12 cycles of denaturing (95°C for 40 s), annealing (50°C for 40 s), and extension (72°C for 40 s). For some DNA templates, the extension products were directly amplified in the conditions of final PCR. The resulting DNA was purified by phenol/chloroform extraction and ethanol precipitation and then dissolved in 20 μl of water and directly used for *in vitro* translation reaction.

Table 3.1 DNA oligomers for the preparation of DNA templates for translation.

	Primer extension		1st PCR		Final PCR	
	Forward	Reverse	Forward	Reverse	Forward	Reverse
red07	KYred01 a.F44	KYred01 a.R44	PatE-pre-Ion b.F47	**KYred05 b.R34**	T7EX5.F22	KYred07 c.R33
red18(3)	KYred14 a.F53	KYred18 a.R45	PatE-pre-Ion b.F47	KYred18(3) b.R43	T7EX5.F22	KYred18(3) b.R43
red23	KYred14 a.F53	KYred18 a.R45	PatE-pre-Ion b.F47	KYred23 b.R43	T7EX5.F22	KYred18 c.R20
red24	KYred14 a.F53	KYred18 a.R45	PatE-pre-Ion b.F47	KYred24 b.R43	T7EX5.F22	KYred18 c.R20
red25	KYred14 a.F53	KYred18 a.R45	PatE-pre-Ion b.F47	KYred25 b.R43	T7EX5.F22	KYred18 c.R20
red26	KYred14 a.F53	KYred18 a.R45	PatE-pre-Ion b.F47	KYred26 b.R43	T7EX5.F22	KYred18 c.R20
red27	KYred14 a.F53	KYred18 a.R45	PatE-pre-Ion b.F47	KYred27 b.R43	T7EX5.F22	KYred18 c.R20
red28(2)	KYred14 a.F53	KYred18 a.R45	PatE-pre-Ion b.F47	KYred28(2) b.R43	T7EX5.F22	KYred18 c.R20
red29	KYred14 a.F53	KYred18 a.R45	PatE-pre-Ion b.F47	KYred29 b.R43	T7EX5.F22	KYred18 c.R20
red116	KYred14 a.F53	KYred18 a.R45	PatE-pre-Ion b.F47	**red108 b.R43**	T7EX5.F22	KYred18 c.R20
red117	KYred14 a.F53	KYred18 a.R45	PatE-pre-Ion b.F47	**red101 b.R43**	T7EX5.F22	KYred18 c.R20
red119	KYred14 a.F53	KYred18 a.R45	PatE-pre-Ion b.F47	**red111 b.R43**	T7EX5.F22	KYred18 c.R20
red120	KYred14 a.F53	KYred18 a.R45	PatE-pre-Ion b.F47	**red112 b.R43**	T7EX5.F22	KYred18 c.R20
red121	KYred14 a.F53	KYred18 a.R45	PatE-pre-Ion b.F47	**red113 b.R43**	T7EX5.F22	KYred18 c.R20
red122	KYred14 a.F53	KYred18 a.R45	PatE-pre-Ion b.F47	**red114 b.R43**	T7EX5.F22	KYred18 c.R20
red123	KYred14 a.F53	KYred18 a.R45	PatE-pre-Ion b.F47	**red115 b.R43**	T7EX5.F22	KYred18 c.R20
red133	KYred14 a.F53	KYred18 a.R45	PatE-pre-Ion b.F47	red133 b.R43	T7EX5.F22	KYred18 c.R20
red134(2)	KYred14 a.F53	KYred18 a.R45	PatE-pre-Ion b.F47	red134(2) b.R43	T7EX5.F22	KYred18 c.R20
red135	KYred14 a.F53	KYred18 a.R45	PatE-pre-Ion b.F47	red135 b.R43	T7EX5.F22	KYred18 c.R20
red136	KYred14 a.F53	KYred18 a.R45	PatE-pre-Ion b.F47	red136 b.R43	T7EX5.F22	KYred18 c.R20
red172	KYred14 a.F53	KYred18 a.R45	PatE-pre-Ion b.F47	red172 b.R43	T7EX5.F22	KYred18 c.R20
red173	KYred14 a.F53	KYred18 a.R45	PatE-pre-Ion b.F47	red173 b.R43	T7EX5.F22	KYred18 c.R20
red174	KYred14 a.F53	KYred18 a.R45	PatE-pre-Ion b.F47	red174 b.R43	T7EX5.F22	KYred18 c.R20
red175	KYred14 a.F53	KYred18 a.R45	PatE-pre-Ion b.F47	red175 b.R43	T7EX5.F22	KYred18 c.R20
red176	KYred14 a.F53	KYred18 a.R45	PatE-pre-Ion b.F47	red176 b.R43	T7EX5.F22	KYred18 c.R20
red177	KYred14 a.F53	KYred18 a.R45	PatE-pre-Ion b.F47	red177 b.R43	T7EX5.F22	KYred18 c.R20
red178	KYred14 a.F53	KYred18 a.R45	PatE-pre-Ion b.F47	red178 b.R43	T7EX5.F22	KYred18 c.R20
red179	KYred14 a.F53	KYred18 a.R45	PatE-pre-Ion b.F47	red179 b.R43	T7EX5.F22	KYred18 c.R20
red180	KYred14 a.F53	KYred18 a.R45	PatE-pre-Ion b.F47	red180 b.R43	T7EX5.F22	KYred18 c.R20
red181	KYred14 a.F53	KYred18 a.R45	PatE-pre-Ion b.F47	red181 b.R43	T7EX5.F22	KYred18 c.R20
red182	KYred14 a.F53	KYred18 a.R45	PatE-pre-Ion b.F47	**red99 b.R43**	T7EX5.F22	KYred18 c.R20
red183	KYred14 a.F53	KYred18 a.R45	PatE-pre-Ion b.F47	red183 b.R43	T7EX5.F22	KYred18 c.R20
red184	KYred14 a.F53	KYred18 a.R45	PatE-pre-Ion b.F47	red184 b.R43	T7EX5.F22	KYred18 c.R20
red185	KYred14 a.F53	KYred18 a.R45	PatE-pre-Ion b.F47	red185 b.R43	T7EX5.F22	KYred18 c.R20
red186	KYred14 a.F53	KYred18 a.R45	PatE-pre-Ion b.F47	red186 b.R43	T7EX5.F22	KYred18 c.R20
red187	KYred14 a.F53	KYred18 a.R45	PatE-pre-Ion b.F47	**red103 b.R43**	T7EX5.F22	KYred18 c.R20
red188	KYred14 a.F53	KYred18 a.R45	PatE-pre-Ion b.F47	**red104 b.R43**	T7EX5.F22	KYred18 c.R20
red189	KYred14 a.F53	KYred18 a.R45	PatE-pre-Ion b.F47	**red102 b.R43**	T7EX5.F22	KYred18 c.R20
red203	KYred14 a.F53	KYred18 a.R45	PatE-pre-Ion b.F47	red203 b.R43	T7EX5.F22	**red203 b.R43**
red276	KYred14 a.F53	KYred18 a.R45	PatE-pre-Ion b.F47	red276 b.R43	T7EX5.F22	KYred18 c.R20
red277	KYred14 a.F53	KYred18 a.R45	PatE-pre-Ion b.F47	red277 b.R43	T7EX5.F22	KYred18 c.R20
red278	KYred14 a.F53	KYred18 a.R45	PatE-pre-Ion b.F47	red278 b.R43	T7EX5.F22	KYred18 c.R20
red279	KYred14 a.F53	KYred18 a.R45	PatE-pre-Ion b.F47	red279 b.R43	T7EX5.F22	KYred18 c.R20

Organic synthesis of model compounds

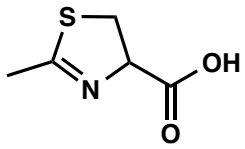

2-methyl-4,5-dihydrothiazole-4-carboxylic acid (1a)[169]

This compound was synthesized according to the literature[169] yielding the thiazoline moiety from *N*-acetyl cysteine in 85% yield..

^{1}H NMR (300 MHz, DMSO-*d*6): δ 5.10–5.04 (m, 1H), 3.66–3.50 (m, 2H), 2.23 (d, *J* = 1.8 Hz, 3H).

HR-ESI-MS: Calculated for $C_5H_7NO_2S$ $[M+H]^+$: 146.02703, Found: 146.0275.

Note that doublet for methyl group and multiplet for proton at α position probably due to long range coupling for homoallylic system as well as multiplet for protons at β position in side chain, were consistent with a literature[170]

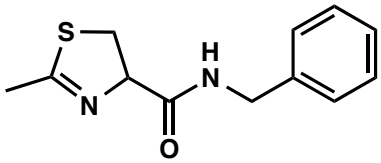

***N*-benzyl-2-methyl-4,5-dihydrothiazole-4-carboxamide (1)**

N,*N*-diisopropylethylamine (293 μL, 1.68 mmol) was added to a mixture of 2-methyl-4,5-dihydrothiazole-4-carboxylic acid (1a) (102 mg, 0.701 mmol), benzylamine (92 μL, 0.84 mmol), and HBTU (322 mg, 0.848 mmol) in 3 mL of *N*,*N*-dimethylformamide and the reaction mixture was stirred at room temperature for 2 h. After the reaction, ethyl acetate was added and the organic layer was washed with brine. The organic layer was dried over Na_2SO_4 and concentrated under reduced pressure. The residue was purified by flash silica gel chromatography to obtain 1 (74.0 mg, 0.304 mmol, in 43% yield).

^{1}H NMR (300 MHz, $CDCl_3$): δ 7.38–7.28 (m, 5H), 7.04 (br, 1H), 5.05–4.98 (m, 1H), 4.57–4.42 (m, 2H), 3.72–3.58 (m, 2H), 2.23 (d, *J* =1.8 Hz, 3H),

^{13}C NMR (75 MHz, $CDCl_3$): δ 171.3, 170.6, 137.9, 128.7, 127.8, 127.5, 79.1, 43.4, 36.7, 20.5. HR-ESI-MS: Calculated for $C_{12}H_{14}N_2OS$ $[M+H]^+$: 235.08996, Found: 235.0897.

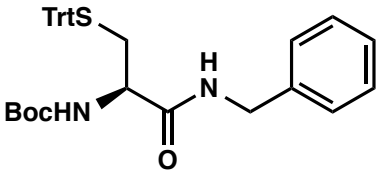

Boc-Cys(Trt)-NHBn (2a)[171]

N,*N*-diisopropylethylamine (1.23 mL, 7.06 mmol) was added to a cooled mixture of Boc-Cys(Trt)-OH (1.16 g, 2.49 mmol) and HBTU (961 mg, 2.54 mmol) in 8 mL of *N*,*N*-dimethylformamide and the reaction mixture was stirred on ice for 5 min and then benzylamine (300 μL, 2.75 mmol) was added and the reaction mixture was stirred at room temperature for 2 h. After the reaction, ethyl acetate was added and the organic layer was washed with 1 M HCl and brine. The organic layer was dried over Na_2SO_4 and concentrated under reduced pressure. The residue was purified by flash silica gel chromatography to obtain 2a (1.19 g, 2.15 mmol, in 86% yield).

^{1}H NMR (300 MHz, $CDCl_3$): δ 7.42–7.18 (m, 20H), 6.23 (br, 1H), 4.76 (br, 1H), 4.38 (d, J = 5.7 Hz, 2H), 3.87 (br, 1H), 2.76 (dd, J = 7.1, 13.1 Hz, 1H), 2.56 (dd, J = 5.4, 12.9 Hz, 1H) 1.38 (s, 9H)

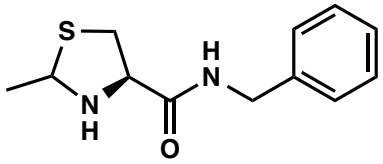

(4*R*)-*N*-benzyl-2-methylthiazolidine-4-carboxamide (2)

1 mL of trifluoroacetic acid was added to a mixture of Boc-Cys(Trt)-NHBn 2a (465 mg, 1.00 mmol), and triisopropylsilane (308 μL, 1.50mmol) in 1 mL of dichloromethane and the reaction mixture was stirred at room temperature for 30 min. after the iterative addition of dichloromethane and concentration under reduced pressure, the residue was dissolved in 800 μL of tetrahydrofuran. The

solution was then basified to pH 9–10 by NaOH aq. Then acetaldehyde (67.2 μL, 1.2 mmol) in 150 μL of tetrahydrofuran was added to the solution and the resulting mixture was further stirred at room temperature for 3 h. The reaction mixture was concetrated under reduced pressure and the remaining water layer was extracted by chloroform. The organic layer was washed with brine and dried over Na_2SO_4 and concentrated under reduced pressure. The residue was purified by flash silica gel chromatography to obtain 2 (158.4 mg 0.670 mmol, 67% in two steps).

^{1}H NMR (300 MHz, $CDCl_3$): δ (The major diastereomer) 7.51 (br, 1H), 4.36 (br, 1H), 4.45 (d, J = 5.7 Hz, 2H), 4.28 (br, 1H), 3.63 (dd, J = 3.9, 11.1 Hz, 1H), 3.34–3.28 (m, 1H, and including 1H from the minor diasterreomer.), 2.11 (br, 1H), 1.54 (d, J = 6.3 Hz, 3H), (The minor diastereomer) 6.72 (br, 1H), 4.64 (br, 1H), 4.48 (d, J = 6.3 Hz, 2H), 3.84 (br, 1H), 3.21 (dd, J = 8.1, 10.5 Hz, 1H), 2.32 (br, 1H), 1.52 (d, J = 6.6 Hz, 3H).

^{13}C NMR (75 MHz, $CDCl_3$): δ (The major diastereomer) 171.2, 138.2, 128.8, 127.6, 127.5, 66.2, 64.5, 43.4, 36.9, 20.7. (The minor diastereomer) 170.8, 137.8, 128.8, 127.9, 127.7, 67.1, 65.2, 43.6, 37.8, 22.2. The ratio between major and minor was estimated as 1.6, which would be derived from stereochemistry at 2-position of thiazolidine, HR-ESI-MS: Calculated for $C_{12}H_{16}N_2OS$ $[M+H]^+$: 237.10561, Found: 237.1064.

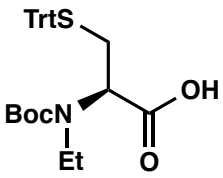

Boc-EtCys(Trt)-OH (3a)

1 mL of methanol-acetic acid (9:1) containing 100 μL of acetaldehyde (1.8 mmol) was added dropwise on ice, into a cooled mixture of H-Cys(Trt)-OH (547 mg, 1.50 mmol) and sodiumcyanoborohydride (95.1 mg, 1.51 mmol) in 15 mL of methanol-acetic acid (9:1). The resulting mixture was stirred for 20 min on ice, and then was concentrated under reduced pressure. The resulting mixture was acidified by 1M HCl, and then the water layer was extracted by chloroform. Combined organic layer was dried over Na2SO4, concentrated in reduced pressure and

the residue was used in the following reaction without any purification. Then, the crude sample was dissolved in 8 mL of 1,4-dioxane and stirred at room temperature and after the addition of 8 mL of 1 M $NaHCO_3$ and Boc_2O in dioxane (393 mg, 1.80 mmol), the mixture was stirred for 16 h. the reaction mixture was then acidified by 1 M HCl to pH 2, and extracted by chloroform. The combined organic layer was concentrated in reduced pressure and the residue was purified by flash silica gel chromatography to obtain 3a (406.2 mg, 0.827 mmol, 83% in two steps).

^{1}H NMR (300 MHz, $CDCl_3$): mixture of two isomers. δ 7.45–7.18 (m, 15H), 3.45, 3.27, 2.90 and 2.68 (br, 2H), 3.15 (t, J = 7.2 Hz, 1H), 2.90 and 2.68 (br, 2H), 1.42 and 1.34 (s, 9H), 0.954 (t, J = 7.2 Hz, 3H). HR-ESI-MS: Calculated for $C_{29}H_{33}NO_4S$ $[M-H]^-$: 490. 20575, Found: 490.2049.

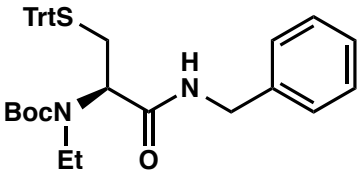

Boc-EtCys(Trt)-NHBn (3b)

N,*N*-diisopropylethylamine (488 μL, 2.80 mmol) was added to a mixture of Boc-EtN-Cys(Trt)-OH (3a) (592 mg, 1.20 mmol), benzylamine (153 μL, 1.40 mmol), and HBTU (534 mg, 1.41 mmol) in 6 mL of *N*,*N*-dimethylformamide and the reaction mixture was stirred at room temperature for 1 h. After the reaction, ethyl acetate was added and the organic layer was washed with 1 M HCl and brine. The organic layer was dried over Na_2SO_4 and concentrated under reduced pressure. The residue was purified by flash silica gel chromatography to obtain 3b (624 mg, 1.07 mmol, in 89% yield).

^{1}H NMR (300 MHz, $CDCl_3$): δ 7.45–7.17 (m, 20H), 6.61 (br, 1H), 4.38–4.27 (br, 2H), 4.09 (br ,1H), 3.01 (br, 2H), 2.78 (br, 1H), 2.65–2.58 (br, 1H), 1.38 (s, 9H), 0.91 (br, 3H). HR-ESI-MS: Calculated for $C_{36}H_{40}N_2O_3S$ $[M+H]^+$: 581.28324, Found: 581.2837.

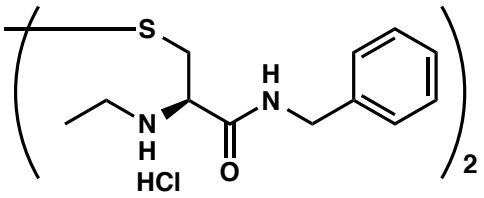

EtCys-NHBn disulfide dihydrochloride (3-dimer)

1.5 mL of trifluoroacetic acid was added to a mixture of Boc-EtN-Cys(Trt)-NHBn 3b (300mg, 0.517 mmol), and triisopropylsilane (128 μL, 0.622 mmol) in 1.5 mL of dichloromethane and the reaction mixture was stirred at room temperature for 20 min. after the iterative concentration under reduced pressure and addition of 4 M HCl in ethyl acetate, the residue was purified by flash silica gel chromatography. During the proceedures of isolation, dimerization took place judged by TLC analysis. Then, after air oxidation of the corresponding monomer, 3-dimer was collected (36.9 mg, 0.0674 mmol, in 26% yield).

^{1}H NMR (300 MHz, $CDCl_3$): δ 7.92 (t, J = 5.4 Hz, 3H) 7.35–7.24 (m, 5H), 4.54–4.36 (m, 2H), 3.45 (dd, J = 4.5, 8.4 Hz, 1H), 3.26 (dd, J = 4.5, 13.8 Hz, 1H), 2.82 (dd, J = 8.4, 13.8 Hz, 1H) 1.92 (br, 1H), 1.07 (t, J = 7.2 Hz, 3H). ^{13}C NMR (75 MHz, $CDCl_3$): δ 172.7, 138.3, 128.7, 127.7, 127.4, 61.1, 43.2, 43.0, 41.5, 15.3. HR-ESI-MS: Calculated for $C_{24}H_{34}N_4O_2S_2$ $[M+H]^+$: 475.21959, Found: 475.2182.

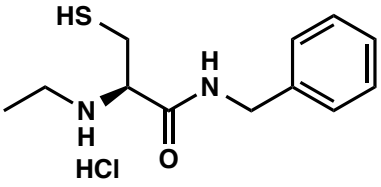

H-EtCys-NHBn hydrochloride (3)

EtCys-NHBn disulfide dihydrochloride was mixed with Immobilized TCEP Disulfide Reducing Gel, which was equilibrated with the deuterated buffer (1M NaOAc buffer pD 5) prior to the disulfide reduction. 1 mL of Immobilized TCEP Disulfide Reducing Gel (50% slurry) was washed twice with D_2O and once with deuterated buffer, by filtration followed by incubation with 1mL of D_2O or deuterated buffer at room temperature for 30 min. The slurry was again filtered and

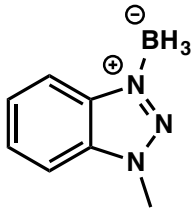

1-methyl benzotriazole borane[172]

This compound was synthesized according to the literature[172] yielding the triazole borane complex in 42% yield. ^{1}H NMR (300 MHz, $CDCl_3$): δ 8.20–8.17 (m, 1H), 7.71–7.58 (m, 3H), 4.38 (s, 2H), 3.43–1.90 (br, 3H).

Ribosomal synthesis of precursor peptides and azoline-containing peptides by a cell-free translation system with or without the cyclodehydratase PatD

The cell-free translation system contained all the components required for the ribosomal expression of peptides from template DNAs. The final concentration of each component is listed below; 50 mM HEPES·K (pH 7.6), 100 mM KOAc, 2 mM GTP, 2 mM ATP, 1 mM CTP, 1 mM UTP, 20 mM creatine phosphate, 12 mM $Mg(OAc)_2$, 2 mM spermidine, 2 mM DTT, 1.5 mg/mL E. coli total tRNA (Roche), 1.2 μM ribosome, 0.6 μM MTF, 2.7 μM IF1, 0.4 μM IF2, 1.5 μM IF3, 30 μM EF-Tu, 30 μM EF-Ts, 0.26 μM EF-G, 0.25 μM RF2, 0.17 μM RF3, 0.5 μM RRF, 4 μg/mL creatine kinase, 3 μg/mL myokinase, 0.1 μM pyrophosphatase, 0.1 μM nucleotide-diphosphatase kinase, 0.1 μM T7 RNA polymerase, 0.73 μM AlaRS, 0.03 μM ArgRS, 0.38 μM AsnRS, 0.13 μM AspRS, 0.02 μM CysRS, 0.06 μM GlnRS, 0.23 μM GluRS, 0.09 μM GlyRS, 0.02 μM HisRS, 0.4 μM IleRS, 0.04 μM LeuRS, 0.11 μM LysRS, 0.03 μM MetRS, 0.68 μM PheRS, 0.16 μM ProRS, 0.04 μM SerRS, 0.09 μM ThrRS, 0.03 μM TrpRS, 0.02 μM TyrRS, 0.02 μM ValRS, 500 μM each proteinogenic amino acids, and 100 μM 10-HCO-H_4folate.

The translation reaction was performed at 37°C for 1 h typically at 2 μL scale, in the presence of 0.2 μL of DNA template, with or without 6 μM of the cyclodehydratase PatD. For the synthesis of peptides containing N-terminal acetyl phenyl alanine (^{Ac}F), the following procedures were adopted.

Aminoacylation of tRNA by activated amino acids by means of flexyzyme

As general procedures, 42 μM of tRNA and 42 μM of flexizyme, (eFx or dFx) was heated at 95°C for 2 min in the presence of 83 mM HEPES·K (pH 7.5) and gradually cooled at 25°C for 5 min. 33% vol. of 600 mM $MgCl_2$ was added to the mixture, and the reaction mixture was further incubated at 25°C for 5 min. After cooling the mixture on ice, the 25% vol. of activated amino acid in DMSO was added and the reaction was performed for several hours (typically 2–24 h). After the incubation, the aminoacylation was quenched by the addition of 400% vol. of 0.3 M NaOAc (pH 5.2). After ethanol precipitaion in acidic conditions, pellet was washed twice with 70% ethanol

containing 0.1 M NaOAc (pH5.2) and once with 70% ethanol, and the resulting pellet was dissolved in 1 mM NaOAc just before adding into translation mixture.

In the specific case in this chapter, tRNA $^{fMet}_{CAU}$–eFx (on ice, 2 h) was adopted for the incorporation of acetyl phenylalanine

Ribosomal synthesis of peptides containing non-proteinogenic structures by a customized cell-free translation system

In the customized cell-free translation mixture, aminoacyl tRNA prepared by flexizyme was typically added into the system at 50 μM based on the amount of total tRNA, regardless of aminoacylation efficiency. And instead, corresponding amino acid was removed from the system.

In the case of experiments in this chapter, methionine as well as 10-HCO-H_4folate were removed from the translation system for the incorporation of acetyl phenylalanine.

Post-translational modification reaction with reducing agents

Typically, to the translation–cyclodehydration product, was added 50% vol. of 1 M sodium cyanoborohydride in 1M NaOAc (pH 5). The resulting mixture was further incubated at 25°C for 24 h. In several experiments, the reaction time was shortened or prolonged.

In the case of reducing agent screening, 33% vol. of 1 M solution/suspension of each reducing agent in buffer with various pH was added, and incubated for denoted times. In such cases, reducing agents were added into either 1 M NaOAc (pH 5), 500 mM HEPES·K (pH 7.5), or 500 mM CHES·K (pH 9).

Alkylation of free thiol by 2-iodoacetamide

After the incubation of a thiazoline-containing peptide with sodium cyanoborohydride, buffer exchange was performed by gel filtration, by 1M HEPES·K (pH 8) containing 0.1 M KOAc. To the filtrate was added 33% vol. of alkylation mixture composed of 30 mM TCEP and 30 mM 2-iodoacetamide in 0.8M HEPES·K (pH 8) and the reaction mixture was further incubated at 25°C for 3 h.

Radical mediated desulfurization of Ψ[CH_2NH]-containing peptide

After the incubation of a thiazoline-containing peptide, with sodium cyanoborohydride, buffer exchange was performed by gel filtration, by 1 M HEPES·K (pH 7.4). To the filtrate was added 50% vol. of desulfurization mixture containing 100 mM VA-044, 0.3 M TCEP, and 100 mM glutathione in 0.5 M HEPES·K (pH 7.4) and the reaction mixture was further incubated at 60°C for 30 min.

MALDI-TOF-MS and MALDI-TOF-MS/MS

The translation mixture, cyclodehydration product, oxidation product, or acid-hydrolysis product was desalted through solid phase extraction (SPE) column (C-Tip C18; Nikkyo Technos), which was equilibrated with elution-solution (80% acetonitrile and 0.5% acetic acid in H_2O) and then with wash-solution (4% acetonitrile and 0.5% acetic acid in H_2O), prior to the sample injection. After the sample injection the column was washed twice with wash-solution (4% acetonitrile and 0.5% acetic acid in H_2O), and eluted with matrix-solution (elution-solution containing half-saturated matrix). As mentioned in supporting results, in the cases of (methyl)oxazoline-containing peptides derived from Ser/Thr residues, acceleration of hydrolysis by the addition of acetic acid into wash-solution, elute-solution, and matrix-solution was observed. In such cases, these solutions were prepared without acetic acid, and denoted in the figures. MALDI-TOF-MS was carried out on an ultrafleXtreme (Bruker Daltonics) externally calibrated with peptide calibration standard II (Bruker Daltonics), in reflector mode.

MALDI-TOF-MS/MS was carried out on an ultrafleXtreme (Bruker Daltonics) and the MS/MS spectra were analyzed on flexAnalysis (Bruker Daltonics) manually.

Chapter 4 General conclusion

In conclusion, I have developed novel methods involving the post-translational enzymatic cyclodehydration by PatD and chemical modifications such as oxidation and reduction on *in vitro* expressed peptides to synthesize backbone-modified peptides inspired by naturally-occurring structural diversity in peptidic natural products, which were reviewed in chapter 1.

In chapter 2, *in vitro* synthetic method of thiazole-containing peptides was developed by integrating a cell-free translation system, a post-translational cyclodehydratase PatD, and chemical oxidation reaction by hydrogen peroxide. The oxidation protocol was originated from a serendipitous observation that one of two consecutive thiazolines was oxidized during MALDI-TOF-MS analysis suggesting oxidation-prone character of the two consecutive thiazolines. For chemical modification, hydrogen peroxide was found to efficiently oxidize the two consecutive thiazollines to intoroduce conjugated thiazole-thiazoline structure in peptidic backbone with a wide variety of peptide sequences. In addition, the structure of oxidation product was identified by a site-specific deuterium labeling method, which was originally developed in this study. The labeling method would be powerful tool for studies on post-translational modification enzymes.

In chapter 3, *in vitro* synthetic method of Ψ[CH_2NH]-containing peptides as well as thiazolidine-containing peptides was developed by integrating a cell-free translation system, a post-translational cyclodehydratase PatD, and chemical reduction by sodium cyanoborohydride. The synthetic method was based on two-step reduction of peptide-embedded thiazoline, which was originally found and characterized by model reactions in this study. The reduction, which is formal site-selective reduction of amide bond in polypeptide, enabled facile synthesis of peptides containing Ψ[CH_2NH] structrure as well as thiazolidine, with a wide variety of sequences.

In conclusion, in this research I have developed novel methods involving the post-translational enzymatic cyclodehydration by PatD and chemical modifications on ribosomally synthesized peptides to yield peptides with various backbone modifications such as thiazoles (Chapter 2) and Ψ[CH_2NH] structures as well as thiazolidines (Chapter 3). The installation of thiazoles and thiazolidines, which are prevailing in bioactive peptidic natural products as well as

Ψ[CH_2NH] structures, which is one of the well known peptidomimetic structures, would provide unique structural scaffolds into peptides, which possibly leads to the development of novel bioactive peptides.

List of accomplishments

【Publications】

1. "Laser-induced oxidation of a peptide-embedded thiazoline by an assistance of adjacent thiazoline", Yasuharu Kato, Yuki Goto, Hiroaki Suga, *Peptide Science 2015,* **2016**, 27-28
2. "One-pot synthesis of azoline-containing peptides in a cell-free translation system integrated with a posttranslational cyclodehydratase", Yuki Goto, Yumi Ito, Yasuharu Kato, Shotaro Tsunoda, Hiroaki Suga, *Chem. Biol.*, **2014**, 21, 766-774.
3. "Attempts at *in Vitro* Reconstitution of a Post-translational Dehydrogenase toward Synthesis of Azole-containing Peptides.", Yasuharu Kato, Yuki Goto, Hiroaki Suga, *Peptide Science 2014*, **2015**, 137-138

【Oral presentations】

4. "翻訳後修飾による複素環含有ペプチドの in vitro 生合成法の開発", 加藤保治, 後藤佑樹, 菅裕明, サントリー生物有機科学研究所報告会, 大阪, 2015 年 3 月
5. "Development of post-translational modification reactions toward in vitro synthesis of peptides with heterocyclic backbones", Yasuharu Kato, Yuki Goto, Hiroaki Suga, 日本化学会第 95 春季年会, 千葉, 2015 年 3 月
6. "Oxidation of azolines assisted by an adjacent azoline moiety toward in vitro synthesis of azole-containing peptides", Yasuharu Kato, Yuki Goto, Hiroaki Suga, 第 52 回ペプチド討論会,平塚, 2015 年 11 月
7. "In vitro biosynthesis of backbone-modified peptides by post-translational modification reactions", Yasuharu Kato, Yuki Goto, Hiroaki Suga, 日本化学会第 96 春季年会, 京都, 2016 年 3 月, (年会ハイライト講演)
8. "アゾリン含有ペプチドの in vitro 合成法の確立とその応用", 加藤保治, 伊藤悠美、角田翔太郎、後藤 佑樹, 菅裕明, 日本薬学会第 136 年会, 横浜, 2016 年 3 月, (大学院生シンポジウム招待講演)
9. "翻訳後修飾による主鎖骨格修飾ペプチド合成法の開発", 加藤保治, 後藤佑樹, 菅裕明, 第 10 回バイオ関連化学シンポジウム, 金沢, 2016 年 9 月
10. "Combination of enzymatic and chemical post-translational modifications for synthesis of various backbone-modified peptides", Yasuharu Kato, Yuki Goto, Hiroaki Suga, 日本化学会第 97 春季年会, 横浜, 2017 年 3 月
11. "翻訳後修飾による主鎖修飾ペプチド合成法の開発とその応用", 加藤保治, 後藤佑樹, 菅裕明, 日本薬学会第 137 年会, 仙台, 2016 年 3 月, (大学院生シンポジウム招待講演)

【Poster presentations】

12. “翻訳後修飾によるアゾール含有ペプチド合成法の開発”, 加藤保治, 後藤佑樹, 菅裕明, 第 14 回東京大学生命科学シンポジウム, 東京, 2014 年 4 月
13. “主鎖骨格にアゾールを有するペプチドの翻訳合成法の開発” 加藤保治, 後藤佑樹, 菅裕明, 日本ケミカルバイオロジー学会第 9 回年会, 大阪, 2014 年 6 月
14. “翻訳後修飾によるアゾール含有ペプチド人工生合成法の開発”, 加藤保治, 後藤佑樹, 菅裕明, 新規素材探索研究会第 13 回セミナー, 横浜, 2014 年 6 月
15. “翻訳後修飾によるアゾール含有ペプチド合成法の開発”, 加藤保治, 後藤佑樹, 菅裕明, 第 2 回バイオ関連化学シンポジウム若手フォーラム, 岡山, 2014 年 9 月
16. “翻訳後修飾によるアゾール含有ペプチド合成法の開発”, 加藤保治, 後藤佑樹, 菅裕明, 第 8 回バイオ関連化学シンポジウム, 岡山, 2014 年 9 月
17. “Artificial post-translational modifications toward synthesis of azole-containing peptides”, 加藤保治, 後藤佑樹, 菅裕明, 第 51 回ペプチド討論会, 徳島, 2014 年 10 月
18. “Development of post-translational modification reactions for the synthesis of Ψ(CH_2NH)-containing peptides”, Yasuharu Kato, Yuki Goto, Hiroaki Suga, The 21st ZESTY Network Seminar, 東京, 2015 年 7 月
19. “ヘテロ環骨格含有ペプチドの合成にむけた新規翻訳後修飾反応の開発”, 加藤保治, 後藤佑樹, 菅裕明, 日本化学会第 95 春季年会アドバンスト・テクノロジー・プログラム, 千葉, 2015 年 3 月
20. “In vitro synthesis of azoline-containing peptides and its applications for various backbone-modified peptides”, Yasuharu Kato, Yuki Goto, Hiroaki Suga, The 15th Tateshina Conference on organic Chemistry,長野, 2015 年 11 月
21. Development of post-translational modification reactions for the synthesis of peptides with Ψ(CH_2NH) structures, Yasuharu Kato, Yuki Goto, Hiroaki Suga, The 2015 International Chemical Congress of Pacific Basin Societies (Pacfichem 2015), Hawaii, 2015 年 12 月
22. “Development of post-translational modifications toward novel bioacitive peptides”, Yasuharu Kato, Yuki Goto, Hiroaki Suga, 日本化学会第 96 春季年会アドバンスト・テクノロジー・プログラム, 京都, 2016 年 3 月
23. “In vitro synthesis of various backbone-modified peptides by post-translational modification reactions”, Yasuharu Kato, Yuki Goto, Hiroaki Suga, 日本化学会第 97 春季年会アドバンスト・テクノロジー・プログラム, 横浜, 2017 年 3 月

References

1. Chothia, C. & Janin, J. Principles of protein-protein recognition. *Nature* **256**, 705-708 (1975).
2. Jones, S. & Thornton, J.M. Principles of protein-protein interactions. *Proceedings of the National Academy of Sciences* **93**, 13-20 (1996).
3. Bogan, A.A. & Thorn, K.S. Anatomy of hot spots in protein interfaces. *Journal of molecular biology* **280**, 1-9 (1998).
4. Arkin, M.R. & Wells, J.A. Small-molecule inhibitors of protein–protein interactions: progressing towards the dream. *Nature reviews Drug discovery* **3**, 301-317 (2004).
5. Wells, J.A. & McClendon, C.L. Reaching for high-hanging fruit in drug discovery at protein–protein interfaces. *Nature* **450**, 1001-1009 (2007).
6. Arkin, M.R., Tang, Y. & Wells, J.A. Small-molecule inhibitors of protein-protein interactions: progressing toward the reality. *Chemistry & biology* **21**, 1102-1114 (2014).
7. Scott, D.E., Bayly, A.R., Abell, C. & Skidmore, J. Small molecules, big targets: drug discovery faces the protein-protein interaction challenge. *Nature Reviews Drug Discovery* **15**, 533-550 (2016).
8. Rask-Andersen, M., Masuram, S. & Schiöth, H.B. The druggable genome: evaluation of drug targets in clinical trials suggests major shifts in molecular class and indication. *Annual review of pharmacology and toxicology* **54**, 9-26 (2014).
9. Nevola, L. & Giralt, E. Modulating protein–protein interactions: the potential of peptides. *Chemical Communications* **51**, 3302-3315 (2015).
10. Gao, M., Cheng, K. & Yin, H. Targeting Protein-Protein Interfaces Using Macrocyclic Peptides. *Biopolymers* **104**, 310-316 (2015).
11. Nevola, L. & Giralt, E. Modulating protein-protein interactions: the potential of peptides. *Chemical Communications* **51**, 3302-3315 (2015).
12. Pelay-Gimeno, M., Glas, A., Koch, O. & Grossmann, T.N. Structure-Based Design of Inhibitors of Protein-Protein Interactions: Mimicking Peptide Binding Epitopes. *Angewandte*

Chemie-International Edition **54**, 8896-8927 (2015).

13. Araghi, R.R. & Keating, A.E. Designing helical peptide inhibitors of protein-protein interactions. *Current Opinion in Structural Biology* **39**, 27-38 (2016).
14. Lipinski, C.A., Lombardo, F., Dominy, B.W. & Feeney, P.J. Experimental and computational approaches to estimate solubility and permeability in drug discovery and development settings. *Advanced Drug Delivery Reviews* **23**, 3-25 (1997).
15. Ahlbach, C.L. et al. Beyond cyclosporine A: conformation-dependent passive membrane permeabilities of cyclic peptide natural products. *Future medicinal chemistry* **7**, 2121-2130 (2015).
16. Siegert, T.R., Bird, M.J., Makwana, K.M. & Kritzer, J.A. Analysis of Loops that Mediate Protein-Protein Interactions and Translation into Submicromolar Inhibitors. *Journal of the American Chemical Society* **138**, 12876-12884 (2016).
17. London, N., Raveh, B. & Schueler-Furman, O. Druggable protein–protein interactions–from hot spots to hot segments. *Current opinion in chemical biology* **17**, 952-959 (2013).
18. Tanaka, Y. et al. Structural basis for the drug extrusion mechanism by a MATE multidrug transporter. *Nature* **496**, 247-251 (2013).
19. Yamagishi, Y. et al. Natural product-like macrocyclic N-methyl-peptide inhibitors against a ubiquitin ligase uncovered from a ribosome-expressed de novo library. *Chemistry & biology* **18**, 1562-1570 (2011).
20. Matsunaga, Y., Bashiruddin, N.K., Kitago, Y., Takagi, J. & Suga, H. Allosteric Inhibition of a Semaphorin 4D Receptor Plexin B1 by a High-Affinity Macrocyclic Peptide. *Cell Chemical Biology* **23**, 1341-1350 (2016).
21. Ecker, D.M., Jones, S.D. & Levine, H.L. in MAbs 9-14 (Taylor & Francis, 2015).
22. Van Weemen, B. & Schuurs, A. Immunoassay using antigen—enzyme conjugates. *FEBS letters* **15**, 232-236 (1971).
23. Engvall, E. & Perlmann, P. Enzyme-linked immunosorbent assay (ELISA) quantitative assay of immunoglobulin G. *Immunochemistry* **8**, 871-874 (1971).
24. Eisenstein, M. Westward expansion. *Nature Methods* **2**, 796-796 (2005).

25. Renart, J., Reiser, J. & Stark, G.R. Transfer of proteins from gels to diazobenzyloxymethyl-paper and detection with antisera: a method for studying antibody specificity and antigen structure. *Proceedings of the National Academy of Sciences* **76**, 3116-3120 (1979).

26. Towbin, H., Staehelin, T. & Gordon, J. Electrophoretic transfer of proteins from polyacrylamide gels to nitrocellulose sheets: procedure and some applications. *Proceedings of the National Academy of Sciences* **76**, 4350-4354 (1979).

27. Brahmer, J.R. et al. Phase I study of single-agent anti–programmed death-1 (MDX-1106) in refractory solid tumors: safety, clinical activity, pharmacodynamics, and immunologic correlates. *Journal of Clinical Oncology* **28**, 3167-3175 (2010).

28. Wang, C. et al. In vitro characterization of the anti-PD-1 antibody nivolumab, BMS-936558, and in vivo toxicology in non-human primates. *Cancer immunology research* **2**, 846-856 (2014).

29. Schafer, P. et al. Apremilast, a cAMP phosphodiesterase‐4 inhibitor, demonstrates anti‐inflammatory activity in vitro and in a model of psoriasis. *British journal of pharmacology* **159**, 842-855 (2010).

30. Song, M.-Y. et al. Characterization of a novel anti-human TNF-α murine monoclonal antibody with high binding affinity and neutralizing activity. *Experimental & molecular medicine* **40**, 35-42 (2008).

31. Magnenat, L. et al. in mAbs 127-139 (Taylor & Francis, 2017).

32. Ernst, J.A. et al. Isolation and characterization of the B-cell marker CD20. *Biochemistry* **44**, 15150-15158 (2005).

33. Yu, Y. et al. A humanized anti-VEGF rabbit monoclonal antibody inhibits angiogenesis and blocks tumor growth in xenograft models. *PLoS One* **5**, e9072 (2010).

34. Liang, W.-C. et al. Cross-species vegf-blocking antibodies completely inhibit the growth of human tumor xenografts and measure the contribution of stromal vegf. *Journal of Biological Chemistry* (2005).

35. Glanville, J. et al. Precise determination of the diversity of a combinatorial antibody library

gives insight into the human immunoglobulin repertoire. *Proceedings of the National Academy of Sciences* **106**, 20216-20221 (2009).

36. Georgiou, G. et al. The promise and challenge of high-throughput sequencing of the antibody repertoire. *Nature biotechnology* **32**, 158-168 (2014).
37. Passioura, T., Katoh, T., Goto, Y. & Suga, H. Selection-based discovery of druglike macrocyclic peptides. *Annual review of biochemistry* **83**, 727-752 (2014).
38. Gray, B.P. & Brown, K.C. Combinatorial peptide libraries: mining for cell-binding peptides. *Chemical reviews* **114**, 1020-1081 (2013).
39. Strieker, M., Tanović, A. & Marahiel, M.A. Nonribosomal peptide synthetases: structures and dynamics. *Current opinion in structural biology* **20**, 234-240 (2010).
40. Winn, M., Fyans, J., Zhuo, Y. & Micklefield, J. Recent advances in engineering nonribosomal peptide assembly lines. *Natural product reports* **33**, 317-347 (2016).
41. Kries, H. Biosynthetic engineering of nonribosomal peptide synthetases. *Journal of Peptide Science* **22**, 564-570 (2016).
42. Fischbach, M.A. & Walsh, C.T. Assembly-line enzymology for polyketide and nonribosomal peptide antibiotics: logic, machinery, and mechanisms. *Chemical reviews* **106**, 3468-3496 (2006).
43. Arnison, P.G. et al. Ribosomally synthesized and post-translationally modified peptide natural products: overview and recommendations for a universal nomenclature. *Natural product reports* **30**, 108-160 (2013).
44. Oman, T.J. & Van Der Donk, W.A. Follow the leader: the use of leader peptides to guide natural product biosynthesis. *Nature chemical biology* **6**, 9-18 (2010).
45. McIntosh, J.A., Donia, M.S. & Schmidt, E.W. Ribosomal peptide natural products: bridging the ribosomal and nonribosomal worlds. *Natural product reports* **26**, 537-559 (2009).
46. Humphrey, J.M. & Chamberlin, A.R. Chemical synthesis of natural product peptides: coupling methods for the incorporation of noncoded amino acids into peptides. *Chemical Reviews* **97**, 2243-2266 (1997).
47. Knerr, P.J. & van der Donk, W.A. Discovery, biosynthesis, and engineering of lantipeptides.

Annual review of biochemistry **81**, 479-505 (2012).

48. Morris, S.L., Walsh, R.C. & Hansen, J. Identification and characterization of some bacterial membrane sulfhydryl groups which are targets of bacteriostatic and antibiotic action. *Journal of Biological Chemistry* **259**, 13590-13594 (1984).
49. Wever, W.J. et al. Chemoenzymatic synthesis of thiazolyl peptide natural products featuring an enzyme-catalyzed formal [4+ 2] cycloaddition. *Journal of the American Chemical Society* **137**, 3494-3497 (2015).
50. Allgaier, H., Jung, G., Werner, R.G., Schneider, U. & Zähner, H. Elucidation of the structure of epidermin, a ribosomally synthesized, tetracyclic heterodetic polypeptide antibiotic. *Angewandte Chemie International Edition in English* **24**, 1051-1053 (1985).
51. Komiyama, K. et al. A new antibiotic, cypemycin. Taxonomy, fermentation, isolation and biological characteristics. *The Journal of antibiotics* **46**, 1666-1671 (1993).
52. Minami, Y. et al. Structure of cypemycin, a new peptide antibiotic. *Tetrahedron letters* **35**, 8001-8004 (1994).
53. HAYASHI, F. et al. The structure of PA48009: the revised structure of duramycin. *The Journal of antibiotics* **43**, 1421-1430 (1990).
54. Hamada, T., Sugawara, T., Matsunaga, S. & Fusetani, N. Polytheonamides, unprecedented highly cytotoxic polypeptides, from the marine sponge theonella swinhoei: 1. Isolation and component amino acids. *Tetrahedron letters* **35**, 719-720 (1994).
55. Hamada, T., Matsunaga, S., Yano, G. & Fusetani, N. Polytheonamides A and B, Highly Cytotoxic, Linear Polypeptides with Unprecedented Structural Features, from the Marine Sponge, Theonella s winhoei. *Journal of the American Chemical Society* **127**, 110-118 (2005).
56. Tugyi, R. et al. Partial D-amino acid substitution: Improved enzymatic stability and preserved Ab recognition of a MUC2 epitope peptide. *Proceedings of the National Academy of Sciences of the United States of America* **102**, 413-418 (2005).
57. Carroll, A.R. et al. Patellins 1-6 and Trunkamide A: Novel Cyclic Hexa-, Hepta-and Octa-peptides From Colonial Ascidians, Lissoclinum sp. *Australian journal of chemistry* **49**,

659-667 (1996).

58. Wipf, P. & Uto, Y. Total synthesis and revision of stereochemistry of the marine metabolite trunkamide A. *The Journal of organic chemistry* **65**, 1037-1049 (2000).

59. Donia, M.S., Ravel, J. & Schmidt, E.W. A global assembly line to cyanobactins. *Nature chemical biology* **4**, 341 (2008).

60. Donia, M.S. & Schmidt, E.W. Linking chemistry and genetics in the growing cyanobactin natural products family. *Chemistry & biology* **18**, 508-519 (2011).

61. Sivonen, K., Leikoski, N., Fewer, D.P. & Jokela, J. Cyanobactins—ribosomal cyclic peptides produced by cyanobacteria. *Applied microbiology and biotechnology* **86**, 1213-1225 (2010).

62. McIntosh, J.A., Donia, M.S., Nair, S.K. & Schmidt, E.W. Enzymatic basis of ribosomal peptide prenylation in cyanobacteria. *Journal of the American Chemical Society* **133**, 13698-13705 (2011).

63. McIntosh, J.A., Lin, Z., Tianero, M.D.B. & Schmidt, E.W. Aestuaramides, a natural library of cyanobactin cyclic peptides resulting from isoprene-derived Claisen rearrangements. *ACS chemical biology* **8**, 877-883 (2013).

64. Ireland, C. & Scheuer, P.J. Ulicyclamide and ulithiacyclamide, two new small peptides from a marine tunicate. *Journal of the American Chemical Society* **102**, 5688-5691 (1980).

65. Bulaj, G. et al. Synthetic μO-conotoxin MrVIB blocks TTX-resistant sodium channel NaV1. 8 and has a long-lasting analgesic activity. *Biochemistry* **45**, 7404-7414 (2006).

66. Fontaine, L. & Hols, P. The inhibitory spectrum of thermophilin 9 from Streptococcus thermophilus LMD-9 depends on the production of multiple peptides and the activity of BlpGSt, a thiol-disulfide oxidase. *Applied and environmental microbiology* **74**, 1102-1110 (2008).

67. Bulaj, G. et al. Efficient oxidative folding of conotoxins and the radiation of venomous cone snails. *Proceedings of the National Academy of Sciences* **100**, 14562-14568 (2003).

68. Derksen, D.J., Stymiest, J.L. & Vederas, J.C. Antimicrobial leucocin analogues with a disulfide bridge replaced by a carbocycle or by noncovalent interactions of allyl glycine

residues. *Journal of the American Chemical Society* **128**, 14252-14253 (2006).

69. Ishida, K., Matsuda, H., Murakami, M. & Yamaguchi, K. Kawaguchipeptin A, a novel cyclic undecapeptide from cyanobacterium Microcystis aeruginosa (NIES-88). *Tetrahedron* **52**, 9025-9030 (1996).

70. Ishida, K., Matsuda, H., Murakami, M. & Yamaguchi, K. Kawaguchipeptin B, an antibacterial cyclic undecapeptide from the cyanobacterium Microcystis aeruginosa. *Journal of natural products* **60**, 724-726 (1997).

71. Parajuli, A. et al. A Unique Tryptophan C-Prenyltransferase from the Kawaguchipeptin Biosynthetic Pathway. *Angewandte Chemie-International Edition* **55**, 3596-3599 (2016).

72. Okada, M. et al. Stereospecific prenylation of tryptophan by a cyanobacterial post-translational modification enzyme. *Organic & Biomolecular Chemistry* **14**, 9639-9644 (2016).

73. Magnuson, R., Solomon, J. & Grossman, A.D. Biochemical and genetic characterization of a competence pheromone from B. subtilis. *Cell* **77**, 207-216 (1994).

74. Okada, M. et al. Structure of the Bacillus subtilis quorum-sensing peptide pheromone ComX. *Nature chemical biology* **1**, 23-24 (2005).

75. Okada, M. et al. Chemical structure of posttranslational modification with a farnesyl group on tryptophan. *Bioscience, biotechnology, and biochemistry* **72**, 914-918 (2008).

76. Roy, R.S., Gehring, A.M., Milne, J.C., Belshaw, P.J. & Walsh, C.T. Thiazole and oxazole peptides: biosynthesis and molecular machinery. *Natural product reports* **16**, 249-263 (1999).

77. White, T.R. et al. On-resin N-methylation of cyclic peptides for discovery of orally bioavailable scaffolds. *Nature chemical biology* **7**, 810-817 (2011).

78. Kansy, M., Senner, F. & Gubernator, K. Physicochemical high throughput screening: parallel artificial membrane permeation assay in the description of passive absorption processes. *Journal of medicinal chemistry* **41**, 1007-1010 (1998).

79. Czekster, C.M., Ge, Y. & Naismith, J.H. Mechanisms of cyanobactin biosynthesis. *Current Opinion in Chemical Biology* **35**, 80-88 (2016).

80. Dunbar, K.L., Melby, J.O. & Mitchell, D.A. YcaO domains use ATP to activate amide backbones during peptide cyclodehydrations. *Nature chemical biology* **8**, 569-575 (2012).

81. Koehnke, J. et al. The cyanobactin heterocyclase enzyme: a processive adenylase that operates with a defined order of reaction. *Angewandte Chemie International Edition* **52**, 13991-13996 (2013).

82. Li, Y.-M., Milne, J.C., Madison, L.L., Kolter, R. & Walsh, C.T. From peptide precursors to oxazole and thiazole-containing peptide antibiotics: microcin B17 synthase. *Science* **274**, 1188 (1996).

83. Leikoski, N. et al. Analysis of an inactive cyanobactin biosynthetic gene cluster leads to discovery of new natural products from strains of the genus Microcystis. *PLoS One* **7**, e43002 (2012).

84. Hamada, Y., Shibata, M. & Shioiri, T. New methods and reagents in organic synthesis. 55. Total syntheses of patellamides B and C, cytotoxic cyclic peptides from a tunicate 1. Their proposed structures should be corrected. *Tetrahedron letters* **26**, 5155-5158 (1985).

85. Hamada, Y., Shibata, M. & Shioiri, T. New methods and reagents in organic synthesis. 56. Total syntheses of patellamides B and C, cytotoxic cyclic peptides from a tunicate 2. Their real structures have been determined by their syntheses. *Tetrahedron letters* **26**, 5159-5162 (1985).

86. Hamada, Y., Shibata, M. & Shioiri, T. New methods and reagents in organic synthesis. 58.: A synthesis of patellamide a, a cytotoxic cyclic peptide from a tunicate. Revision of its proposed structure. *Tetrahedron letters* **26**, 6501-6504 (1985).

87. Schmidt, U. & Griesser, H. Total synthesis and structure determination of patellamide B. *Tetrahedron letters* **27**, 163-166 (1986).

88. Schmidt, E.W. et al. Patellamide A and C biosynthesis by a microcin-like pathway in Prochloron didemni, the cyanobacterial symbiont of Lissoclinum patella. *Proceedings of the National Academy of Sciences of the United States of America* **102**, 7315-7320 (2005).

89. Williams, A.B. & Jacobs, R.S. A marine natural product, patellamide D, reverses multidrug resistance in a human leukemic cell line. *Cancer letters* **71**, 97-102 (1993).

90. Donia, M.S. et al. Natural combinatorial peptide libraries in cyanobacterial symbionts of marine ascidians. *Nature chemical biology* **2**, 729-735 (2006).

91. Agarwal, V., Pierce, E., McIntosh, J., Schmidt, E.W. & Nair, S.K. Structures of cyanobactin maturation enzymes define a family of transamidating proteases. *Chemistry & biology* **19**, 1411-1422 (2012).

92. Dunbar, K.L. et al. Discovery of a new ATP-binding motif involved in peptidic azoline biosynthesis. *Nature chemical biology* **10**, 823-829 (2014).

93. Lee, J., McIntosh, J., Hathaway, B.J. & Schmidt, E.W. Using marine natural products to discover a protease that catalyzes peptide macrocyclization of diverse substrates. *Journal of the American Chemical Society* **131**, 2122-2124 (2009).

94. McIntosh, J.A. et al. Circular logic: nonribosomal peptide-like macrocyclization with a ribosomal peptide catalyst. *Journal of the American Chemical Society* **132**, 15499-15501 (2010).

95. Koehnke, J. et al. The mechanism of patellamide macrocyclization revealed by the characterization of the PatG macrocyclase domain. *Nature structural & molecular biology* **19**, 767-772 (2012).

96. Bent, A.F. et al. Structure of PatF from Prochloron didemni. *Acta Crystallographica Section F: Structural Biology and Crystallization Communications* **69**, 618-623 (2013).

97. Goto, Y., Ito, Y., Kato, Y., Tsunoda, S. & Suga, H. One-pot synthesis of azoline-containing peptides in a cell-free translation system integrated with a posttranslational cyclodehydratase. *Chemistry & biology* **21**, 766-774 (2014).

98. Shimizu, Y. et al. Cell-free translation reconstituted with purified components. *Nature biotechnology* **19**, 751-755 (2001).

99. Schmeing, T.M. & Ramakrishnan, V. What recent ribosome structures have revealed about the mechanism of translation. *Nature* **461**, 1234-1242 (2009).

100. Young, R. & Bremer, H. Polypeptide-chain-elongation rate in Escherichia coli B/r as a function of growth rate. *Biochemical Journal* **160**, 185-194 (1976).

101. Bilgin, N., Claesens, F., Pahverk, H. & Ehrenberg, M. Kinetic properties of Escherichia coli

ribosomes with altered forms of S12. *Journal of molecular biology* **224**, 1011-1027 (1992).

102. Bouadloun, F., Donner, D. & Kurland, C. Codon-specific missense errors in vivo. *The EMBO journal* **2**, 1351 (1983).

103. Crick, F., Barnett, L., Brenner, S. & Watts-Tobin, R. General Nature of the Genetic Code for Proteins. *Nature* **192**, 1227-1232 (1961).

104. Nirenberg, M.W. & Matthaei, J.H. The dependence of cell-free protein synthesis in E. coli upon naturally occurring or synthetic polyribonucleotides. *Proceedings of the National Academy of Sciences* **47**, 1588-1602 (1961).

105. Nirenberg, M. Historical review: Deciphering the genetic code–a personal account. *Trends in biochemical sciences* **29**, 46-54 (2004).

106. Chapeville, F. et al. On the role of soluble ribonucleic acid in coding for amino acids. *Proceedings of the National Academy of Sciences* **48**, 1086-1092 (1962).

107. Ellman, J.A., Mendel, D. & Schultz, P.G. Site-specific incorporation of novel backbone structures into proteins. *Science* **255**, 197 (1992).

108. Noren, C.J., Anthony-Cahill, S.J., Griffith, M.C. & Schultz, P.G. A general method for site-specific incorporation of unnatural amino acids into proteins. *Science* **244**, 182 (1989).

109. Wang, L., Brock, A., Herberich, B. & Schultz, P.G. Expanding the genetic code of Escherichia coli. *Science* **292**, 498-500 (2001).

110. Josephson, K., Hartman, M.C. & Szostak, J.W. Ribosomal synthesis of unnatural peptides. *Journal of the American Chemical Society* **127**, 11727-11735 (2005).

111. Goto, Y., Katoh, T. & Suga, H. Flexizymes for genetic code reprogramming. *Nature protocols* **6**, 779-790 (2011).

112. Murakami, H., Ohta, A., Ashigai, H. & Suga, H. A highly flexible tRNA acylation method for non-natural polypeptide synthesis. *Nature Methods* **3**, 357 (2006).

113. Goto, Y., Murakami, H. & Suga, H. Initiating translation with D-amino acids. *RNA* **14**, 1390-1398 (2008).

114. Fujino, T., Goto, Y., Suga, H. & Murakami, H. Reevaluation of the D-amino acid compatibility with the elongation event in translation. *Journal of the American Chemical*

Society **135**, 1830-1837 (2013).

115. Katoh, T., Tajima, K. & Suga, H. Consecutive Elongation of D-Amino Acids in Translation. *Cell Chemical Biology* (2016).

116. Fujino, T., Goto, Y., Suga, H. & Murakami, H. Ribosomal Synthesis of Peptides with Multiple β-Amino Acids. *Journal of the American Chemical Society* **138**, 1962-1969 (2016).

117. Kawakami, T., Murakami, H. & Suga, H. Messenger RNA-programmed incorporation of multiple N-methyl-amino acids into linear and cyclic peptides. *Chemistry & biology* **15**, 32-42 (2008).

118. Kawakami, T., Murakami, H. & Suga, H. Ribosomal Synthesis of Polypeptoids and Peptoid − Peptide Hybrids. *Journal of the American Chemical Society* **130**, 16861-16863 (2008).

119. Ohta, A., Murakami, H., Higashimura, E. & Suga, H. Synthesis of polyester by means of genetic code reprogramming. *Chemistry & biology* **14**, 1315-1322 (2007).

120. Ohta, A., Murakami, H. & Suga, H. Polymerization of α - Hydroxy Acids by Ribosomes. *ChemBioChem* **9**, 2773-2778 (2008).

121. Goto, Y. et al. Reprogramming the translation initiation for the synthesis of physiologically stable cyclic peptides. *ACS chemical biology* **3**, 120-129 (2008).

122. Sako, Y., Goto, Y., Murakami, H. & Suga, H. Ribosomal synthesis of peptidase-resistant peptides closed by a nonreducible inter-side-chain bond. *ACS chemical biology* **3**, 241-249 (2008).

123. Sako, Y., Morimoto, J., Murakami, H. & Suga, H. Ribosomal synthesis of bicyclic peptides via two orthogonal inter-side-chain reactions. *Journal of the American Chemical Society* **130**, 7232-7234 (2008).

124. Yamagishi, Y., Ashigai, H., Goto, Y., Murakami, H. & Suga, H. Ribosomal synthesis of cyclic peptides with a fluorogenic oxidative coupling reaction. *ChemBioChem* **10**, 1469-1472 (2009).

125. Melby, J.O., Nard, N.J. & Mitchell, D.A. Thiazole/oxazole-modified microcins: complex natural products from ribosomal templates. *Current opinion in chemical biology* **15**, 369-378 (2011).

126. Carmeli, S., Moore, R.E., Patterson, G.M., Corbett, T.H. & Valeriote, F.A. Tantazoles, unusual cytotoxic alkaloids from the blue-green alga Scytonema mirabile. *Journal of the American Chemical Society* **112**, 8195-8197 (1990).

127. Carmeli, S., Moore, R.E. & Patterson, G.L. Mirabazoles, minor tantazole-related cytotoxins from the terrestrial blue-green alga Scytonema mirabile. *Tetrahedron letters* **32**, 2593-2596 (1991).

128. Gaumont, A.-C., Gulea, M. & Levillain, J. Overview of the Chemistry of 2-Thiazolines. *Chemical reviews* **109**, 1371-1401 (2009).

129. Charette, A.B. & Chua, P. Mild method for the synthesis of thiazolines from secondary and tertiary amides. *The Journal of Organic Chemistry* **63**, 908-909 (1998).

130. Raman, P., Razavi, H. & Kelly, J.W. Titanium (IV)-mediated tandem deprotection− cyclodehydration of protected cysteine N-amides: biomimetic syntheses of thiazoline-and thiazole-containing heterocycles. *Organic letters* **2**, 3289-3292 (2000).

131. Numajiri, Y., Takahashi, T., Takagi, M., Shin-ya, K. & Doi, T. Total synthesis of largazole and its biological evaluation. *Synlett* **2008**, 2483-2486 (2008).

132. Sakakura, A., Kondo, R., Umemura, S. & Ishihara, K. Dehydrative cyclization of serine, threonine, and cysteine residues catalyzed by molybdenum (VI) oxo compounds. *Tetrahedron* **65**, 2102-2109 (2009).

133. Seebeck, F.P. & Szostak, J.W. Ribosomal synthesis of dehydroalanine-containing peptides. *Journal of the American Chemical Society* **128**, 7150-7151 (2006).

134. Hofmann, F.T., Szostak, J.W. & Seebeck, F.P. In vitro selection of functional lantipeptides. *Journal of the American Chemical Society* **134**, 8038-8041 (2012).

135. Pace, C.N., Vajdos, F., Fee, L., Grimsley, G. & Gray, T. How to measure and predict the molar absorption coefficient of a protein. *Protein science* **4**, 2411-2423 (1995).

136. Zipperer, A. et al. Human commensals producing a novel antibiotic impair pathogen colonization. *Nature* **535**, 511-516 (2016).

137. Drechsel, H. et al. Structure elucidation of yersiniabactin, a siderophore from highly virulent Yersinia strains. *European Journal of Organic Chemistry* **1995**, 1727-1733 (1995).

138. Cox, C.D., Rinehart, K.L., Moore, M.L. & Cook, J.C. Pyochelin: novel structure of an iron-chelating growth promoter for Pseudomonas aeruginosa. *Proceedings of the National Academy of Sciences* **78**, 4256-4260 (1981).

139. Miller, D.A., Luo, L., Hillson, N., Keating, T.A. & Walsh, C.T. Yersiniabactin synthetase: a four-protein assembly line producing the nonribosomal peptide/polyketide hybrid siderophore of Yersinia pestis. *Chemistry & biology* **9**, 333-344 (2002).

140. Patel, H.M. & Walsh, C.T. In vitro reconstitution of the Pseudomonas aeruginosa nonribosomal peptide synthesis of pyochelin: characterization of backbone tailoring thiazoline reductase and N-methyltransferase activities. *Biochemistry* **40**, 9023-9031 (2001).

141. Malins, L.R. & Payne, R.J. Synthetic amino acids for applications in peptide ligation–desulfurization chemistry. *Australian Journal of Chemistry* **68**, 521-537 (2015).

142. Dawson, P.E., Miur, T.W., Clark-Lewis, I. & Kent, S.B. Synthesis of proteins by native chemical ligation. *Science* **266**, 776-780 (1994).

143. Kent, S. et al. Through the looking glass–a new world of proteins enabled by chemical synthesis. *Journal of Peptide Science* **18**, 428-436 (2012).

144. Yan, L.Z. & Dawson, P.E. Synthesis of peptides and proteins without cysteine residues by native chemical ligation combined with desulfurization. *Journal of the American Chemical Society* **123**, 526-533 (2001).

145. Crich, D. & Banerjee, A. Native chemical ligation at phenylalanine. *Journal of the American Chemical Society* **129**, 10064-10065 (2007).

146. Haase, C., Rohde, H. & Seitz, O. Native chemical ligation at valine. *Angewandte Chemie International Edition* **47**, 6807-6810 (2008).

147. Chen, J., Wan, Q., Yuan, Y., Zhu, J. & Danishefsky, S.J. Native chemical ligation at valine: a contribution to peptide and glycopeptide synthesis. *Angewandte Chemie* **120**, 8649-8652 (2008).

148. Yang, R., Pasunooti, K.K., Li, F., Liu, X.-W. & Liu, C.-F. Dual native chemical ligation at lysine. *Journal of the American Chemical Society* **131**, 13592-13593 (2009).

149. Ajish Kumar, K., Haj‐Yahya, M., Olschewski, D., Lashuel, H.A. & Brik, A. Highly

efficient and chemoselective peptide ubiquitylation. *Angewandte Chemie International Edition* **48**, 8090-8094 (2009).

150. Chen, J., Wang, P., Zhu, J., Wan, Q. & Danishefsky, S.J. A program for ligation at threonine sites: application to the controlled total synthesis of glycopeptides. *Tetrahedron* **66**, 2277-2283 (2010).

151. Harpaz, Z., Siman, P., Kumar, K. & Brik, A. Protein synthesis assisted by native chemical ligation at leucine. *ChemBioChem* **11**, 1232-1235 (2010).

152. Shang, S., Tan, Z., Dong, S. & Danishefsky, S.J. An advance in proline ligation. *Journal of the American Chemical Society* **133**, 10784-10786 (2011).

153. Siman, P., Karthikeyan, S.V. & Brik, A. Native chemical ligation at glutamine. *Organic letters* **14**, 1520-1523 (2012).

154. Malins, L.R., Cergol, K.M. & Payne, R.J. Peptide ligation–desulfurization chemistry at arginine. *ChemBioChem* **14**, 559-563 (2013).

155. Thompson, R.E., Chan, B., Radom, L., Jolliffe, K.A. & Payne, R.J. Chemoselective peptide ligation–desulfurization at aspartate. *Angewandte Chemie International Edition* **52**, 9723-9727 (2013).

156. Cergol, K.M., Thompson, R.E., Malins, L.R., Turner, P. & Payne, R.J. One-Pot Peptide Ligation–Desulfurization at Glutamate. *Organic letters* **16**, 290-293 (2013).

157. Malins, L.R., Cergol, K.M. & Payne, R.J. Chemoselective sulfenylation and peptide ligation at tryptophan. *Chemical Science* **5**, 260-266 (2014).

158. Sayers, J., Thompson, R.E., Perry, K.J., Malins, L.R. & Payne, R.J. Thiazolidine-Protected beta-Thiol Asparagine: Applications in One-Pot Ligation-Desulfurization Chemistry. *Organic Letters* **17**, 4902-4905 (2015).

159. Wan, Q. & Danishefsky, S.J. Free‐radical‐based, specific desulfurization of cysteine: a powerful advance in the synthesis of polypeptides and glycopolypeptides. *Angewandte Chemie International Edition* **46**, 9248-9252 (2007).

160. Choudhary, A. & Raines, R.T. An Evaluation of Peptide‐Bond Isosteres. *ChemBioChem* **12**, 1801-1807 (2011).

161. Szelke, M. et al. Potent new inhibitors of human renin. (1982).

162. Oh, H.-S., Ko, S.-S., Cho, H. & Lee, K.-H. Design and synthesis of antibacterial pseudopeptides with a potent antibacterial activity and more improved stability from a short cationic antibacterial peptide. *Bull. Korean Chem. Soc* **26**, 161-164 (2005).

163. Kim, S.-M., Kim, J.-M., Joshi, B.P., Cho, H. & Lee, K.-H. Indolicidin-derived antimicrobial peptide analogs with greater bacterial selectivity and requirements for antibacterial and hemolytic activities. *Biochimica et Biophysica Acta (BBA)-Proteins and Proteomics* **1794**, 185-192 (2009).

164. Xu, G.G., Zhang, Y., Mercedes-Camacho, A.Y. & Etzkorn, F.A. A reduced-amide inhibitor of Pin1 binds in a conformation resembling a twisted-amide transition state. *Biochemistry* **50**, 9545-9550 (2011).

165. Geyer, A., Mueller, G. & Kessler, H. Conformational Analysis of a Cyclic RGD Peptide Containing a .psi.[CH2-NH] Bond: A Positional Shift in Backbone Structure Caused by a Single Dipeptide Mimetic. *Journal of the American Chemical Society* **116**, 7735-7743 (1994).

166. Zivec, M., Jakopin, Z. & Gobec, S. Recent advances in the synthesis and applications of reduced amide pseudopeptides. *Current medicinal chemistry* **16**, 2289-2304 (2009).

167. Assem, N., Natarajan, A. & Yudin, A.K. Chemoselective peptidomimetic ligation using thioacid peptides and aziridine templates. *Journal of the American Chemical Society* **132**, 10986-10987 (2010).

168. Kourouklis, D., Murakami, H. & Suga, H. Programmable ribozymes for mischarging tRNA with nonnatural amino acids and their applications to translation. *Methods* **36**, 239-244 (2005).

169. Chen, H., O'Connor, S., Cane, D.E. & Walsh, C.T. Epothilone biosynthesis: assembly of the methylthiazolylcarboxy starter unit on the EpoB subunit. *Chemistry & biology* **8**, 899-912 (2001).

170. Emtenäs, H., Alderin, L. & Almqvist, F. An enantioselective ketene− imine cycloaddition method for synthesis of substituted ring-fused 2-pyridinones. *The Journal of organic*

chemistry **66**, 6756-6761 (2001).

171. Koniev, O. et al. Selective irreversible chemical tagging of cysteine with 3-arylpropiolonitriles. *Bioconjugate chemistry* **25**, 202-206 (2014).

172. Liao, W. et al. 1, 2, 3-Triazole-boranes: stable and efficient reagents for ketone and aldehyde reductive amination in organic solvents or in water. *Chemical Communications*, 6436-6438 (2009).

Acknoledgement

本研究を遂行し、学位論文をまとめるにあたり、ご指導ご鞭撻をいただいた菅裕明教授に心より感謝申し上げます。菅研究室の研究環境は十分すぎると言ってもいいほどで、研究の律速段階が自分自身であるという環境は、自己を鍛錬する場として最適なものだったと思います。菅先生のもとに集まった研究室のメンバーは国籍から研究のバックグラウンドにいたるまで多種多様であり、刺激的な研究生活・学生生活を送ることができました。ミーティングでの議論を通して、実験の細かい点を追求するだけでなく、研究を大局的に見る視点、そして何より研究を通して新しい世界を切り開こうという姿勢を少しでも会得できていたらと思います。菅研究室での 5 年間は、これから研究者として生きて行く上で欠かせない経験だったと確信しています。

本研究を進める上で、直接的に実験の指導をしていただきました後藤佑樹准教授に心より感謝申し上げます。翻訳後修飾の研究テーマを示していただいてから今日にいたるまで数え切れないほどのご指導をいただきました。研究がうまく進まず、苦しい中であっても実験データと向き合って方向性を探り続けることの困難さと重要さを学びました。5 年間ご指導をいただく中で、目指すべき研究者像の輪郭を描くことができました。

研究発表に関してご助言をいただきました、狩野直和准教授に感謝申し上げます。専門分野の異なる視点からご指摘をいただくことで、自分自身の研究を客観的に見る機会を得ることができました。また、研究に関するご助言および研究室運営を通して研究をサポートいただきました、加藤敬行助教に感謝申し上げます。おかげさまで研究に全力投球することができました。

研究を進めるにあたり、様々なご指導、ご助言をいただきました研究室の先輩方に感謝申し上げます。特に、分子生物学の研究をしていた私に有機化学の実験法をご指導いただきました、樋口岳博士、山田光博博士に感謝申し上げます。また、修士課程および博士課程で研究室生活を共にした、石橋正成氏、井関めぐみ氏、岩根由彦氏、高辻諒氏、角田翔太郎氏、西尾洸祐氏、村上直央氏に感謝申し上げます。特に岩根氏、高辻氏、西尾氏とは 5 年間、学生生活を共に過ごしました。互いに切磋琢磨し、支え合える同期がいてくれたおかげでなんとか卒業を迎えることができたと思っています。加えて、研究室の後輩の皆様に感謝申し上げます。研究で煮詰まったときでも無駄話に付き合ってもらうことで、元気を分けていただきました。

なお、本研究を遂行するにあたり、日本学術振興会より 2 年間、特別研究員奨励費の助成をいただきました。感謝申し上げます。

最後に、これまでの学生生活を暖かく見守ってくれた両親に感謝の意を表し、本論文の末尾の言葉とさせていただきます。